Misallocation May Kill: Evidence from the World's Largest Energy-Saving Program*

Yuan Chen† Qirui Wang‡

March 25, 2026

Abstract

This paper examines the mortality consequences of China's Top 1,000 Energy-Saving Program, the world's largest energy-conservation initiative regulating the 1,008 largest energy-consuming firms. In sharp contrast to its policy goal, regions more exposed to the program experienced higher mortality rates. The absence of environmental improvement, driven by cross-firm spillovers, and a negative income channel explain this pattern. The evidence is consistent with a Hsieh and Klenow (2009)-type misallocation framework in which distortionary, size-based regulations exert limited effects on pollution but large adverse effects on output and welfare, illustrating how poorly targeted environmental policies can backfire.

JEL Codes: I12, I18, L51, P28, Q48, Q52, R12

*We are grateful to discussions with Treb Allen, Dengke Chen, Hui Ding, Jonathan Skinner, and Jun Zhang, as well as comments of Qiaoyi Chen and Zhao Chen. We acknowledge data support from School of Economics, Fudan University and National Earth System Science Data Center, National Science & Technology Infrastructure of China. We have no relevant or material financial interests that relate to the research described in this paper. All errors are our own.

†Fudan University. Email: chenyuan23@m.fudan.edu.cn

‡Dartmouth College. Email: Qirui.Wang@dartmouth.edu

1 Introduction

Climate change imposes substantial economic and human costs, including lower agricultural output, slower productivity growth, and higher mortality risk (Schlenker and Roberts 2009; Dell et al. 2012; Somanathan et al. 2021; Carleton et al. 2022). Policies to restrict carbon emissions have therefore become central to climate and development debates. In theory, a universal carbon tax is first-best (Nordhaus 2008), yet limited regulatory capacity often leads governments to adopt *size-dependent* regulations that target the largest firms for compliance.[1]

However, such size-dependent regulations can introduce distortionary effects, misallocating resources away from productive firms and reducing aggregate productivity (Guner et al. 2008; Restuccia and Rogerson 2008; Hsieh and Klenow 2009), or even raising aggregate pollution (Qi et al. 2021). Moreover, by lowering income in affected regions, these policies may also deteriorate public health, as income is among the most robust determinants of health outcomes (Pritchett and Summers 1996; Banerjee et al. 2021; Sun et al. 2021; Richterman et al. 2023; Walker et al. 2024). The welfare consequences of such policies are therefore theoretically ambiguous and require empirical evaluation.

Despite the prominence of this question, empirical evidence remains scant. Existing studies either rely on numerical simulation (Qi et al. 2021; da Hora and Vaz 2024) or examine regulation-induced reallocation of pollution and workers without assessing its consequences for health, the ultimate objective of environmental policy (Henderson 1996; Becker and Henderson 2000; Walker 2013; Chen et al. 2025).[2] Indeed, the Top 1,000 Program, the focus of this paper, has been widely regarded as a policy success. The World Bank's review of China's energy-efficiency experience concludes that "the program proved successful and made a substantial contribution to China's overall achievement of its energy-intensity reduction target" (De Gouvello et al. 2021, p. 37).

This paper provides a counterexample. We show that a distortionary, size-based environmental regulation can, quite literally, be fatal. Studying China's Top 1,000 Energy Conservation Program, the largest energy-conservation initiative in history, we document missing environmental gains but increased mortality in regions more exposed to the program. The program served as the flagship initiative under China's 11th Five-Year Plan (2006-2011), which aimed to reduce energy use per unit of GDP by 20 percent. The regulated firms consumed 670 million tons of coal equivalent (TCE) in 2004, accounting for 33 percent of total national energy use. Given that most regulated firms were established long prior to the program's launch, the policy provides a quasi-experimental setting for identifying its impacts.

We uncover four main findings. First, the regulation induced substantial reallocation of pollution and labor within prefectures but little change across them. Using high-resolution pollution and geo-coded firm census data, we construct a 3 km $\times$ 3 km grid-cell panel. Cells hosting regulated firms, characterized by lower pollution intensity and higher wages in the baseline, experienced a 0.6 percent decline in aerosol optical depth (AOD) concentrations and an 18.9 percent fall in employment relative to other cells in the same prefecture, yet aggregate pollution and employment at the prefecture level remained unchanged. Second, consistent with labor moving toward lower-

[1] In addition to China's *Top 1,000 Program* launched in 2006, examples include China's *Emissions Trading System* initiated in 2013, the EU's *Industrial Emissions Directive*, and the U.S. *Clean Air Act*. Size-dependent regulatory coverage under these policies is determined either by explicit size thresholds or through rank-based targeting of the largest firms (Cui et al. 2021; Becker and Henderson 2000; Ozaltun et al. 2025).

[2] There is also related work on pollution leakage across regions within a country (Chen et al. 2018b; Curt et al. 2025) or across countries through "north-south" trade, as reviewed in Copeland et al. (2022). Among them, Tanaka et al. (2022) is a rare exception directly examining mortality effects of pollution spillovers.

wage areas, average household consumption fell by 2 percent at the mean exposure. Household investments in health and climate adaptation also shifted: preventive medical outlays, electricity use, and air-conditioner ownership all fell, while curative medical spending increased. Third, mortality rates rose sharply following the program's introduction. Prefectures with average exposure saw mortality increase by 2.3 percent, and heat-related vulnerability intensified: the mortality gradient with respect to days above 30°C rose by 0.2 percentage point, about 30 percent higher than baseline. Excess mortality is concentrated in cardiorespiratory causes, which account for most of the aggregate increase and are known to be highly sensitive to heat. Across demographic groups, the burden of excess deaths falls disproportionately on populations most exposed to income losses, including urban residents, men, and the working-age and elderly. Together, these findings align with a Hsieh and Klenow (2009)-type misallocation framework, in which distortionary regulations reduce aggregate income through inefficient factor allocation. In this case, the negative health effects from income reduction appear to have fully offset, if not outweighed, any direct pollution benefits, resulting in higher mortality overall.

Our work contributes to two strands of literature. First, we revisit the health impacts of environmental regulation through the lens of household income. A large body of research documents the health benefits of pollution control policies (Chay and Greenstone 2003; Chay et al. 2003; Greenstone and Hanna 2014; Tanaka 2015; Deschênes et al. 2017; Fan et al. 2023), yet these studies largely overlook potential health costs arising from the negative income effects of such regulations. A related literature examines how environmental regulation affects firm productivity (Henderson 1996; Becker and Henderson 2000; Greenstone 2002; He et al. 2020) and labor demand (Berman and Bui 2001; Walker 2011, 2013; Gray et al. 2014; Liu et al. 2023), but seldom connects these income effects to health outcomes. By linking income, consumption, and mortality, our study provides one of the first comprehensive welfare assessments of a large-scale energy-conservation program.

Second, we contribute to the misallocation literature by providing direct evidence that distortionary policies can have fatal welfare consequences. Following the canonical frameworks of Restuccia and Rogerson (2008) and Hsieh and Klenow (2009), a vast literature quantifies the welfare cost of misallocation (Baqaee and Farhi 2020; Edmond et al. 2023; Carrillo et al. 2023; Atkin et al. 2025), and recent work in environmental economics shows that factor misallocation can raise emission intensity and reduce welfare (Tombe and Winter 2015; Qi et al. 2021). Yet, to our knowledge, no prior study links such distortionary policies to observed welfare outcomes in real-world data.[3] In a concurrent study, Chen et al. (2025) document widespread spillovers from the Top 1,000 Program, particularly through ownership networks, and evaluate its welfare implications using a calibrated industry model. Their analysis focuses on production-side responses and model-implied aggregate welfare, whereas we provide direct evidence on realized mortality, the program's most critical welfare consequence. By uncovering the program's reallocation toward less-regulated, dirtier entities, we reveal a markedly more adverse welfare outcome than Chen et al. (2025). Diverging from their conclusion that aggregate energy use fell by 4 percent at the cost of a 3.5 percent output loss, we find no evidence of energy saving or environmental improvement in more regulated prefectures but a 2.3 percent increase in mortality, let alone potential dead weight losses due to redistribution.

The remainder of the paper is organized as follows. Section 2 describes the policy background.

[3] A complementary body of work in the healthcare sector documents that misallocation of medical inputs deteriorates healthcare quality and increases mortality (Chandra and Staiger 2020; Chandra et al. 2023; Raja 2025).

Section 3 describes the data. Section 4 presents the empirical results. Section 5 concludes.

2 The Top 1,000 Program

China's energy consumption surged during the early 2000s, driven by rapid industrialization and urban expansion. Confronted with rising emissions, growing energy dependence, and mounting climate concerns, the Chinese government made energy efficiency a central objective in the 11th National Economic and Social Development Five-Year Plan, which set a binding goal to reduce energy use per unit of GDP by 20 percent. As the flagship program to realize this target, the National Development and Reform Commission (NDRC) launched the *Top 1,000 Energy Conservation Program* in 2006 (Price et al. 2010; Zhou et al. 2010; Ke et al. 2012). The program covered 1,008 enterprises in nine energy-intensive industries whose annual energy consumption exceeded 180,000 tons of coal equivalent (TCE) in 2004. Collectively, these firms accounted for roughly one-third of national and nearly one-half of industrial energy use, making the Top 1,000 Program the cornerstone of China's early energy conservation strategy.

Local governments implemented the program by assigning each regulated firm specific energy-saving targets and energy-use quotas proportional to its 2004 consumption. To strengthen compliance, the NDRC linked provincial officials' promotion prospects to firms' energy-saving performance, creating strong local enforcement incentives. Between 2007 and 2010, more than 90 percent of regulated firms met their annual targets, and the final compliance rate reached 98.3 percent (NDRC 2011).[4]

Several institutional features make the Top 1,000 Program a useful quasi-experimental setting to study the distributional consequences of distortionary regulation. First, firm eligibility was based on 2004 energy use, well before the program's announcement, which rules out manipulation of treatment status. Second, the program imposed firm-specific energy quotas that effectively acted as implicit production taxes.[5] Finally, most regulated firms were old and state-affiliated, reflecting China's early industrial planning priorities. As shown in Panel A of Figure 1, firms established before 1970 accounted for about half of total employment among regulated firms in 2004. Their locations were largely shaped by the mid-20th-century industrial geography. In particular, Panel A of Appendix Figure G.1 shows that Top 1,000 firms clustered tightly along the historical railway network, a central determinant of industrial siting during the 1950s and 1960s (Fan and Zou 2021; Heblich et al. 2022).

3 Data

To evaluate the impact of the Top 1,000 Program, we assemble comprehensive data on firms, pollution, household, and mortality from multiple sources. Details of data source and variable construction are reported in Appendix A. Summary statistics are reported in Appendix Tables G.1 and G.2.

We identify regulated firms from the NDRC list and merge them with the 2004 *National Economic Census* (NBS 2004), which covers the universe of industrial firms and reports their

[4]Appendix B provides additional background on the Top 1,000 Program and clarifies key aspects of its implementation and enforcement.

[5]Using detailed firm-level data, Chen et al. (2025) show that regulated firms reduced energy use primarily by scaling down output, consistent with the near-perfect complementarity between energy and other inputs documented in Ryan (2018) and Bretschger and Jo (2024).

location, industry, employment, output, and financial accounts. Regulated firms are widely distributed: 247 of 345 prefectures host at least one Top 1,000 firm, and in these prefectures, they account for roughly 12 percent of local industrial employment on average (Appendix Table G.1). Consistent with the program design, regulated firms are substantially larger and more productive: in 2004, their output per worker was 1.78 log points higher, their skill-adjusted wage 0.98 log points higher, and their pollution intensity about 0.12 log points lower than that of unregulated firms (Figure 1).[6]

To track firm dynamics and reallocation, we use the *Annual Survey of Industrial Firms* (ASIF) for 2001-2009 (NBS 2001-2009a), which covers all large industrial enterprises responsible for over 90 percent of total output. We geocode all firms and aggregate them to $0.03^\circ \times 0.03^\circ$ (about 3 km $\times$ 3 km) grid cells, which capture fine-grained variation in industrial activity and naturally account for firm entry and exit.

Environmental performance is measured using satellite-derived aerosol optical depth (AOD), which captures light extinction by airborne particulates such as sulfates, nitrates, and black carbon (van Donkelaar et al. 2006). Because Top 1,000 firms are major emitters of sulfur dioxide, fume, and dust, they are key contributors to local AOD levels. Appendix Figure G.2 shows that AOD is highly correlated with aggregate SO_2 emissions and $PM_{2.5}$ concentrations at prefecture-year level. We use 1 km $\times$ 1 km MODIS AOD data from NASA's TERRA and AQUA satellites (Lyapustin et al. 2015), aggregated to our 3 km grid cells.[7]

Household responses are analyzed using the *Urban Household Survey* (UHS), covering 159 prefectures across 16 provinces during 2002-2009 (NBS 2002-2009b). It records detailed expenditure categories—including healthcare spending, electricity use, and air-conditioner ownership—which allow us to examine behavioral adjustments following the policy shock. We focus on urban residents because Top 1,000 firms are primarily large nonagricultural employers, implying that urban households were most directly exposed to the program. This focus is later corroborated by our heterogeneity analysis in Section 4.3.

Health outcomes are drawn from multiple mortality sources. Our baseline analysis uses annual prefecture-level mortality rates from the *China Regional Statistical Yearbook* for 1999-2011 (NBS 2000-2012). We supplement these data with cancer mortality for years 1990-1992, 2004-2005, and 2014 from CHCAMS (2017), which combines national retrospective cause-of-death surveys, cancer registries, and the Disease Surveillance Points system.[8] We focus on lung cancer, the fourth leading cause of death in 2013 (Zhou et al. 2016), as the most pollution-related disease. To further explore heterogeneity, we collect province-by-gender level cause-of-death data for 1990 and 2013 from the 2013 Global Burden of Disease Study (Zhou et al. 2016), as well as mortality by region, gender, and age data from the 2000 and 2010 population censuses (NBS 2000, 2010).[9]

[6]We focus on unregulated firms in the same industries in Panel D, because the sampling scheme of pollution data, as detailed in Appendix A.1, prevents us from credibly estimating pollution intensity for clean industries.

[7]Unlike the Shen et al. (2024) $PM_{2.5}$ dataset, AOD data are not calibrated with self-reported pollution readings, which may suffer from misreporting (Ghanem and Zhang 2014; Greenstone et al. 2022). Alternative sources such as MERRA-2 SO_2 concentrations are available only at a coarser resolution ($0.5^\circ \times 0.625^\circ$).

[8]The original data are provided at the county level, which we aggregate to the prefecture level using simple averages.

[9]Except for the prefecture-level mortality from the regional yearbook, all mortality data are age-adjusted.

4 Results

4.1 Misallocation and Missing Environmental Improvement

To study how the Top 1,000 Program reshaped the spatial allocation of production, labor, and pollution within local markets, we first characterize the areas directly exposed to the regulation. Using grid-cell aggregates, we compare cells hosting regulated firms with others in the same prefecture. Panels A and B of Figure 2 show that grid cells hosting regulated firms were cleaner—in the sense of lower pollution intensity—and had higher skill-adjusted wages, consistent with the productivity and environmental premiums of regulated firms documented in Panels B-D of Figure 1. Moreover, within prefectures, pollution intensity increases and skill-adjusted wages decline with distance from grid cells hosting regulated firms, indicating a pronounced spatial gradient in economic activity and environmental conditions.

We next examine how this spatial structure responds to the introduction of the Top 1,000 Program. Specifically, we use our grid cell level panel to estimate:

$$Y_{it} = \sum_{\tau \neq 2005} \beta_\tau (\text{Top } 1{,}000_i \times \text{Year}_t) + \boldsymbol{\gamma}' \boldsymbol{x}_{it} + \varepsilon_{it}, \tag{1}$$

where the dependent variable is the outcome for grid cell i in year t, and the treatment variable Top $1{,}000_i$ is a dummy that equals one if grid cell i hosts at least one Top 1,000 firm and zero otherwise. The control vector $\boldsymbol{x}_{it}$ includes grid cell fixed effects and prefecture-by-year fixed effects, so that the coefficients β_τ's only collect *relative* changes within prefectures. Without further notice, in all of the following regressions we cluster the standard errors ε_{it} at prefecture level to allow for arbitrary serial correlation and spatial correlation within prefectures.

Panel C of Figure 2 plots the estimation results. The coefficients fluctuate around zero and are not statistically significant before the program began, but have decreased gradually since 2006. On average, the program reduced AOD level around the regulated firm by 0.6 percent. Given that pollution disperses spatially and that satellite-based AOD is measured with error, this effect is economically meaningful. Motivated by recent environmental studies emphasizing the role of wind in pollution transport (Deryugina et al. 2019; Anderson 2020), Panel A of Appendix Table G.3 further shows that grid cells downwind of Top 1,000 firms also experienced a 0.4 percent relative decline in AOD, while upwind cells exhibit no significant change.

To discern whether this reduction in pollution is due to reduced production, Panel D of Figure 2 plots the event study on labor. The figure shows that prior to the regulation, regulated firms were actually expanding their employment compared with other firms within the same prefecture. However, employment started to drop drastically after the regulation. On average, employment around the regulated firms reduced by 19 percent.[10] Furthermore, Panel B of Appendix Table G.3 shows no systematic labor reallocation associated with wind patterns, indicating that the air-quality improvements observed in downwind areas are driven by regulation on Top 1,000 firms. Appendix Figure G.8 provides additional evidence on reduced industrial activities by plotting the event study on the number of days with satellite-detected active thermal anomalies, an indicator for heat release such as power generation and cement production (Xia et al. 2018; Yang et al.

[10]Due to the presence of pre-trends, the coefficients need to be treated with caution. Following the best recommendation of the literature, we plot fixed length confidence intervals (FLCIs) following the approach of Rambachan and Roth (2023) in Appendix Figure G.7. We show that we can still find significant decrease in labor if allowing for violations of parallel trends that are approximately linear. If any, we might have under-estimated the program effect.

2024).[11] Consistently, we find that the days of active thermal anomalies around these regulated firms decreased significantly after the program.

Next, we examine the aggregate effect of the program by moving attention to changes at prefecture level. Specifically, we perform event studies using

$$Y_{dt} = \sum_{\tau \neq 2005} \beta_\tau (\text{Top 1,000 share}_d \times \text{Year}_t) + \boldsymbol{\gamma}' \boldsymbol{x}_{dt} + \varepsilon_{dt}, \tag{2}$$

which is analogous to specification (1) except that we replace the exposure measure with baseline share of employment in Top 1,000 firms relative to total industrial employment in the prefecture, Top 1,000 share$_d$. Intuitively, the measure captures the importance of these regulated firms for local labor markets. We further show in Appendix F that the measure is consistent with a model of regulation and misallocation in the spirit of Hsieh and Klenow (2009). The control vectors $\boldsymbol{x}_{dt}$ include prefecture effects and province-by-year fixed effects, which absorb any time-invariant prefecture-level unobservables or province-by-year level shocks.

Panels E and F of Figure 2 report the estimated coefficients. Both panels show that, despite reallocation of pollution and labor within prefectures, the effects at aggregate level were very small. Given the mean Top 1,000 share being 11.7%, we estimate a 0.39 (0.117×0.034) percent decrease in prefecture-level average AOD and 0.7 percent (0.117×0.059) decrease in aggregate employment, both of which are not statistically different from zero.[12] The lack of aggregate effect suggests that the direct emission reduction from the contraction of regulated cells were offset by the reallocation of activity toward unregulated cells, whose higher pollution intensities ((Panel A of Figure 2) neutralized the program's local environmental benefits.

The Appendixes explore the robustness of these results. Appendix Figure G.9 shows that the null of environmental improvement is robust to using alternative measures of sulfur dioxide (SO_2) and $PM_{2.5}$ concentration, or using total industrial SO_2 emission and energy consumption. Appendix Table G.6 confirms that *population-weighted* pollution exposure neither changed.[13] In Appendix C, we use micro data on major polluting firms and provide direct evidence that unregulated firms in more exposed prefectures significantly increased their energy use and SO_2 emission after the program began (Appendix Figure G.11). However, Appendix Figure G.12 shows that there is no change in regulation stringency of local governments, measured using a text-based approach based on annual local government reports (Panels A and B)[14] or using total environmental penalties (Panels C and D). The lack of government responses helps to rule out the alternative explanation that local governments endogenously loosened their regulation on other firms to mitigate the economic loss due to the program.

Taken together, in the presence of a spatial gradient in pollution intensity, contractions among regulated firms reallocated production away from relatively cleaner locations within the same prefecture, helping explain the missing aggregate environmental improvement. In terms of labor, employment declined in more productive firms and higher-skill-wage locations and expanded in relatively less productive, lower-wage ones. Such misallocation could reduce aggregate income, which we examine in the next section through its implications for households.

[11] We obtain the data from MODIS Version 6 Global Monthly Fire Location Product (NASA 2025). Additional details are provided in Appendix A.4.

[12] By contrast, if employment layoff of regulated firms were not off-set by expansion of other firms, one would expect a 2.2 (0.117×0.189) percent decrease in prefecture industrial employment.

[13] See Appendix E.1 for details of implementation.

[14] This approach is standard and widely adopted in the environment literature (Chen et al. 2018a,b; Li et al. 2026). Details on the measurement is provided in Appendix A.6.

4.2 Household Responses

We use micro data from UHS to examine whether labor misallocation translated into income losses and lower living standards. We perform event studies analogous to specification (2), except that we use individual or household level observations.[15] In what follows, we frequently summarize the magnitude of the estimated effects for an averagely exposed prefecture by scaling the difference-in-differences coefficients by the mean exposure intensity 11.7%.

Panel A of Figure 3 shows the event study on individual work status. Consistent with the finding in the previous section, we find no significant change in work status, suggesting that workers are reallocated rather than laid off. However, Panel B shows that households' living standard became worse off: household in the averagely exposed prefecture experienced decrease in real expenditure by 1.9 percent. The effect might appear large compared with the documented labor reallocation in the last section. Given the fact that regulated firms paid twice as much as unregulated firms (Panel C of Figure 1), and the industrial sector accounts for 40 percent of non-agricultural employment, a back-of-envelope calculation implies a decrease in income by 0.4 percent ($0.117 \times 0.189 \times 0.5 \times 0.4$). The gap between these the observed income decrease and the back-of-envelope calculation might be explained by the fact that regulated firms are all very upstream firms central to the whole production network.[16] Therefore, the increased cost could propagate through the production network (Acemoglu et al. 2012; Liu 2019) and result in much larger income shock.[17]

Reduced income might squeeze out health expenditure if health is a superior good (Hall and Jones 2007; Acemoglu et al. 2013). Therefore, Panels C and D of Figure 3 plot event studies on preventive and curative medical spendings respectively. Specifically, the UHS reports total medical and health spending, as well as six sub-categories: medical equipment, health care appliances, pharmaceuticals, nutraceuticals, medical treatment, and other medical expenses. We classify nutraceuticals, pharmaceuticals, and health care appliances as preventive spending, and all other sub-categories as curative spending. We conjecture the former is more income-elastic but morbidity-insensitive, while the later might reflect a mix of income and morbidity.

Results in Panel C show that households in the averagely exposed prefecture reduced annual preventive medical spending by 47.3 RMB, a 4.4 percent decrease given the pre-policy mean 1063.85 RMB. The larger decrease in preventive spending also suggests the policy reduced the expenditure share, i.e. households are moving downward along the Engel curve, which we confirm in Appendix Figure G.14. By contrast, Panel D shows that the average household increased curative spending by 17.17 RMB, a 3.5 percent increase given the pre-policy mean 494.72 RMB. As shown in Appendix Figure G.14, the bulk of increase is due to increase in medical treatment expenditure, likely reflecting an increase in morbidity. Together, we estimate that total medical and health spending decreased by 1.9 percent $((47.3 - 17.17)/(1063.85 + 494.72))$, yielding an income elasticity approximately one, consistent with the estimate of Acemoglu et al. (2013).

Finally, Panels E and F examine households' electricity use (physical units) and air-conditioner ownership, important defensive spending to weather shocks highlighted by Deschênes and Green-

[15] We further control for individual or household demographics. In individual level analysis, we control for age, gender, ethnicity, and years of education. In household level analysis, we control for the same set of demographics of the household head.

[16] Appendix Figure G.13 visualizes the upstremaness of these regulated firms using the method of Antràs et al. (2012).

[17] Similar findings are documented in Fieler et al. (2018) and Demir et al. (2023), who use data and theory to show that firm-to-firm production network and endogenous quality choices could amplify export shocks by up to ten times.

stone (2011) and Barreca et al. (2016).[18] We find households reduced electricity use by 2.2 percent and air-conditioner ownership by 0.7 percentage points, suggesting that households might become more vulnerable to temperature shocks after the program. We return to this point later in next section.

4.3 Mortality Effects

The endpoint analysis of this paper examines the health consequences, the ultimate focus of environmental policies. Because many of our mortality data also span the Top 10,000 program initiated in 2012, we augment specification (2) with year fixed effects interacted with employment shares of Top 10,000 firms. Furthermore, because our heterogeneity analysis uses province level data, we only control for region-by-year fixed effects in baseline specifications.[19] Appendix Figure G.19 presents results with province-by-year fixed effects and confirms that results change mildly.

The main threat to our difference-in-differences strategy is that exposure to the Top 1,000 program may be correlated with heterogeneous trends. To address this concern, in addition to our parsimonious baseline specification, we estimate more flexible specifications that allow year fixed effects to vary with a set of baseline prefecture characteristics. These characteristics include the urban population share; the shares of the population aged 0-15 and aged 65 or above; the infant mortality rate; an indicator for Top 1,000 prefectures; an indicator for inclusion in the *Two Control Zones*; and the employment share of *National Specially Monitored Firms*. Together, these interactions absorb differential time trends associated with urbanization, age structure, baseline health conditions, exposure intensity, and concurrent environmental regulations (Chen et al. 2018a; Zhang et al. 2018). Appendix D.1 provides additional details and discussion.[20]

Panel A of Figure 4 plots the event study on (the log of) all-cause mortality rate. The figure shows that prefectures exhibit similar trends before the policy began in 2006, followed by a noticeable increase afterward. Panel B of Figure 4 shows that lung cancer—one of the most air pollution-relevant diseases—exhibits similar patterns, which is consistent with our earlier finding of null environmental improvement.[21] Results are reasonably stable across specifications: in the averagely exposed prefecture, all-cause mortality and lung cancer mortality increased by 2.3-2.9 percent and 2.8-3.1 percent respectively.

Amplified mortality-climate shock gradient. Recent literature on climate change highlights the role of income in mitigating the harm of extreme temperatures (Barreca et al. 2016; Carleton et al. 2022). Motivated by this literature, we next estimate the interaction between the Top 1,000 Program and temperature shocks:

$$Y_{dt} = \sum_{\tau \neq 2004} \beta_\tau (\text{Top 1,000 share}_d \times \text{Year}_t) + \sum_k \sum_{\tau \neq 2004} \beta_\tau^k (\text{TBin}_{dt}^k \times \text{Top 1,000 share}_d \times \text{Year}_t) + \boldsymbol{\gamma}' \boldsymbol{x}_{dt} + \varepsilon_{dt}, \quad (3)$$

[18] The air-conditioner commonly used in China is a split AC system that can generate both cool and hot air.

[19] "Region" is a conventional partition of prefectures and provinces by location and is defined by the first digit of prefecture/province codes. It's similar to "census division" in the US.

[20] Appendix Figure G.16 confirms our earlier results on households are robust to controlling for these heterogeneous trends.

[21] While lung cancer is strongly associated with smoking, our evidence from the UHS data shows no significant changes in tobacco or alcohol consumption (Appendix Figure G.15). This suggests that the observed increase in mortality is likely driven by the more general mechanisms identified in this paper.

where we introduce a triple interaction term between number of days in temperature bin k, TBin_{dt}^{k}, with Top 1,000 share and year dummies. The coefficients β_{τ}^{k} capture how the mortality-temperature gradient changes following the implementation of the program. To address the omitted-variable bias highlighted by Feigenberg et al. (2025), we include the full set of lower-order terms, namely temperature bins themselves and their interactions with the Top 1,000 share and year indicators. We consider two temperature bins—"30°C or above" for hot days and "below 0°C" for cold days—for parsimony, and we add more temperature bins in Appendix Figure G.18.[22]

Panels C and D of Figure 4 show the estimation results. Panel C shows that the association between mortality and hot days remained flat before the policy, but rose sharply after the policy began. On average, the mortality-hot-days gradient increases by 0.21-0.24 percentage points in the averagely exposed prefecture, corresponding to a roughly 30% increase relative to the baseline gradient estimated in Yu et al. (2019). Panel D shows that the effect was asymmetric: there was no economically meaningful change in the association between mortality and cold days, possibly reflecting the mitigating role of China's winter heating policy (Ebenstein et al. 2017). The heterogeneous mortality response by temperature is clearer in Appendix Figure G.17, where we present monthly event studies using population census data.[23] The figure shows that mortality response is most pronounced in summer when the temperature is high, and there is no significant mortality effect in other cooler days. Appendix Figure G.18 confirms that our estimates are robust to controlling for other weather co-variates like humidity, wind speed, precipitation, or pollution level, or to interact the policy variable with more temperature bins.

Estimating temperature-mortality gradients helps isolate the underlying mechanism. Unlike channels such as emission reallocation or healthcare supply responses—which are unlikely to selectively amplify heat-related vulnerability—an intensified heat gradient points toward reduced household capacity for self-protection. This interpretation is supported by our evidence of declining electricity consumption and air-conditioner ownership, as well as the concentration of excess mortality in heat-sensitive causes documented in the heterogeneity analysis.

Heterogeneity. We decompose the overall increase in mortality by cause of death and demographic group using province-by-gender-level Global Burden of Disease (GBD) data from Zhou et al. (2016) and population census tabulations from NBS (2000, 2010). Because baseline mortality rates differ substantially across causes and demographic groups, we focus on each subgroup's share of total excess deaths, following the decomposition approach of Finkelstein et al. (2025). The underlying difference-in-differences estimates are reported in Appendix Figure G.25, with additional details provided in Appendix D.2.

Figure 5 presents the decomposition results together with each subgroup's baseline share of deaths. Panel A shows that the three leading causes of death—cardiovascular diseases, neoplasms, and chronic respiratory diseases—account for 92.3% of total excess deaths. These causes are all known to be strongly associated with heat exposure in prior work (e.g., Barreca (2012); Carleton et al. (2022)). Panels B-D document substantial heterogeneity across demographic groups: excess deaths are concentrated among urban residents (Panel B), males (Panel C), and individuals of working age as well as the elderly (Panel D). These patterns are consistent with the fact that regulated firms are major local employers and that older populations are particularly vulnerable to heat-related health risks.

[22] Nevertheless, we control for the whole set of temperature bins in the control vector: below 0°C, 0-5°C, 5-10°C, 10-15°C, 15-20°C, 20-25°C, and 30°C or above.

[23] Each census wave, which is conducted in November 1st of the survey year, reports deaths by month in the past year.

Robustness. We conduct a broad set of robustness checks, described in detail in Appendix D. Our results are robust to controlling for a wide range of additional heterogeneous trends, to alternative measures of exposure, weighting schemes, and inference procedures (Appendix D.1), to aggregation at the province level that accounts for spatial spillovers and migration (Appendix D.2), and to analyses using individual-level panel data on mortality and health outcomes (Appendix D.3).

Magnitude. Our estimates imply a steep mortality-income gradient: an average income contraction of 1.9 percent is associated with a 2.3 to 2.9 percent increase in mortality, corresponding to an elasticity between 1.2 and 1.5 in absolute value.[24] It is important to interpret this magnitude in light of the type of income variation we study. Our setting captures a negative and potentially persistent income shock, rather than marginal or transitory income gains. In this respect, our estimates are not directly comparable to canonical gradients derived from cross-country or individual-level correlations, which typically range from 0.2 to 0.4 (Pritchett and Summers 1996; Deaton 2003), or to studies examining positive income shocks such as cash transfers (Walker et al. 2024; Richterman et al. 2025; Barham and Rowberry 2013) and pension expansions (Aizer et al. 2016; Huang and Zhang 2021), which generally find elasticities between 0.3 and 0.8. By contrast, studies focusing on negative economic shocks—settings more comparable to ours—document substantially larger mortality responses, with estimated elasticities ranging from 0.60 to 1.54 (Sullivan and von Wachter 2009; Adda and Fawaz 2020; Schwandt and Von Wachter 2019; Burgess et al. 2017; Xiao et al. 2024; Bellemare et al. 2025; Walker et al. 2024). Seen through this lens, our estimates lie toward the upper end of the existing literature but remain well within the range implied by recent evidence on the health consequences of adverse income shocks (see Appendix Table G.5).

Alternative Explanations. We discuss whether factors outside our proposed misallocation framework could account for the rise in mortality in Appendix E. Using granular township-level data, we rule out the possibility that the mortality increase was driven by changes in pollution exposure or internal population sorting (Appendix Tables G.6 and G.7). We also examine the healthcare supply channel and find that while the program led to a decline in the number of doctors, this reduction does not meaningfully account for the observed mortality response (Appendix Table G.8). Finally, we provide more direct evidence supporting the income mechanism by showing that the program-induced deaths predominantly occurred at home (Appendix Figure G.30) and were exclusively concentrated among individuals lacking medical insurance (Appendix Table G.9), a pattern consistent with a scenario where reduced affordability of formal care drives health deterioration.

5 Concluding Remarks

This paper shows that China's *Top 1,000 Program*, the world's largest size-dependent conservation initiative, unexpectedly increased mortality in more exposed regions. Despite targeting the nation's largest energy users, the program failed to improve environmental quality and instead reduced household income, leading to lower preventive health spending and greater vulnerability

[24] These estimates are likely upper bounds given data limitations, as the calculation relies on income contractions measured over the short run (through 2009). As shown in Panel B of Figure 3, the negative effects on household expenditure continue to intensify over time; incorporating potentially larger or more persistent income losses in 2010-2011 would raise the average income contraction over the full horizon.

to temperature shocks. These results highlight how size-based regulations can generate welfare losses through both misallocation and negative income effects, even when aggregate emissions remain unchanged.

Our findings underscore that the design of environmental policy matters as much as its ambition. Threshold-based regulation that targets only large firms can distort resource allocation and weaken welfare. We believe few economists would view our results as an argument against energy regulation itself, but rather as evidence that policy design and implementation deserve greater attention. We hope these findings will provide new perspective for policymakers seeking to reconcile climate objectives with economic efficiency and human well-being.

References

Acemoglu, Daron, Amy Finkelstein, and Matthew J. Notowidigdo, "Income and Health Spending: Evidence from Oil Price Shocks," *Review of Economics and Statistics*, 2013, *95* (4), 1079–1095.

_ , Vasco M. Carvalho, Asuman Ozdaglar, and Alireza Tahbaz-Salehi, "The Network Origins of Aggregate Fluctuations," *Econometrica*, 2012, *80* (5), 1977–2016.

Adda, Jérôme and Yarine Fawaz, "The health toll of import competition," *Economic Journal*, 2020, *130* (630), 1501–1540.

Aizer, Anna, Shari Eli, Joseph Ferrie, and Adriana Lleras-Muney, "The long-run impact of cash transfers to poor families," *American Economic Review*, 2016, *106* (4), 935–971.

Anderson, Michael L., "As the Wind Blows: The Effects of Long-Term Exposure to Air Pollution on Mortality," *Journal of the European Economic Association*, 2020, *18* (4), 1886–1927.

Antràs, Pol, Davin Chor, Thibault Fally, and Russell Hillberry, "Measuring the Upstreamness of Production and Trade Flows," *American Economic Review*, 2012, *102* (3), 412–16.

Atkin, David, Baptiste Bernadac, Dave Donaldson, Tishara Garg, and Federico Huneeus, "The Incidence of Distortions," Technical Report 2025.

Banerjee, Abhijit, Esther Duflo, and Garima Sharma, "Long-Term Effects of the Targeting the Ultra Poor Program," *American Economic Review: Insights*, 2021, *3* (4), 471–86.

Baqaee, David Rezza and Emmanuel Farhi, "Productivity and Misallocation in General Equilibrium," *Quarterly Journal of Economics*, 2020, *135* (1), 105–163.

Barham, Tania and Jacob Rowberry, "Living longer: The effect of the Mexican conditional cash transfer program on elderly mortality," *Journal of Development Economics*, 2013, *105*, 226–236.

Barreca, Alan I., "Climate change, humidity, and mortality in the United States," *Journal of Environmental Economics and Management*, 2012, *63* (1), 19–34.

_ , Karen Clay, Olivier Deschênes, Michael Greenstone, and Joseph S. Shapiro, "Adapting to climate change: The remarkable decline in the US temperature-mortality relationship over the twentieth century," *Journal of Political Economy*, 2016, *124* (1), 105–159.

Becker, Randy and Vernon Henderson, "Effects of Air Quality Regulations on Polluting Industries," *Journal of Political Economy*, 2000, *108* (2), 379–421.

Bellemare, Marc F., Jhih-Yun Liu, and Joleen Hadrich, "Commodity Revenue Shocks and Mortality," *Journal of Human Resources*, December 2025. Published online before print.

Berman, Eli and Linda T. M. Bui, "Environmental regulation and labor demand: evidence from the South Coast Air Basin," *Journal of Public Economics*, 2001, *79* (2), 265–295.

Bretschger, Lucas and Ara Jo, "Complementarity between labor and energy: A firm-level analysis," *Journal of Environmental Economics and Management*, 2024, *124*, 102934.

Burgess, Robin, Olivier Deschenes, Dave Donaldson, and Michael Greenstone, "Weather, Climate Change and Death in India," Working Paper, Energy Policy Institute at the University of Chicago 2017.

Carleton, Tamma, Amir Jina, Michael Delgado, Michael Greenstone, Trevor Houser, Solomon Hsiang, Andrew Hultgren, Robert E. Kopp, Kelly E. McCusker, Ishan Nath, James Rising, Ashwin Rode, Hee Kwon Seo, Arvid Viaene, Jiacan Yuan, and Alice Tianbo Zhang, "Valuing the Global Mortality Consequences of Climate Change Accounting for Adaptation Costs and Benefits," *Quarterly Journal of Economics*, 2022, *137* (4), 2037–2105.

Carrillo, Paul, Dave Donaldson, Dina Pomeranz, and Monica Singhal, "Misallocation

in Firm Production: A Nonparametric Analysis Using Procurement Lotteries," Working Paper 31311, National Bureau of Economic Research November 2023.

Chandra, Amitabh and Douglas O. Staiger, "Identifying Sources of Inefficiency in Healthcare," *The Quarterly Journal of Economics*, 2020, *135* (2), 785–843.

_ , Carrie H. Colla, and Jonathan S. Skinner, "Productivity Variation and Input Misallocation: Evidence from Hospitals," Working Paper 31569, National Bureau of Economic Research August 2023.

Chay, Kenneth, Carlos Dobkin, and Michael Greenstone, "The Clean Air Act of 1970 and Adult Mortality," *Journal of Risk and Uncertainty*, 2003, *27* (3), 279–300.

Chay, Kenneth Y. and Michael Greenstone, "Air Quality, Infant Mortality, and the Clean Air Act of 1970," Working Paper 10053, National Bureau of Economic Research October 2003.

CHCAMS, "Nationwide County-Level Cancer Mortality Rates (1973–1975, 1990–1992, 2004–2005, 2014)," Cancer Hospital, Chinese Academy of Medical Sciences 2017.

Chen, Qiaoyi, Zhao Chen, Zhikuo Liu, Juan Carlos Suárez Serrato, and Daniel Yi Xu, "Regulating Conglomerates: Evidence from an Energy Conservation Program in China," *American Economic Review*, 2025, *115* (2), 408–47.

Chen, Yvonne Jie, Pei Li, and Yi Lu, "Career concerns and multitasking local bureaucrats: Evidence of a target-based performance evaluation system in China," *Journal of Development Economics*, 2018, *133*, 84–101.

Chen, Zhao, Matthew E. Kahn, Yu Liu, and Zhi Wang, "The consequences of spatially differentiated water pollution regulation in China," *Journal of Environmental Economics and Management*, 2018, *88*, 468–485.

Copeland, Brian R., Joseph S. Shapiro, and M. Scott Taylor, "Chapter 2 - Globalization and the environment," in Gita Gopinath, Elhanan Helpman, and Kenneth Rogoff, eds., *Handbook of International Economics*, Vol. 5, Elsevier, 2022, pp. 61–146.

Cui, Jingbo, Chunhua Wang, Junjie Zhang, and Yang Zheng, "The effectiveness of China's regional carbon market pilots in reducing firm emissions," *Proceedings of the National Academy of Sciences*, 2021, *118* (52), e2109912118.

Curt, E. Mark, Weiting Miao, Felix Samy Soliman, Juan Carlos Suárez Serrato, and Daniel Yi Xu, "The Geographic Leakages of Environmental Regulations: Evidence from the Clean Air Act," Technical Report 2025.

da Hora, Jefferson and Paulo Vaz, "Green Misallocation: Allocative Efficiency and Air Pollution," Technical Report 2024.

De Gouvello, Christophe, Robert Taylor, and Yanqin Song, "China: 40-Year Experience in Energy Efficiency Development-Policies, Achievements, and Lessons Learned," 2021.

Deaton, Angus, "Health, Inequality, and Economic Development," *Journal of Economic Literature*, 2003, *41* (1), 113–158.

Dell, Melissa, Benjamin F. Jones, and Benjamin A. Olken, "Temperature Shocks and Economic Growth: Evidence from the Last Half Century," *American Economic Journal: Macroeconomics*, 2012, *4* (3), 66–95.

Demir, Banu, Ana Cecília Fieler, Daniel Yi Xu, and Kelly Kaili Yang, "O-Ring Production Networks," *Journal of Political Economy*, 2023, *132* (1), 200–247.

Deryugina, Tatyana, Garth Heutel, Nolan H. Miller, David Molitor, and Julian Reif, "The Mortality and Medical Costs of Air Pollution: Evidence from Changes in Wind Direction," *American Economic Review*, 2019, *109* (12), 4178–4219.

Deschênes, Olivier and Michael Greenstone, "Climate change, mortality, and adaptation: Evidence from annual fluctuations in weather in the US," *American Economic Journal: Applied*

Economics, 2011, *3* (4), 152–185.

_ , _ , and Joseph S. Shapiro, "Defensive Investments and the Demand for Air Quality: Evidence from the NOx Budget Program," *American Economic Review*, 2017, *107* (10), 2958–89.

Ebenstein, Avraham, Maoyong Fan, Michael Greenstone, Guojun He, and Maigeng Zhou, "New evidence on the impact of sustained exposure to air pollution on life expectancy from China's Huai River Policy," *Proceedings of the National Academy of Sciences*, 2017, *114* (39), 10384–10389.

Edmond, Chris, Virgiliu Midrigan, and Daniel Yi Xu, "How Costly Are Markups?," *Journal of Political Economy*, 2023, *131* (7), 1619–1675.

Fan, Jingting and Ben Zou, "Industrialization from scratch: The "Construction of Third Front" and local economic development in China's hinterland," *Journal of Development Economics*, 2021, *152*, 102698.

Fan, Maoyong, Hanchen Jiang, and Maigeng Zhou, "Beyond particulate matter: New evidence on the causal effects of air pollution on mortality," *Journal of Health Economics*, 2023, *91*, 102799.

Feigenberg, Benjamin, Ben Ost, and Javaeria A. Qureshi, "Omitted Variable Bias in Interacted Models: A Cautionary Tale," *Review of Economics and Statistics*, 2025, *107* (5), 1260–1274.

Fieler, Ana Cecília, Marcela Eslava, and Daniel Yi Xu, "Trade, Quality Upgrading, and Input Linkages: Theory and Evidence from Colombia," *American Economic Review*, 2018, *108* (1), 109–46.

Finkelstein, Amy, Matthew J. Notowidigdo, Frank Schilbach, and Jonathan Zhang, "Lives Versus Livelihoods: The Impact of the Great Recession on Mortality and Welfare," *Quarterly Journal of Economics*, 2025, *140* (3), 2269–2328.

Ghanem, Dalia and Junjie Zhang, "'Effortless Perfection:' Do Chinese cities manipulate air pollution data?," *Journal of Environmental Economics and Management*, 2014, *68* (2), 203–225.

Gray, Wayne B., Ronald J. Shadbegian, Chunbei Wang, and Merve Meral, "Do EPA regulations affect labor demand? Evidence from the pulp and paper industry," *Journal of Environmental Economics and Management*, 2014, *68* (1), 188–202.

Greenstone, Michael, "The Impacts of Environmental Regulations on Industrial Activity: Evidence from the 1970 and 1977 Clean Air Act Amendments and the Census of Manufactures," *Journal of Political Economy*, 2002, *110* (6), 1175–1219.

_ and Rema Hanna, "Environmental Regulations, Air and Water Pollution, and Infant Mortality in India," *American Economic Review*, 2014, *104* (10), 3038–72.

_ , Guojun He, Ruixue Jia, and Tong Liu, "Can Technology Solve the Principal-Agent Problem? Evidence from China's War on Air Pollution," *American Economic Review: Insights*, 2022, *4* (1), 54–70.

Guner, Nezih, Gustavo Ventura, and Yi Xu, "Macroeconomic implications of size-dependent policies," *Review of Economic Dynamics*, 2008, *11* (4), 721–744.

Hall, Robert E. and Charles I. Jones, "The Value of Life and the Rise in Health Spending," *Quarterly Journal of Economics*, 2007, *122* (1), 39–72.

He, Guojun, Shaoda Wang, and Bing Zhang, "Watering Down Environmental Regulation in China," *Quarterly Journal of Economics*, 2020, *135* (4), 2135–2185.

Heblich, Stephan, Marlon Seror, Hao Xu, and Yanos Zylberberg, "Industrial Clusters in the Long Run: Evidence from Million-Rouble Plants in China," Working Paper 30744, National Bureau of Economic Research December 2022.

Henderson, J. Vernon, "Effects of Air Quality Regulation," *American Economic Review*, 1996, *86* (4), 789–813.

Hsieh, Chang-Tai and Peter J. Klenow, "Misallocation and Manufacturing TFP in China and India," *Quarterly Journal of Economics*, 2009, *124* (4), 1403–1448.

Huang, Wei and Chuanchuan Zhang, "The Power of Social Pensions: Evidence from China's New Rural Pension Scheme," *American Economic Journal: Applied Economics*, 2021, *13* (2), 179–205.

Ke, Jing, Lynn Price, Stephanie Ohshita, David Fridley, Nina Zheng Khanna, Nan Zhou, and Mark Levine, "China's industrial energy consumption trends and impacts of the Top-1000 Enterprises Energy-Saving Program and the Ten Key Energy-Saving Projects," *Energy Policy*, 2012, *50*, 562–569.

Li, Taipeng, Lorenzo Trimarchi, Rui Xie, and Guohao Yang, "The unintended consequences of trade protection on the environment," *Journal of Development Economics*, 2026, *178*, 103547.

Liu, Ernest, "Industrial Policies in Production Networks," *Quarterly Journal of Economics*, 2019, *134* (4), 1883–1948.

Liu, Yun, Yifei Zhang, Yuxin Yang, and Xin Chen, "Dark side of environmental regulation: Wage inequality cost," *Journal of Comparative Economics*, 2023, *51* (2), 524–544.

Lyapustin, Alexei, Yujie Wang, and NASA MODAPS SIPS, "MCD19A2 MODIS/Terra + Aqua Aerosol Optical Thickness Daily L2G Global 1 km SIN Grid (Collection 6)," 2015.

MEP, "Environmental Survey and Reporting Database," Ministry of Environmental Protection 2002-2011.

NASA, "Fire Information for Resource Management System (FIRMS): Active Fire Data Attributes for MODIS and VIIRS," Technical Report, NASA Earth Science Data and Information System (ESDIS) Project, Goddard Space Flight Center 2025.

NBS, "Fifth National Population Census," National Bureau of Statistics 2000.

_ , "China Statistical Yearbook For Regional Economy," National Bureau of Statistics 2000-2012.

_ , "Annual Survey of Industrial Firms," National Bureau of Statistics 2001-2009.

_ , "Urban Household Survey (16 provinces)," National Bureau of Statistics 2002-2009.

_ , "First National Economic Census," National Bureau of Statistics 2004.

_ , "Sixth National Population Census," National Bureau of Statistics 2010.

NDRC, "Completion Status of Energy-Saving Targets for the Top 1,000 Enterprises During the 11th Five-Year Plan," Official announcement No. 31 December 2011. National Development and Reform Commission.

Nordhaus, William, *A Question of Balance: Weighing the Options on Global Warming Policies*, Yale University Press, 2008.

Ozaltun, Bora, Joseph S. Shapiro, and Reed Walker, "Size-Based Environmental Regulation: Evidence from Major Clean Air Act Thresholds," Technical Report 2025.

Price, Lynn, Xuejun Wang, and Jiang Yun, "The challenge of reducing energy consumption of the Top-1000 largest industrial enterprises in China," *Energy Policy*, 2010, *38* (11), 6485–6498.

Pritchett, Lant and Lawrence H. Summers, "Wealthier is Healthier," *Journal of Human Resources*, 1996, *31* (4), 841–868.

Qi, Ji, Xin Tang, and Xican Xi, "The Size Distribution of Firms and Industrial Water Pollution: A Quantitative Analysis of China," *American Economic Journal: Macroeconomics*, 2021, *13* (1), 151–83.

Raja, Chandni, "Regulating the Quality of Hospitals: Input Regulation, Factor Market Structure, and Misallocation in Healthcare." Ph.d. thesis, University of California, Los Angeles 2025.

Rambachan, Ashesh and Jonathan Roth, "A More Credible Approach to Parallel Trends," *Review of Economic Studies*, 2023, *90* (5), 2555–2591.

Restuccia, Diego and Richard Rogerson, "Policy distortions and aggregate productivity with heterogeneous establishments," *Review of Economic Dynamics*, 2008, *11* (4), 707–720.

Richterman, Aaron, Christophe Millien, Elizabeth F. Bair, Gregory Jerome, Jean Christophe Dimitri Suffrin, Jere R. Behrman, and Harsha Thirumurthy, "The effects of cash transfers on adult and child mortality in low- and middle-income countries," *Nature*, 2023, *618* (7965), 575–582.

_ , Tra-My Ngoc Bùi, Elizabeth F. Bair, Gregory Jerome, Christophe Millien, Jean Christophe Dimitri Suffrin, Jere R. Behrman, and Harsha Thirumurthy, "The effects of government-led cash transfer programmes on behavioural and health determinants of mortality: a difference-in-differences study," *Lancet*, 2025, *405* (10476), 483–494.

Ryan, Nicholas, "Energy Productivity and Energy Demand: Experimental Evidence from Indian Manufacturing Plants," Working Paper 24619, National Bureau of Economic Research May 2018.

Schlenker, Wolfram and Michael J. Roberts, "Nonlinear temperature effects indicate severe damages to U.S. crop yields under climate change," *Proceedings of the National Academy of Sciences*, 2009, *106* (37), 15594–15598.

Schwandt, Hannes and Till Von Wachter, "Socioeconomic Decline and Death: The Life-Cycle Impacts of Recessions for Labor Market Entrants," Working Paper 26638, National Bureau of Economic Research 2019.

Shen, Siyuan, Chi Li, Aaron van Donkelaar, Nathan Jacobs, Chenguang Wang, and Randall V. Martin, "Enhancing Global Estimation of Fine Particulate Matter Concentrations by Including Geophysical a Priori Information in Deep Learning," *ACS EST Air*, 2024, *1* (5), 332–345.

Somanathan, E., Rohini Somanathan, Anant Sudarshan, and Meenu Tewari, "The Impact of Temperature on Productivity and Labor Supply: Evidence from Indian Manufacturing," *Journal of Political Economy*, 2021, *129* (6), 1797–1827.

Sullivan, Daniel and Till von Wachter, "Job Displacement and Mortality: An Analysis Using Administrative Data," *Quarterly Journal of Economics*, 2009, *124* (3), 1265–1306.

Sun, Sicong, Jin Huang, Darrell L. Hudson, and Michael Sherraden, "Cash Transfers and Health," *Annual Review of Public Health*, 2021, *42*, 363–380.

Tanaka, Shinsuke, "Environmental regulations on air pollution in China and their impact on infant mortality," *Journal of Health Economics*, 2015, *42*, 90–103.

_ , Kensuke Teshima, and Eric Verhoogen, "North-South Displacement Effects of Environmental Regulation: The Case of Battery Recycling," *American Economic Review: Insights*, 2022, *4* (3), 271–88.

Tombe, Trevor and Jennifer Winter, "Environmental policy and misallocation: The productivity effect of intensity standards," *Journal of Environmental Economics and Management*, 2015, *72*, 137–163.

van Donkelaar, Aaron, Randall V. Martin, and Rokjin J. Park, "Estimating ground-level PM2.5 using aerosol optical depth determined from satellite remote sensing," *Journal of Geophysical Research: Atmospheres*, 2006, *111* (D21).

Walker, Michael W., Nick Shankar, Edward Miguel, Dennis Egger, and Grady Killeen, "Can Cash Transfers Save Lives? Evidence from a Large-Scale Experiment in Kenya," Working Paper 32204, National Bureau of Economic Research 2024.

Walker, W. Reed, "Environmental Regulation and Labor Reallocation: Evidence from the Clean

Air Act," *American Economic Review*, 2011, *101* (3), 442–47.

_ , "The Transitional Costs of Sectoral Reallocation: Evidence From the Clean Air Act and the Workforce," *Quarterly Journal of Economics*, 2013, *128* (4), 1787–1835.

Xia, Haiping, Yunhao Chen, and Jinling Quan, "A simple method based on the thermal anomaly index to detect industrial heat sources," *International Journal of Applied Earth Observation and Geoinformation*, 2018, *73*, 627–637.

Xiao, Na, Zhaohui Ye, Huijuan Li et al., "Associations of serial negative income shock and all-cause mortality: a longitudinal study in China," *BMJ Public Health*, 2024, *2* (1), e000414.

Yang, Lin, Yatang Lin, Jin Wang, and Fangyuan Peng, "Achieving Air Pollution Control Targets with Technology-Aided Monitoring: Better Enforcement or Localized Efforts?," *American Economic Journal: Economic Policy*, 2024, *16* (4), 280–315.

Yu, Xiumei, Xiaoyan Lei, and Min Wang, "Temperature effects on mortality and household adaptation: Evidence from China," *Journal of Environmental Economics and Management*, 2019, *96*, 195–212.

Zhang, Bing, Xiaolan Chen, and Huanxiu Guo, "Does central supervision enhance local environmental enforcement? Quasi-experimental evidence from China," *Journal of Public Economics*, 2018, *164*, 70–90.

Zhou, Maigeng, Haidong Wang, Jun Zhu, Wanqing Chen, Linhong Wang, Shiwei Liu, Yichong Li, Lijun Wang, Yunning Liu, Peng Yin, Jiangmei Liu, Shicheng Yu, Feng Tan, Ryan M. Barber, Matthew M. Coates, Daniel Dicker, Maya Fraser, Diego González-Medina, Hannah Hamavid, Yuantao Hao, Guoqing Hu, Guohong Jiang, Haidong Kan, Alan D. Lopez, Michael R. Phillips, Jun She, Theo Vos, Xia Wan, Gelin Xu, Lijing L. Yan, Chuanhua Yu, Yong Zhao, Yingfeng Zheng, Xiaonong Zou, Mohsen Naghavi, Yu Wang, Christopher J. L. Murray, Gonghuan Yang, and Xiaofeng Liang, "Cause-specific mortality for 240 causes in China during 1990-2013: a systematic subnational analysis for the Global Burden of Disease Study 2013," *Lancet*, 2016, *387* (10015), 251–272.

Zhou, Nan, Mark D. Levine, and Lynn Price, "Overview of current energy-efficiency policies in China," *Energy Policy*, 2010, *38* (11), 6439–6452.

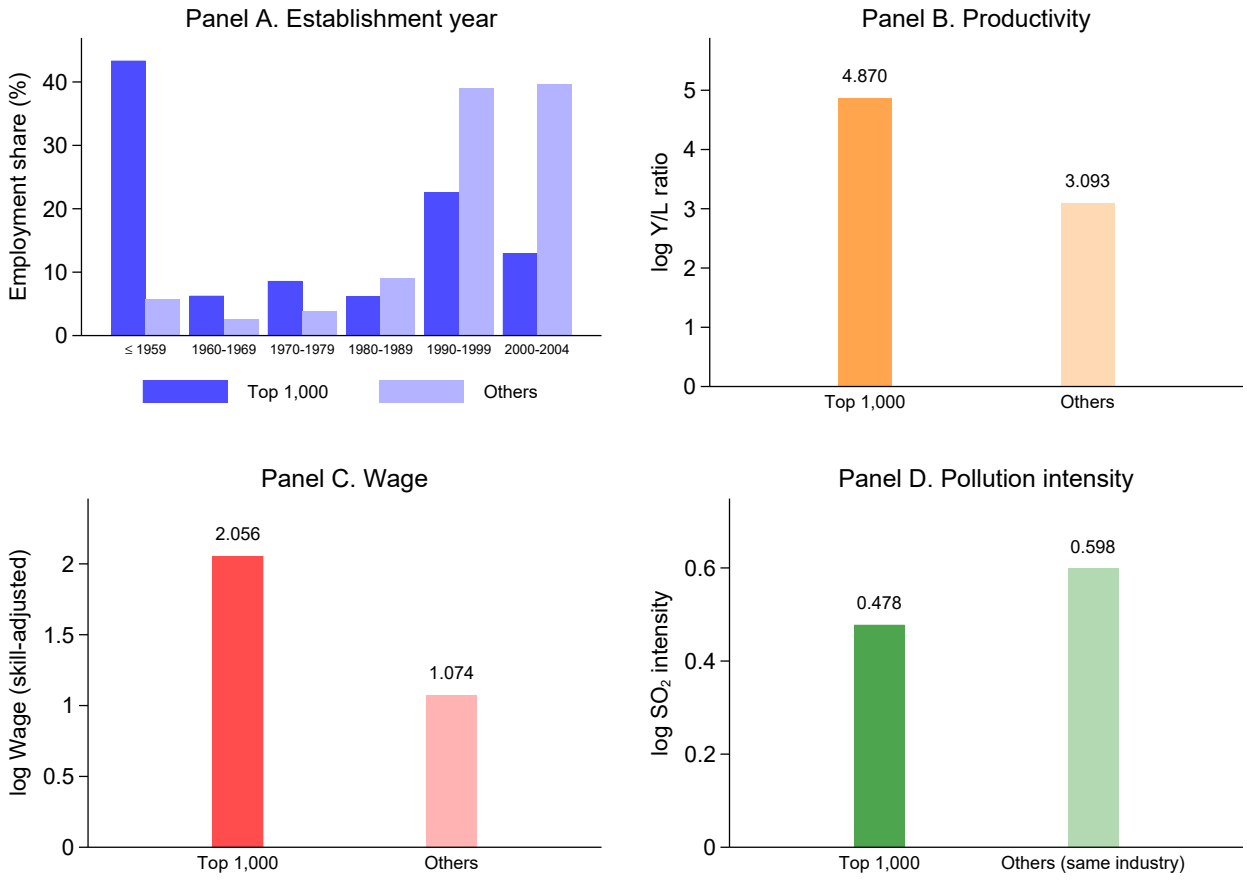


Figure 1: Top 1,000 versus Other Industrial Firms

Notes: Panel A shows the distribution of establishment years, while Panels B–D compare productivity, wages, and pollution intensity between Top 1,000 firms and other industrial firms. Log Y/L ratio is the logarithm of value added per worker; log Wage is the logarithm of payroll per (skill-adjusted) worker; and log SO_2 intensity is the logarithm of sulfur dioxide (SO_2) emissions per unit of output. The skill-adjusted number of workers in firm i is computed as $\widetilde{\text{Employment}}_i = \sum_{g=1}^{G} \text{Employment}_i^g \times \zeta_g$, where $\zeta_g = e^{0.1 \times x_g}$, and x_g denotes the years of education for group $g \in \{\text{middle school } (9), \text{high school } (12), \text{2-year college } (14), \text{bachelor } (16), \text{master } (18)\}$, assuming a Mincer-style 10% return to schooling. Panels A-C use data from the 2004 *Economic Census* (NBS 2004), and Panel D uses data from the 2004 *Environmental Survey and Reporting (ESR)* system (MEP 2002-2011). Pollution intensity in Panel D is computed within industries.
Sources: NBS (2004); MEP (2002-2011).

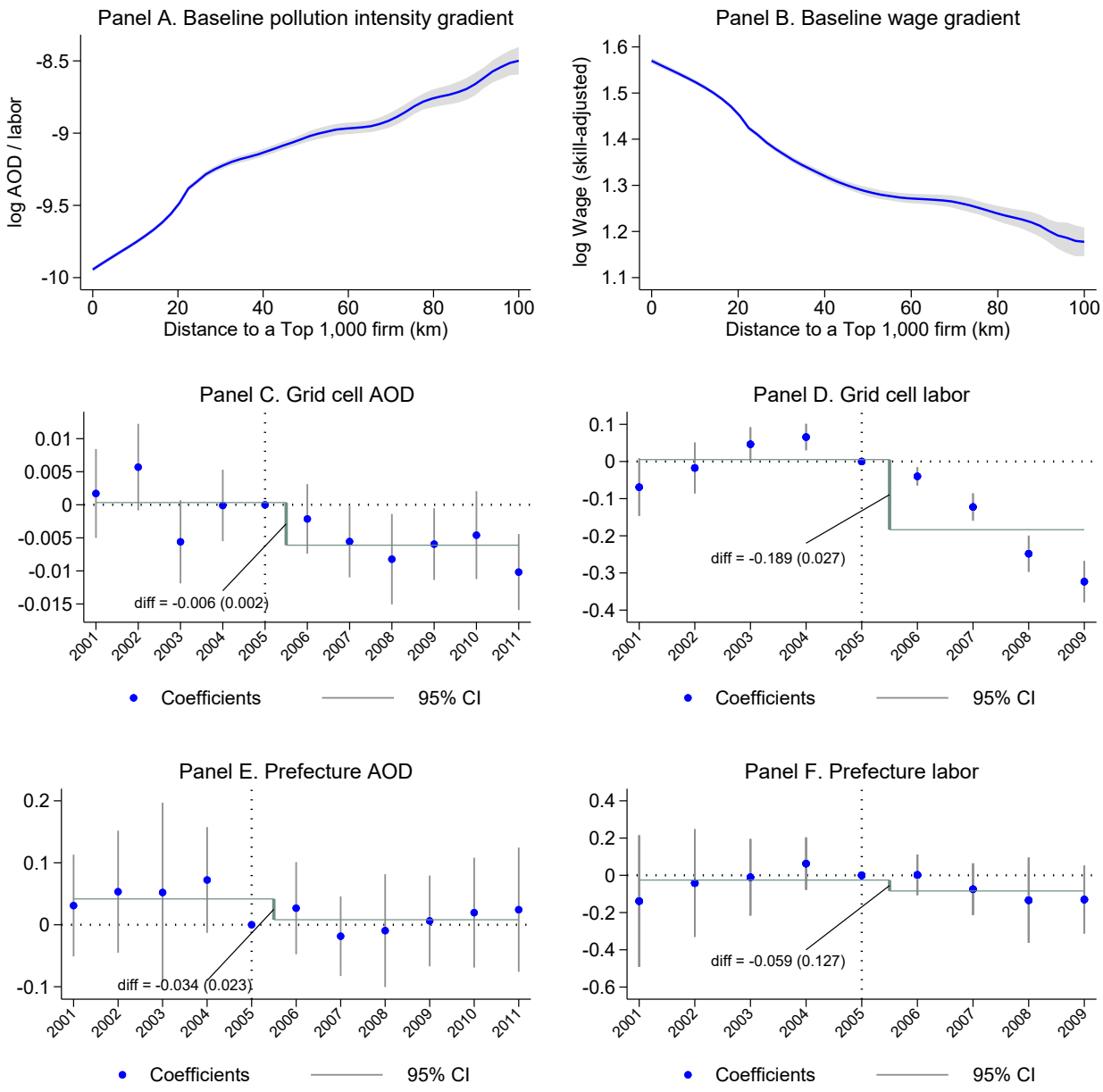


Figure 2: Baseline Spatial Patterns and Policy-Induced Reallocation

Notes: Panels A and B plot polynomial smooths of baseline outcomes in 2004 against the distance to the nearest Top 1,000 firm in the same prefecture. Panel A shows the log AOD per industrial worker, and Panel B shows the log skill-adjusted wage. Both series are estimated using an Epanechnikov kernel with a bandwidth of 10 km. The skill adjustment of wages follows the definition in Figure 1. Each observation is a $0.03° \times 0.03°$ grid cell (32,583 and 32,619 observations in Panels A and B, respectively). Panels C and D report grid-cell-level event-study estimates specification (1). The sample includes 393,439 (Panel C) and 320,943 (Panel D) grid cell-year observations. Regressions include grid cell fixed effects and prefecture-by-year fixed effects. Panels E and F present prefecture-level event studies specification (2), using 3,795 (Panel E) and 3,105 (Panel F) prefecture-year observations. These regressions include prefecture fixed effects and province-by-year fixed effects. The value labeled "diff" denotes the difference between post- and pre-policy means, computed from the event-study coefficients using the Delta method. These estimates may differ slightly from those obtained from a standard difference-in-differences specification. For Panels C-F, 95% confidence intervals are based on standard errors clustered at the prefecture level.
Sources: Lyapustin et al. (2015); NBS (2004, 2001-2009a).

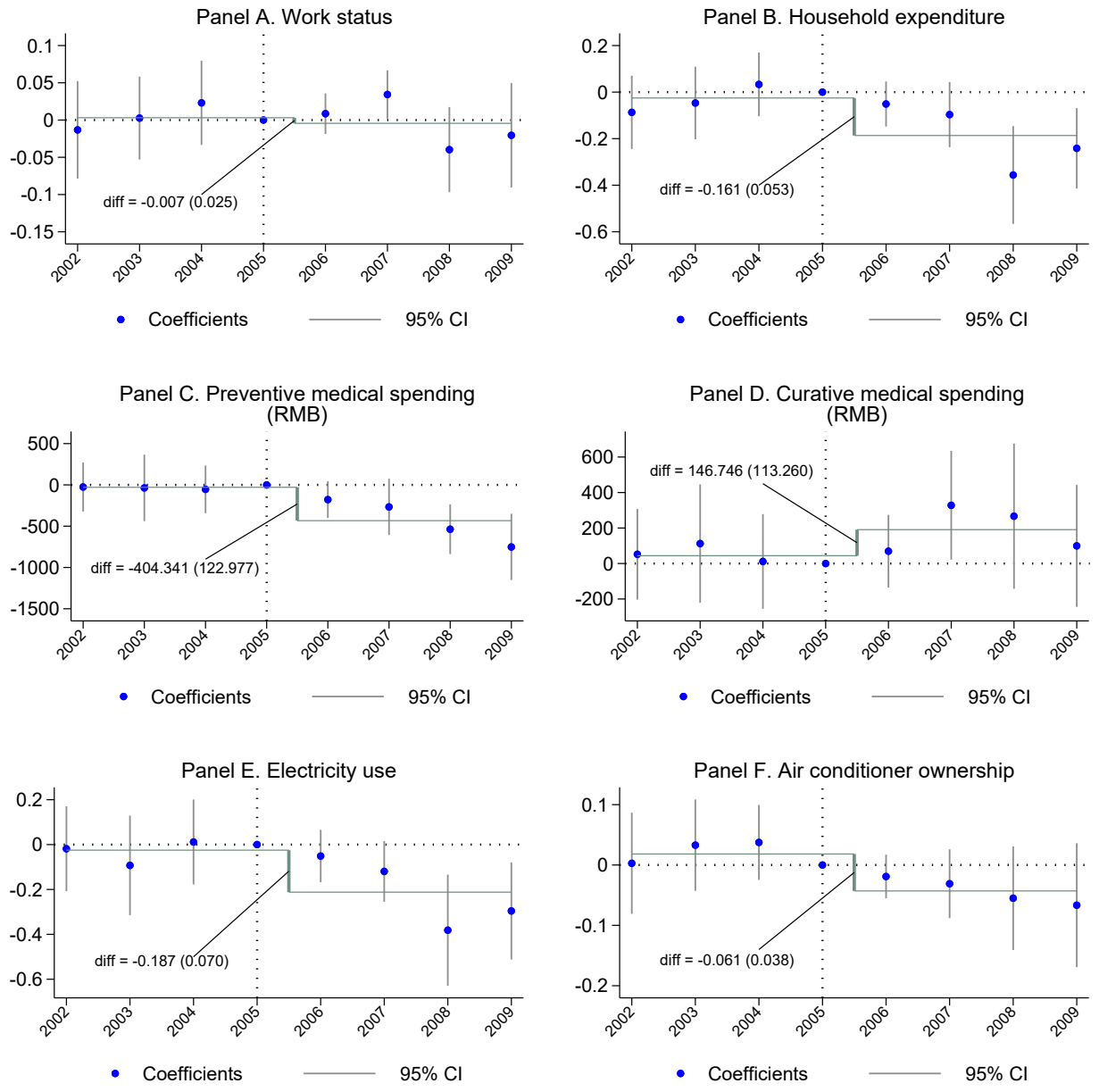


Figure 3: Household Responses to the Top 1,000 Program

Notes: This figure plots the event-study estimates of individual and household responses to the Top 1,000 Program based on the following specification:

$$Y_{\iota dt} = \sum_{t \neq 2005} \beta_t \left(\text{Top 1,000 share}_d \times \text{Year}_t\right) + \boldsymbol{\gamma}' \boldsymbol{x}_{\iota dt} + \varepsilon_{\iota dt},$$

where $Y_{\iota dt}$ denotes outcomes for individual or household ι, prefecture d, and year t. The dependent variable in Panel A is individual work status; the sample is restricted to working-age individuals (16-64 years old), and the variable takes the value of one if the individual is employed and zero otherwise. The dependent variables in Panels B are the logarithm of household total expenditure. Panels C and D use the absolute amount of preventive medical spending (in RMB, including expenditures on *nourishment*, *medicine*, and *health-care devices*) and curative spending (in RMB, all other sub-categories) as dependent variables. The dependent variables in Panels E and F are the logarithm of electricity use (in kWh) and air conditioner ownership, respectively. All regressions include prefecture fixed effects and province-by-year fixed effects, as well as demographics including age, gender, ethnicity, and years of education of each individual (Panel A) or the household head (Panels B-F). The value labeled "diff" denotes the difference between post- and pre-policy means, computed from the event-study coefficients using the Delta method. These estimates may differ slightly from those obtained from a standard difference-in-differences specification. Numbers of observations are: 587,652 (Panel A), 256,077 (Panels B-D), 247,028 (Panel E) and 256,652 (Panel F). 95% confidence intervals are constructed using standard errors clustered at the prefecture level.
Source: NBS (2002-2009b).

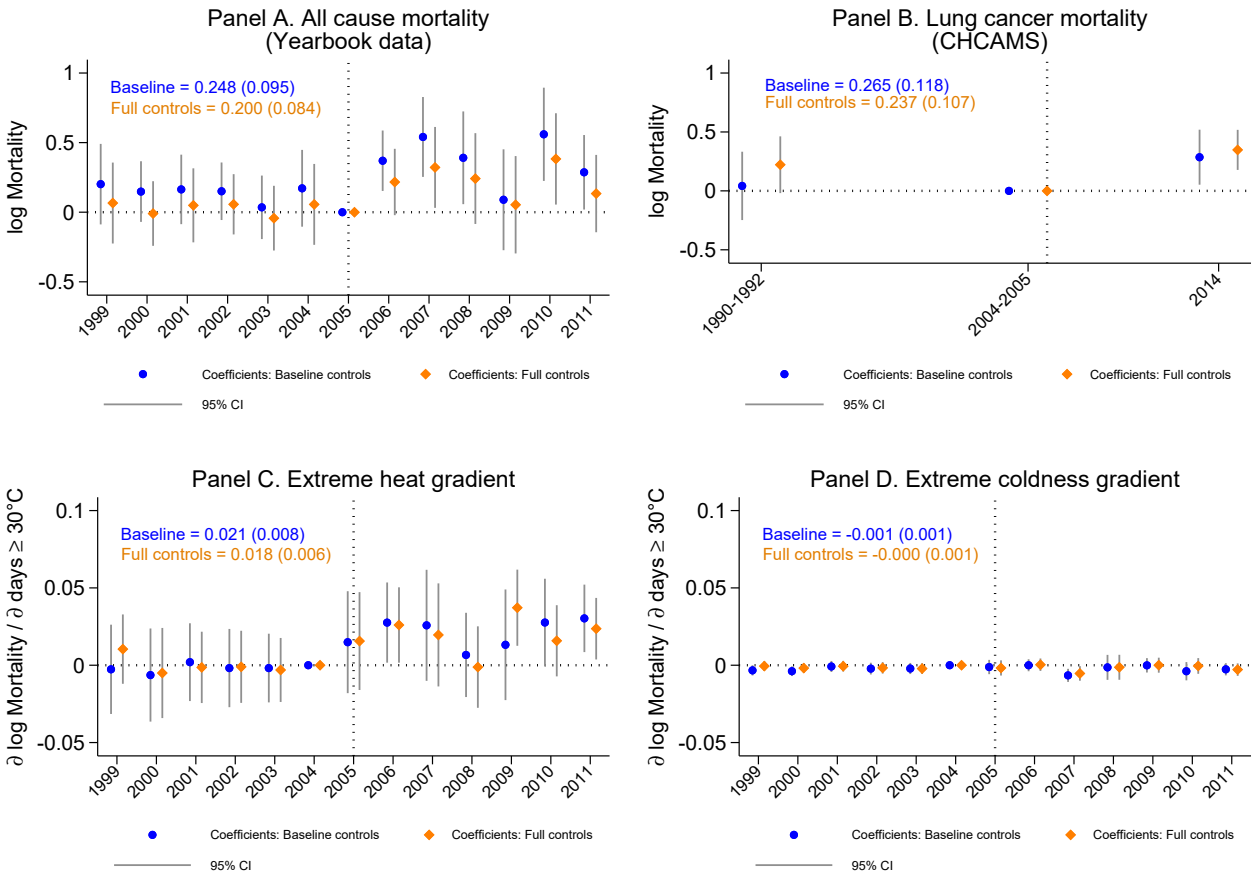


Figure 4: Effects of the Top 1,000 Program on Mortality and Vulnerability

Notes: Panel A and B plots the event studies of the Top 1,000 program on mortality rates, based on the specification

$$Y_{dt} = \sum_{\tau \neq \tau_o} \beta_\tau (\text{Top 1,000 share}_d \times \text{Year}_t) + \boldsymbol{\gamma}' \boldsymbol{x}_{dt} + \varepsilon_{dt}.$$

Panel C and D plots the estimates of the interaction of event studies terms of the Top 1,000 program with temperature shocks (days above 30°C in Panel C and days below 0°C in Panel D) based on the specification:

$$Y_{dt} = \sum_{\tau \neq \tau_o} \beta_\tau (\text{Top 1,000 share}_d \times \text{Year}_t) + \sum_k \sum_{\tau \neq \tau_o} \beta_\tau^k (\text{TBin}_{dt}^k \times \text{Top 1,000 share}_d \times \text{Year}_t) + \boldsymbol{\gamma}' \boldsymbol{x}_{dt} + \varepsilon_{dt},$$

where Y_{dt} denotes mortality outcome for prefecture d, and year t. τ_o is the omitted year depending on data availability, which is set to 2005 in Panels A, 2004-2005 in Panel B, and 2004 in Panels C and D. For Panel B, the analysis utilizes gender-disaggregated data, with the outcomes and error term indexed by $\{s, d, t\}$ to denote gender, prefecture, and survey wave, respectively. Dependent variable in Panels A, C and D is the logarithm of (crude) all-cause mortality rate. Dependent variable in Panel B is the logarithm of lung cancer mortality rate, standardized to Segi's world standard population. Baseline controls include prefecture fixed effects, region-by-year fixed effects, and year fixed effects interacted with baseline employment shares of Top 10,000 firms. Panel B additionally controls for gender fixed effects. Panels C and D additionally include lower-order covariates as discussed in Section 4.3. The "Full controls" specification further allows year fixed effects to vary with baseline prefecture characteristics capturing demographics (urban population share, share of the population with a high school degree or above, share of the population aged 0-15, and share of the population aged 65 or above), health (infant mortality rate), industrial structure (indicator for Top 1,000 prefectures), and concurrent environmental regulations (indicator for inclusion in the *Two Control Zones* and employment shares of *National Specially Monitored Firms*). See Appendix D.1 for details. Coefficients listed on the left-upper corners are differences between post- and pre-policy means, computed from the event-study coefficients using the Delta method. Samples are 4,332 prefecture-year observations (Panel A, C and D) and 2,070 prefecture-gender-year observations (Panel B). All regressions are weighted by base industrial employment. 95% confidence intervals are constructed using standard errors clustered at the prefecture level.
Sources: NBS (2000, 2004, 2000-2012); CHCAMS (2017).

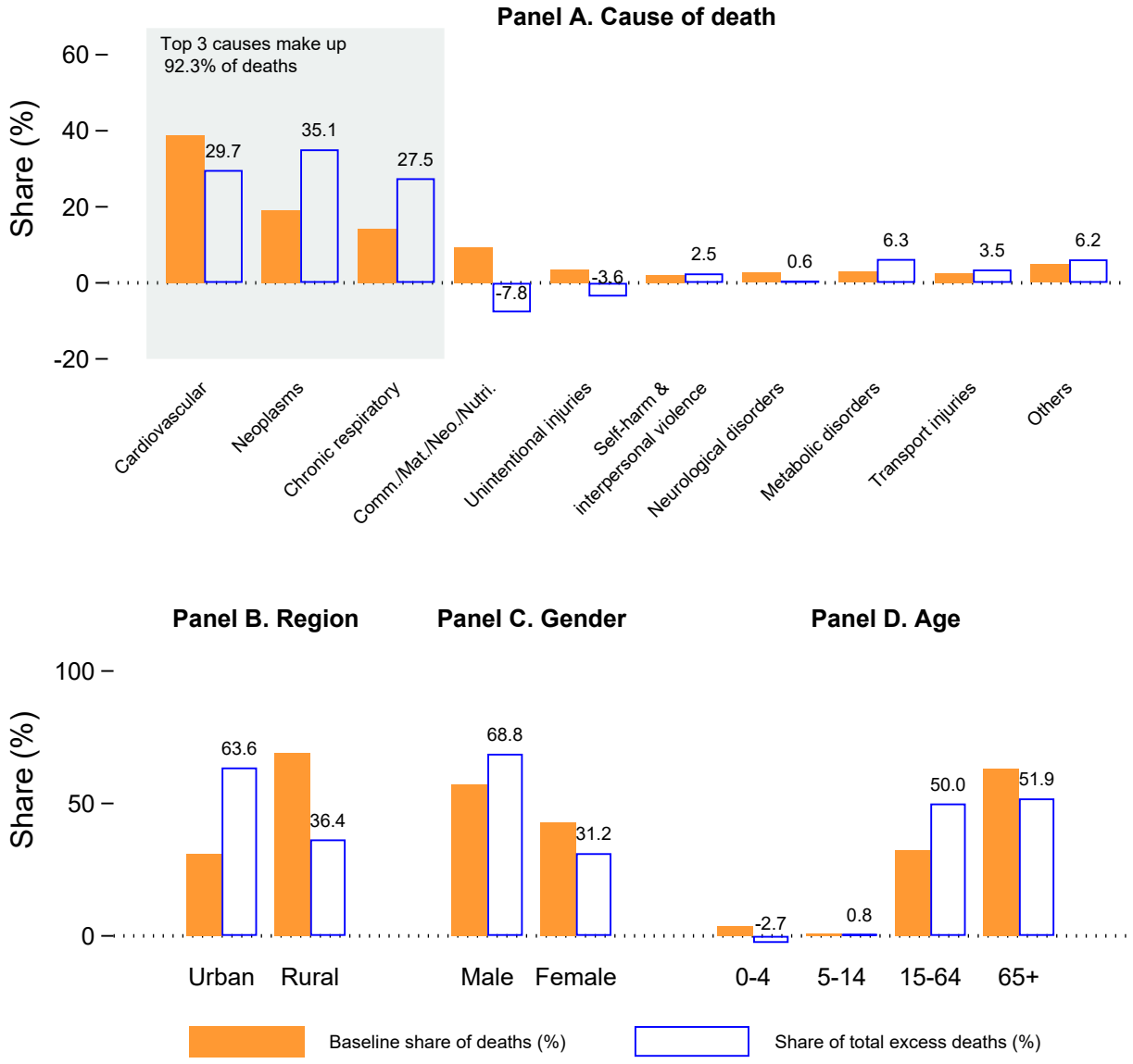


Figure 5: Decomposition of Mortality Increase by Cause and Demographics

Notes: This figure reports baseline shares of deaths s_ι (solid orange bars) and the decomposition of excess deaths induced by the Top 1,000 Program (hollow blue bars) by cause of death (Panel A), region (Panel B), gender (Panel C), and age group (Panel D). Baseline shares of deaths are measured as the average shares of deaths between 1990 and 2013 in Panel A, and between 2000 and 2010 in Panels B-D. The decomposition follows Finkelstein et al. (2025). Specifically, for each cause of death or demographic group ι, we estimate a difference-in-differences specification for log mortality changes over the corresponding period. Given the estimated difference-in-differences coefficient $\hat{\beta}_\iota$, the contribution of group ι to total excess mortality is computed as $\frac{s_\iota \hat{\beta}_\iota}{\sum_{\iota'} s_{\iota'} \hat{\beta}_{\iota'}}$. The underlying regression estimates $\hat{\beta}_\iota$ and their confidence intervals are reported in Appendix Figure G.25. The cause-of-death classification follows the Global Burden of Disease (GBD) 2013. Abbreviations: "Metabolic disorders" is death due to diabetes, urogenital, blood, and endocrine; "Comm./Mat./Neo./Nutri." is death due to communicable, maternal, neonatal, and nutritional.
Sources: Zhou et al. (2016); NBS (2000, 2010).

Online Appendix for

Misallocation May Kill: Evidence from the World's Largest Energy-Saving Program

Yuan Chen, Qirui Wang

This appendix provides supplementary materials and additional analyses. Appendix A provides a detailed description of the data sources and sample construction. Appendix B provides a comprehensive overview of the institutional background of the Top 1,000 Program, including its origins, design, and implementation, as well as anecdotal evidence regarding its impact on household income. Appendix C analyzes the direct effects and potential spillovers of the Top 1,000 Program at the firm level. Appendix D examines the robustness of our main findings concerning the program's impact on mortality. Appendix E discusses alternative mechanisms. Finally, Appendix F develops an energy regulation model based on the misallocation framework of Hsieh and Klenow (2009). Additional tables and figures not reported in the main text are presented in Section G.

A Data Appendix

A.1 Firm Data

Top 1,000 firms. We obtain the list of Top 1,000 firms from the official website of the National Development and Reform Commission (NDRC).[25] Firm characteristics, including industry, location, and initial employment in 2004, are obtained by merging this list with the 2004 *Economic Census* (NBS 2004). Because both datasets contain unique firm identifiers, we successfully match all but one firm in the Top 1,000 list.[26] Figure G.1 shows the geographical distribution of these regulated firms and their baseline employment shares across prefectures. The firms are spatially dispersed, with higher concentrations in the Jing-Jin-Ji Metropolitan Region and the Yangtze River Delta Economic Zone. Panel A of Table G.1 summarizes prefecture-level exposure to the program. Among 345 prefectures, 71.6% host at least one Top 1,000 firm in 2004 (hereafter "Top 1,000 prefectures"). In these prefectures, Top 1,000 firms accounted for 11.7% of baseline industrial employment.

Top 10,000 firms. We obtain the list of Top 10,000 firms from the official website of the National Development and Reform Commission (NDRC),[27] and merge it with the 2004 *Economic Census*, following the same procedure as for the Top 1,000 firms. We identify 8,992 Top 10,000 firms in the census, and 8,299 after excluding the Top 1,000 firms. As reported in Table G.1, these firms are distributed across 333 prefectures and accounted for 9.7% of baseline industrial

[25] The website is: `https://www.ndrc.gov.cn/xxgk/zcfb/tz/200604/t20060414_965934.html`. [Accessed on May 6th, 2023.]

[26] The only unmatched firm is *Baosteel Group Guangdong Shaoguan Iron and Steel Co., Ltd.*, which was not classified as an industrial firm in 2004.

[27] The website is: `https://www.ndrc.gov.cn/xxgk/zcfb/tz/201112/t20111229_964360.html`. [Accessed on May 6th, 2023.]

employment in those prefectures.

Annual Survey of Industrial Firms (ASIF). The firm panel comes from the Annual Survey of Industrial Firms (ASIF) for 2001-2009, a census of above-scale firms collected by the National Bureau of Statistics (NBS) of China. The sample expanded from 169,028 firms in 2001 to 434,701 in 2009.[28] Although the data don't cover the universe of firms, above-scale firms accounted for over 70% of industrial employment and over 90% of industrial output (Brandt et al. 2014).

The data include detailed information on firms' location, industry, ownership type, exporting activity, number of employees, and a wide range of accounting variables. The data also report detailed information on firms' name and addresses. We use these information to geolocate all firms via the AMap API. We use coordinates of zip codes when precise geolocation is not available.[29] We aggregate firms to $0.03° \times 0.03°$ (about 3 km $\times$ 3 km) grid cells, which naturally account for firm entry and exit. Our working sample includes 61,685 distinct cells, with an average of six firms and 1,493 workers per cell.

Industrial Product Output Database. We obtain monthly firm-by-product panel on physical output from the National Bureau of Statistics (NBS 2000-2006), which provides high frequency information on the production of Top 1,000 firms. The raw data contain 12,449,626 observations on 265,559 firms and 2,234 products. We are able to match 896 Top 1,000 firms and 5,131 Top 10,000 firms with the data. We refer readers to Rubens (2023) for more details of the data.

Environmental Survey and Reporting (ESR) database. Pollution and energy use data are obtained from the *Environmental Survey and Reporting* (ESR) database maintained by the former Ministry of Environmental Protection (MEP 2002-2011). The ESR sample is constructed by ranking all pollution sources within each county according to their emissions of sulfur dioxide (SO_2) and chemical oxygen demand (COD), and including those that jointly accounted for the top 85% of total emissions. The dataset reports plant-level pollutant quantities and energy inputs (coal, oil, and gas), allowing analysis of both firm-level responses and aggregate emission changes. The raw data contain approximately 843,345 firm-year observations for 248,997 firms.[30]

We clean the dataset following Chen et al. (2025). First, we exclude about 12% of observations corresponding to non-manufacturing firms, especially those in the energy-generation sector (CIC code 4411), as data for thermal power plants were no longer reported since 2006. Second, when analyzing firm energy use, we exclude industries where electricity consumption accounts for more than 30% of total energy consumption,[31] since the ESR data do not contain information on electricity use. Third, we remove extreme observations in which the absolute year-to-year percentage change in emissions or energy use exceeds 10, or where values are identical to those reported in the previous year.[32]

[28]The sample consists of "above-scale" industrial firms. From 1998 to 2006, this category includes all state-owned enterprises (SOEs) and non-state firms with annual sales exceeding 5 million RMB. Starting in 2007, the universal inclusion of SOEs was discontinued. In 2011, the revenue threshold for all firms was further raised to 20 million RMB. Although using the term "firm", an observation is closer to the definition of establishment in the United States, and establishments of multi-branch firms show up as single observation in the data.

[29]A zip code zone is close to a township in China.

[30]See He et al. (2020) and Chen et al. (2025) for more details on the dataset.

[31]Industry-level energy composition is obtained from the *China Energy Statistical Yearbook* (2005) (NBS 2005b).

[32]In the raw data, a non-negligible number of firms repeatedly report identical pollution or energy use values over consecutive years (e.g., 21,600 kg of SO_2 emissions from 2008-to 2010), which likely reflects misreporting.

Related firms. As highlighted by Chen et al. (2025), many of the Top 1,000 firms belong to larger conglomerates. To capture these ownership linkages, we obtain data on firm ownership networks from *Tianyancha*,[33] which compiles information from the *China Administrative Registration Database (CARD)* maintained by the State Administration for Industry and Commerce. Following Chen et al. (2025), we define related firms as (i) wholly owned subsidiaries of regulated firms; (ii) firms partially owned by regulated firms; (iii) shareholders of regulated firms; and (iv) firms fully or partially owned by those shareholders. Ownership links are required to involve at least a 25% equity stake at each level of investment. To ensure economic relevance, we further restrict related firms to those operating in the same four-digit industry (in 2004) as the regulated firms, since production shifts across industries are unlikely.

We identify 1,701 related firms within the same four-digit industry that can be matched to the 2004 Economic Census. These figures are comparable to, though slightly smaller than, those in Chen et al. (2025), who report 2,466 related firms in the same four-digit industry.[34] After excluding regulated firms themselves, we are left with 1,186 related firms. Although the number of related firms is large, they are considerably smaller in scale than regulated firms. As shown in Table G.1, among 263 prefectures that host at least one related firm, related firms only account for 2.3% of industrial employment.

National Specially Monitored Firms (NSMF) firms. We obtain the list of *National Specially Monitored Firms* (NSMF) from the official website of the central government,[35] and merge it with the 2004 *Economic Census*, following the same procedure as for the Top 1,000 firms. We identify 4,986 NSMF firms in the census, among which 455 are Top 1,000 firms.

A.2 Mortality and Health Data

Our baseline analysis uses annual prefecture-level mortality rates from the *China Regional Statistical Yearbook* for 1999-2011 (NBS 2000-2012). Because the raw series exhibit implausible fluctuations, we rescale prefecture-level mortality rates to provincial totals from the *China Population & Employment Statistics Yearbook* (NBS 2023)—a more reliable source that closely mirrors mortality statistics from census yearbooks and the Disease Surveillance Points (DSP) system (Figure G.3). Figure G.4 further illustrates the correction procedure: Panel A shows the raw and corrected for Beijing, while Panel B compares corrected prefecture-level mortality rates with census data, showing marked improvement in consistency. We conduct a comprehensive set of robustness checks in Section D to confirm that our findings are not sensitive to the correction procedure.[36]

[33]The website is: `https://www.tianyancha.com/`. We scraped the conglomerate ownership networks in August 2024. Because the website is continuously updated, our data may differ slightly from the information currently available online.

[34]The discrepancy arises because Chen et al. (2025) match their ownership data with the ASIF for 2001-2011, whereas our sample is based on the 2004 Economic Census. When we instead match the *Tianyancha* data with ASIF, we identify 2,573 related firms in the same four-digit industry.

[35]The website is: `https://www.zhb.gov.cn/plan/gdgc/200703/t20070329_102191.htm`. [Accessed May 6, 2024.]

[36]First, our results are robust to the inclusion of province-by-year fixed effects, which absorb the correction factors so that we're only exploring the variation of the raw data (Figure G.19). Second, our results are robust to using independently measured data from population census, the Global Burden of Disease Study 2013, and individual panels (Sections D.2 and D.3).

Province-level mortality data. We compile province-level mortality data from multiple official and research sources. all-cause mortality rates for 1990-2022 are obtained from the *China Population & Employment Statistics Yearbook* (2023 edition) (NBS 2023). In our empirical analysis we focus on 1990-2018 to avoid the impact of COVID-19. In addition, we extract gender- and cause-specific (age-standardized) mortality rates for 1990 and 2013 from Zhou et al. (2016), who report age-standardized death rates for 240 causes by gender and year.[37] We construct province-gender-year-level mortality rates based on the Global Burden of Disease (GBD) 2013 classification. Our analysis covers the three mutually exclusive and exhaustive GBD categories: (i) communicable, maternal, neonatal, and nutritional diseases; (ii) non-communicable diseases (NCDs); and (iii) injuries. To provide a granular understanding of the program's impact, we further disaggregate the latter two categories into their most prevalent components in China. Specifically, for NCDs, we include neoplasms, cardiovascular diseases, chronic respiratory diseases, neurological disorders, and metabolic disorders (comprising diabetes, urogenital, blood, and endocrine diseases). For injuries, we focus on transport injuries, unintentional injuries, and deaths from self-harm and interpersonal violence.

Chinese Longitudinal Healthy Longevity Survey (CLHLS). We use individual-level death records from the Chinese Longitudinal Healthy Longevity Survey (CLHLS) (CLHLS 2002-2011). The CLHLS was first launched in 1998, with follow-up surveys conducted every three years in randomly selected half of all counties and cities across 22 of China's 31 provinces. The early waves focused on individuals aged 80 and above, but beginning in 2002 the survey expanded to include respondents aged 65 or older. Accordingly, our analysis draws on the longitudinal waves from 2002 to 2011, which include four rounds of surveys conducted in 2002, 2005, 2008, and 2011. In each wave, surviving respondents were re-interviewed, while deceased individuals were replaced by new participants to maintain the sample size. Importantly, family members of deceased respondents were interviewed to provide detailed information about the deceased, including their date of death. Using these records, we construct an individual-level panel of 14,049 elderly respondents observed between 2002 and 2011. Because only province identifiers are provided in the dataset, we link these individual records to province level exposure in our analysis.

China Health and Nutrition Survey (CHNS). Finally, we use individual-level health data from the China Health and Nutrition Survey (CHNS) (Zhang et al. 2014). The CHNS employs a multistage, random-cluster sampling design to survey households across nine provinces. Unlike the CLHLS, which focuses on older adults, the CHNS covers respondents of all age groups. The survey has conducted ten waves from 1989 to 2015. In each wave, participants report whether they have felt ill or suffered an injury during the past four weeks.[38] For our analysis, we focus on the 2004, 2006, 2009, and 2011 waves, as information on heart disease, a key outcome of interest, is largely missing in earlier rounds. We focus on a balanced panel of individuals to avoid migration bias. The final sample includes 5,621 individuals from 49 prefectures across these nine provinces.

[37] This represents the highest-quality cause-of-death dataset for China. It adheres to rigorous GBD 2013 methodologies, integrated multiple authoritative data sources (e.g., disease surveillance systems, cancer registries), and incorporated China-specific optimizations such as garbage code redistribution and urban-rural weighting, ensuring robustness. The dataset further enhances reliability through bias adjustment, spatiotemporal modeling, and quantification of uncertainty, providing unparalleled granularity and validity for subnational epidemiological research.

[38] See Table G.2 for specific survey questions.

A.3 Meteorological Data

Daily meteorological data are from the NOAA Integrated Surface Database (NOAA 2024). Starting with 394 national stations, we exclude 32 with missing observations exceeding 10% of the sample period, resulting in a balanced panel of 362 stations. Data including daily temperature, precipitation, relative humidity, and wind speed. Each prefecture is matched to the closest stations based on the distances between their centroids and the stations. We calculate the annual frequency of daily mean temperatures across eight discrete bins: below 0°C, 0-5°C, 5-10°C, 10-15°C, 15-20°C, 20-25°C, 25-30°C, and above 30°C.

A.4 Satellite and Monitor Data

Aerosol Optical Depth (AOD). We measure local environmental performance using satellite-derived Aerosol Optical Depth (AOD) retrieved from the NASA Moderate Resolution Imaging Spectroradiometer (MODIS). Specifically, we use the MCD19A2 (Collection 6.1) product, which is a Level-2 gridded (L2G) dataset derived from both Terra and Aqua MODIS inputs. This product utilizes the Multi-Angle Implementation of Atmospheric Correction (MAIAC) algorithm, which provides a significant improvement in spatial resolution (1 km) and accuracy over land surfaces compared to previous algorithms (Lyapustin et al. 2015). We aggregate the 1 km pixels into $0.03^\circ \times 0.03^\circ$ grid cells (approximately 3 km). For the validation against ground-based emissions in Appendix Figure G.2, we further calculate prefecture-level annual means using 2010 administrative boundaries. As discussed in Section 3, this satellite-derived measure provides an objective proxy for pollution exposure that is immune to potential misreporting in ground-level monitors (Ghanem and Zhang 2014).

Auxiliary pollution data. We supplement the AOD data with several alternative measures of air pollution drawn from independent sources. First, we use calibrated $PM_{2.5}$ concentration data from Shen et al. (2024), available at a $0.01^\circ \times 0.01^\circ$ spatial resolution. This dataset represents the latest version of the widely used van Donkelaar et al. (2016) $PM_{2.5}$ product and has been extensively validated and applied in the literature (see, e.g., Finkelstein et al. (2025)). Second, we obtain independently measured SO_2 and $PM_{2.5}$ concentration data from the Modern-Era Retrospective Analysis for Research and Applications, version 2 (MERRA-2; Modeling and Assimilation Office GMAO), which are available at a $0.5^\circ \times 0.625^\circ$ spatial resolution.[39] Both satellite-based measures are aggregated to the prefecture level using 2010 administrative boundaries. Finally, following Ebenstein et al. (2017), we construct ground monitor SO_2 concentration data by digitizing multiple volumes of China's *Environmental Yearbooks* (MEP 2002-2009) and *Environmental Quality Annual Reports* (MEP 2007-2012). The two sources are cross-validated against each other to ensure internal consistency. The resulting dataset forms an unbalanced panel, expanding from 97 prefectures in 2001 to 323 prefectures in 2011. Importantly, unlike PM_{10}, prior studies find little evidence of systematic manipulation in official SO_2 monitoring data, suggesting that these readings provide reliable measures of ambient SO_2 concentrations (Ghanem and Zhang 2014; Greenstone et al. 2022).[40] To our knowledge, these sources together cover all major pollution measures available for China during the 2001-2011 period.

[39]The raw MERRA-2 data do not report $PM_{2.5}$ concentrations directly. We construct $PM_{2.5}$ concentrations following the methodology in Buchard et al. (2016).

[40]Local governments have limited incentives to manipulate SO_2 readings, as PM_{10}—rather than SO_2—is the primary determinant of non-"blue-sky" days in most Chinese cities (Ghanem and Zhang 2014).

Thermal Anomalies. We obtain active fire and thermal anomaly data from NASA's Fire Information for Resource Management System (FIRMS). We specifically use the MODIS Collection 6.1 (MCD14ML) standard quality product, which provides science-grade observations with a three-month lag to ensure higher accuracy than near-real-time data. To capture industrial heat release—such as power generation and cement production—we follow the literature (Xia et al. 2018) and restrict our primary indicator to *Static Land Sources* (Type 2). For quality control, we retain only observations with a confidence level ≥ 50 and a Fire Radiative Power (FRP) ≥ 5. The raw point-level data are aggregated to our $0.03^\circ \times 0.03^\circ$ grid cells by rounding coordinates to the nearest 0.03 multiple. Our primary variable is the annual sum of thermal anomalies detected within each cell. As a placebo test, we also construct a measure for non-industrial thermal anomalies (Type $\neq 2$), such as wildfires, applying the same confidence threshold to ensure comparability.

A.5 Household Behavior

Data on household behavior are obtained from the *Urban Household Survey* (UHS) for 2002-2009 (NBS 2002-2009b), a rich dataset containing detailed information on individual employment, income, and household consumption. The UHS, administered by the National Bureau of Statistics, is a nationally representative survey of urban households and is often regarded as the Chinese counterpart of the U.S. *Current Population Survey*. The UHS covers urban China and has used a consistent questionnaire since 1986, though it is considered nationally representative only from 2002 onward; our description therefore focuses on this latter period. The survey adopts a three-stage stratified random sampling design, similar to that of the *Current Population Survey* in the United States (Meng 2012; Ge and Yang 2014; Feng et al. 2017). We have access to data for 16 provinces and 159 prefectures.[41] The sample size increases from 77,103 (25,593) individuals (households) in 2002 to 103,743 (35,817) individuals (households) in 2009.

A.6 Government Behavior

Environmental penalty. We use environmental administrative punishment records obtained from CnOpenData,[42] a data consulting company that compiles enforcement data disclosed by municipal Environmental Protection Bureaus (EPBs). These records are used to capture local environmental regulatory enforcement. The construction and application of this dataset follow the approach in Kong and Liu (2024). Importantly, the dataset includes only penalties issued by municipal EPBs, excluding those issued by provincial authorities or the Ministry of Ecology and Environment, thereby ensuring that the measure reflects enforcement intensity at the municipal level.

Government Work Report. To capture local governments' emphasis and effort on environmental protection, we compile the full texts of municipal Government Work Reports (GWRs) for prefectures from 2001 to 2010. The reports are obtained from CnOpenData.[43] Our final balanced panel includes 320 prefecture-level cities over the sample period. We conduct a textual analysis

[41] The 16 provinces are Beijing, Shanxi, Liaoning, Heilongjiang, Shanghai, Jiangsu, Anhui, Jiangxi, Shandong, Henan, Hubei, Guangdong, Chongqing, Sichuan, Yunnan, and Gansu.

[42] `https://www.cnopendata.com/data/m/ESG/envl-penalty.html` [Accessed on Sep 29th, 2025.]

[43] `https://www.cnopendata.com/data/m/text/chinese-government-work-report.html` [Accessed on Sep 29th, 2025.]

based on word frequency counts of key terms regarding *environment*, *environmental regulation*, *air pollution*, and *energy saving*, to construct indicators that reflect the intensity of local environmental concerns. We also collected prefecture-level energy-saving targets from local government work reports and policy documents released in 2006 to disentangle the effect of the Top 1,000 Program from the overall energy-saving mandates.

A.7 Measuring Travel Time

Data Sources. In Section D.1, we use bilateral travel times to calculate indirect exposure to the Top 1,000 program. To compute travel times between locations, we rely on data on highways, national trunk roads, state roads, and railway networks in 2000, obtained from the China Data Center at the University of Michigan. We supplement these data with the road networks in 2010, obtained from Baum-Snow et al. (2017), for robustness. Additionally, as emphasized by Ma and Tang (2024), accounting for terrain is essential when calculating travel speeds. To do so, we collect elevation data at a 30 arc-second resolution from GTOPO30 via the USGS.

Constructing Speed Maps. Based on these road and auxiliary datasets, we construct 1 km $\times$ 1 km resolution speed maps for China. For each pixel, we assume its speed equals the maximum speed among all available transport modes. Following Ma and Tang (2024), we assign speeds of 22.8 km/h, 40 km/h, 93.75 km/h, 62.5 km/h, and 75 km/h for waterways, normal paved roads, railways, state roads and provincial trunk roads, and highways, respectively, in plains.[44] We then adjust these speeds based on terrain, again following Ma and Tang (2024). Specifically, we classify China into four terrain types: plains, low rolling hills (LRH), hills, and mountains, following the classification in Appendix B.2 of Ma and Tang (2024). The terrain-adjusted assumptions are:

- **Highways:** Travel speed on LRH or hills is the same as on plains, but on mountains it is 80/120 of the speed on plains.
- **Paved roads, state roads, and provincial trunk roads:** Travel speed on LRH is the same as on plains, but on hills or mountains it is 80/100 of the speed on plains.
- **Railways:** Travel speed on LRH is 100/120 of the speed on plains, and on hills or mountains it is 80/120 of the speed on plains.

Figure G.5 plots the speed maps.

Fast Marching Method. Following Allen and Arkolakis (2014), we use the Fast Marching Method (FMM) to calculate bilateral travel times between prefecture pairs, based on the speed maps shown in Figure G.5. For inter-prefecture pairs, we use the travel time between their centroids. For intra-prefecture travel, we use the average travel time from the centroid to all other grid points within the same prefecture.

[44] We assume that the design speed is 1.6 times the average travel speed for railways, state roads and provincial trunk roads, and highways. For example, Table 1 in Ma and Tang (2024) reports a design speed of 120 km/h for highways in plains, so we assume an average speed of $120 \div 1.6 = 75$ km/h. The factor 1.6 is taken from Table 4 in Ma and Tang (2024).

B Policy Details of the Top 1,000 Program

This section provides additional institutional background on the origin, design, and implementation of the *Top 1,000 Enterprises Energy-Saving Program*. Section B.1 describes the policy's design and firm-selection rules, highlighting why regulatory effort was concentrated on a small set of large energy users. Section B.2 explains the implementation and enforcement mechanisms that generated high compliance among regulated firms. Section B.3 discusses why firms predominantly responded through output reduction rather than energy-efficiency improvements. Finally, Section B.4 presents qualitative evidence illustrating how the program affected firm operations and local income dynamics.

B.1 Policy Origins and Design

The *Top 1,000 Enterprises Energy-Saving Program* was launched in April 2006 as the central administrative instrument to achieve the binding energy-conservation targets set under China's 11th Five-Year Plan. The program targeted 1,008 industrial enterprises that together accounted for approximately 33 percent of national energy consumption and 47 percent of total industrial energy use in 2004 (NDRC 2006). By concentrating regulatory effort on a small number of large energy users, the central government was able to exert control over nearly half of industrial energy consumption while keeping monitoring and enforcement administratively tractable.

Firm selection was based on a backward-looking threshold: industrial enterprises consuming at least 180,000 tons of coal equivalent (TCE) in 2004 were included in the regulated list. Because eligibility relied on pre-determined energy consumption measured two years prior to the program's announcement, firms could not strategically adjust contemporaneous behavior to avoid regulation. This retroactive selection rule sharply limits concerns about endogenous participation and underpins our difference-in-differences design.

The program's stated objective was to achieve cumulative energy savings of 100 million TCE by 2010, accounting for roughly 45 percent of the national energy-saving mandate (Price et al. 2010; Ke et al. 2012). Targets were assigned through a top-down administrative process: provincial quotas were first determined at the central level and then allocated to regulated firms based largely on industry-level benchmarks and historical energy use, rather than firm-specific assessments of marginal abatement costs or technological potential (NDRC and NBS 2007). As a result, firms with widely different production technologies and adjustment costs faced comparable energy-saving requirements, a feature central to the misallocation mechanism we document.

Focusing on the largest firms also offered substantial administrative advantages. The *Energy Conservation Law* authorized regulators to designate "key energy-using units," mandate regular reporting, and require the establishment of dedicated energy management posts within regulated enterprises. Large firms typically maintain centralized and standardized energy accounts, making monitoring easier and falsification more difficult than for smaller establishments. Moreover, approximately 70 percent of the Top 1,000 enterprises were state-owned, allowing regulators to leverage political incentives by linking compliance to executive performance evaluations and compensation. Together, these features explain why the government could regulate a large share of industrial energy use at relatively low administrative cost and with high expected compliance.

B.2 Implementation and Enforcement

Implementation of the Top 1,000 Program relied on a centralized *Target Responsibility System* (TRS). In July 2006, the National Development and Reform Commission (NDRC) signed Energy Conservation Responsibility Agreements with provincial governments, which in turn contracted directly with each regulated enterprise within their jurisdiction. These contracts specified firm-level *absolute* energy-saving targets to be met by the end of 2010, transforming energy conservation into a binding administrative mandate for firm managers (Price et al. 2010).

Compliance was enforced through a political incentive mechanism commonly referred to as the "one-vote veto" Regions failing to meet annual energy-saving targets were stripped of honorary titles, and responsible officials received failing performance evaluations, directly affecting promotion prospects (NDRC 2007). By tying energy conservation outcomes to the political careers of mayors and party secretaries, the TRS sharply reduced local protectionism and induced local governments to prioritize enforcement even at the cost of short-run output losses (Chen et al. 2018).

To operationalize enforcement, regulators established a multi-layered monitoring system. The *Energy Conservation Law* required regulated firms to create dedicated energy management posts and submit regular reports. In addition, firms were subject to mandatory third-party energy audits—costing roughly 200,000 RMB per firm on average—to verify energy balances and fuel invoices (Price et al. 2010; Zhao et al. 2014). Local governments further formed temporary Energy Conservation Leadership Groups, often chaired by provincial governors or city mayors, and deployed cross-bureau Special Inspection Teams to conduct intensive on-site supervision (Liu et al. 2014).

B.3 Why Output Reduction Dominated Efficiency Improvement

Although firms could in principle comply with energy-saving targets by either improving energy efficiency or reducing output, enforcement in practice focused on *total energy consumption* rather than efficiency metrics. Auditing firm-level efficiency gains proved administratively infeasible: firms could exploit price fluctuations, reallocate output across units, or selectively apply alternative accounting formulas, making reliable verification difficult for regulators (Price et al. 2011). As a result, authorities prioritized monitoring physical energy inputs—such as electricity usage and coal deliveries—through "live energy consumption monitoring systems" that allowed for real-time cross-verification with grid records and fuel invoices (Price et al. 2011; Ke et al. 2012).

Under this regime, firms faced binding caps on total energy consumption. Exceeding these caps triggered immediate administrative sanctions, most notably mandatory power rationing and production shutdowns (Price et al. 2010; Zhao et al. 2014; Chen et al. 2025). Enforcement took multiple forms, including coordinated suspension schedules for continuous-process industries, sudden forced power cuts, quota-based electricity rationing, and on-site supervised shutdowns as firms approached consumption limits. These measures made non-compliance extremely costly and highly visible.

Given short evaluation cycles and severe penalties, firms rationally prioritized output reductions over deep technological upgrades. Energy-efficiency investments involved substantial upfront costs and long payback periods. For example, large-scale projects such as waste-heat recovery systems or supercritical generation units typically required several years for approval, construction, and testing (Zhao et al. 2014), often exceeding the remaining horizon of the 11th Five-Year Plan. By contrast, production cuts—such as idling lines or decommissioning units—offered an immediate

and reliable way to meet binding quotas.

In addition, fiscal incentives reinforced this adjustment margin. Beginning in 2007, the central government established transfer payment programs rewarding the *scale* of decommissioned capacity rather than subsidizing new investment. Between 2007 and 2011, these programs disbursed over 26.9 billion RMB from the central government and more than 10 billion RMB from local governments (MOF 2012). Because these payments were typically disbursed ex post and did not cover the full replacement cost of capital, they did little to relax firms' financing constraints for deep efficiency upgrades, further biasing adjustment toward output contraction.

For state-owned enterprises, these incentives were amplified by governance arrangements. Energy-saving performance was directly tied to executive compensation and promotion prospects: annual bonuses—often accounting for 30–50 percent of total income—were fully contingent on meeting energy consumption targets, and failure triggered a one-vote veto that blocked career advancement regardless of other performance metrics (Chen et al. 2025). Together, these institutional features explain why the Top 1,000 Program achieved compliance primarily through administrative output curtailment rather than market-driven efficiency improvements.

The resulting production cuts translated into sharp income losses for workers in highly exposed regions, a channel we document empirically in the main text. The following subsection provides illustrative anecdotal evidence on these income effects.

B.4 Anecdotal Evidence on the Income Effect of the Top 1,000 Program

To complement the institutional background and our quantitative analysis, this subsection presents qualitative evidence illustrating how the *Top 1,000 Program* generated sizable economic shocks through income losses among workers and households. We focus on two highly exposed regions—Tangshan and Shanxi—and one flagship firm, Shougang Group. Together, these cases illustrate the adjustment costs imposed by abrupt environmental enforcement in energy-intensive areas.

Case 1: Tangshan Prefecture. Tangshan is one of China's most steel-intensive cities and among the most exposed to the Top 1,000 Program (Top 1,000 employment share = 0.2833, above the 90th percentile nationally). Major producers such as Tangshan Iron and Steel Group and Tangshan Guofeng Iron and Steel were included in the regulated list. Contemporary media reports document frequent production suspensions following inspections, directly disrupting firm operations and worker earnings.

According to the *China Securities Journal* (Li and Li 2010), steel plants were repeatedly forced to shut down blast furnaces for several consecutive days due to electricity restrictions, rendering essential equipment inoperable. During these shutdowns, workers were typically retained on-site but paid only subsistence allowances—often 10–20 RMB per day—far below regular wages. Firms also incurred substantial losses from forced stoppages, including maintenance costs approaching one million RMB per blast furnace cycle.

These disruptions generated persistent income losses beyond the immediate shutdowns. Reports in *China Economy and Informatization* (Zhang 2010) describe prolonged periods of partial operation, extended worker leave, and sharp declines in household income, particularly in families where multiple members were employed by the same plant.

Case 2: Shanxi Province. Shanxi was among the most heavily exposed provinces under the program, with an average prefecture-level Top 1,000 share of 0.2 (above the 85th percentile nationally). As part of enforcement, provincial authorities implemented the so-called "Three Suspensions" policy—suspending electricity, operations, and credit—leading to widespread shutdowns of coal, coking, and steel enterprises.[45]

The social consequences of these measures were widely documented. A CCTV investigation captured workers facing imminent demolitions of production facilities, while provincial leaders publicly acknowledged that large-scale layoffs were unavoidable during the adjustment process. Thousands of workers lost their jobs across multiple prefectures in a short period.

Income losses often persisted beyond temporary unemployment. For example, *China Youth Daily*[46] reports the case of a disabled coal miner whose mine was permanently closed before his compensation claim was resolved, leaving him in extreme poverty. Such accounts illustrate how enforcement-induced shutdowns translated into long-lasting economic hardship for affected households.

Case 3: Shougang Group. At the firm level, Shougang (Capital Steel) provides a prominent example of large-scale adjustment under the Top 1,000 Program. Beginning in 2005, the company undertook major production cuts and relocation, generating 64,700 surplus workers.[47] Only 19,100 workers were absorbed into new projects, while others were transferred, retired early, or laid off.

Prior to restructuring, skilled workers earned roughly 4,000–5,000 RMB per month. After relocation, wages fell to about 60–70% of previous levels, with disposable income declining further once commuting and housing costs were accounted for. Older workers unable to adapt to new production technologies often accepted early retirement, receiving pensions of around 2,000 RMB per month.

Discussion. Across regions and firms, these cases reveal a common pattern: compliance with the Top 1,000 Program was achieved through production curtailment and shutdowns, generating sharp and sometimes persistent income losses for workers and households. These qualitative accounts align closely with our empirical findings and support the interpretation that the program operated as a negative income shock in highly exposed areas, contributing to the observed increases in mortality.

C Firm Level Impact of the Top 1,000 Program

In Section 4.1, we document policy-induced spatial reallocation using evidence at both the grid-cell and prefecture levels. We show that, within grid cells hosting regulated firms the Top 1,000 Program led to pronounced declines in aerosol pollution, employment, and industrial activity. Yet, at the prefecture level, there is no significant changes in aggregate pollution, employment, or other environmental indicators after the Program (Figure 2).

Beyond this baseline evidence on spatial reallocation, this appendix section examines firm-level responses to the program. Previous literature has studied the direct impact of the Top 1,000

[45] China Central Television (2007), "Shanxi: Cutting Off the Arm to Cure Pollution," *News Probe*, September 9, 2007.

[46] China Youth Daily (2010), "A Miner's Unfinished Compensation: The Hidden Pain Behind Mine Closures," April 27, 2010. Available at: `https://zqb.cyol.com/content/2010-04/27/content_3201961.htm`

[47] Economic Daily (2009), "Restructuring of Shougang: 64,700 Surplus Workers Reassigned or Retired."

Program on regulated firms, with Chen et al. (2025) providing particularly detailed and robust evidence. We first synthesize these findings to characterize how regulated firms adjusted to the policy. We then use micro data on major polluting firms to provide direct evidence that unregulated firms in more exposed prefectures experienced positive spillovers, significantly increasing their energy use and SO_2 emissions. Taken together, the responses of regulated and unregulated firms confirm the reallocation mechanism underlying the misallocation documented in the main analysis.

C.1 Direct Impact on Regulated Firms

Existing evidence based on detailed firm-level data provides a clear picture of how regulated enterprises complied with the Top 1,000 Program. Using administrative records, Chen et al. (2025) show that the policy imposed binding, target-based energy-saving requirements on regulated firms, leading to substantial reductions in both energy use and pollutant emissions. These reductions were achieved primarily through scale contraction rather than technological upgrading: total energy consumption declined by 13-16 percent, while output fell by 10-23 percent following the program's introduction. Importantly, regulated firms did not experience statistically significant improvements in energy efficiency relative to unregulated firms in the five years after the policy.[48] This adjustment pattern is consistent with the institutional features of the program discussed in Section B.3, which emphasized binding short-term energy-use targets and monitoring of total energy consumption rather than verifiable efficiency improvements.

Other firm-level studies reinforce this characterization of firms' responses. Ai et al. (2021) find that binding energy-use targets raised production costs and slowed output expansion among regulated firms, while Han et al. (2020) show that reductions in energy use were not accompanied by increased substitution toward cleaner energy sources such as natural gas or diesel.

Complementing large-sample analyses, Zhao et al. (2014) provide detailed case-study evidence from a large state-owned thermal power producer included in the Top 1,000 list. Between 2007 and 2010, the firm permanently shut down six old, low-efficiency generating units (Units 1-6), with a combined capacity of 365 MW, roughly one-third of its total capacity in 2005. Interview and administrative records clarify why capacity shutdowns dominated the adjustment margin. Environmental targets were evaluated over short horizons, while approval and construction of large-scale power generation projects typically require several years. Facing binding near-term targets and direct administrative pressure from the NDRC, the firm retired existing units to achieve immediate reductions in energy use rather than pursuing gradual efficiency improvements.[49]

To further clarify how regulated firms adjusted on the production margin, we examine firm-by-product output dynamics using monthly industrial product data from the ASIF (NBS 2000-2006). The purpose of this exercise is not to estimate the long-run effect of the policy on firm output, but rather to verify that regulated firms responded by reducing physical production rather than reallocating output across products or reporting margins. Following Chen et al. (2025), we use firms in the Top 10,000 as the control group and implement an event-study design that normalizes

[48] Although average energy efficiency increased by roughly 20 percent for both Top 1,000 firms and unregulated firms during this period, regulated firms did not exhibit differential gains relative to comparable control firms (Chen et al. 2025). This pattern is consistent with Wang and Yang (2025), who document systematic gaps between official policy assessments and estimates based on more rigorous empirical methods.

[49] The study also reports that these shutdowns were accompanied by provincial fiscal compensation exceeding 30 million RMB, underscoring the administrative and non-market nature of the adjustment process.

2005Q4 as the reference period.[50] The specification includes firm-product fixed effects, product-year-quarter fixed effects, and province-year-quarter fixed effects, with standard errors clustered two-way at the firm and product levels.

Figure G.10 shows a clear and immediate decline in product-level output among regulated firms following the program's implementation. At the firm-product level, output at Top 1,000 firms falls by approximately 8.7 percent relative to the control group. Because ASIF product data are only available through 2006Q4, this analysis captures production responses over at most four post-policy quarters. Given existing evidence that the effects of the Top 1,000 Program intensified during 2007-2010, this estimate should be interpreted as a lower bound on the policy-induced contraction in physical output.

C.2 Firm Level Spillover of the Top 1,000 Program

In Section 4.1, we interpret the absence of aggregate prefecture-level effects as being consistent with a reallocation of production and pollution toward dirtier regions under the Top 1,000 Program. If such reallocation operates through local markets, a corresponding pattern should emerge at the firm level: within the same prefecture, unregulated firms may expand production and energy use in response to contractions among regulated firms.

We use the Environmental Survey and Reporting (ESR) Database to examine the responses of unregulated firms in prefectures with different exposure to the Top 1,000 Program. Given that coal is the primary energy source for industrial firms in China, we use coal consumption as a proxy for energy consumption in our analysis. The exposure measure is the baseline employment share of Top 1,000 firms in each prefecture, and the empirical specification follows equation (2). All regressions exclude Top 1,000 firms themselves and focus exclusively on unregulated firms, while controlling for firm fixed effects, industry by year fixed effects, province by year fixed effects and Top 1,000 county by year fixed effects.

Figure G.11 reports the responses of unregulated firms. Panel A shows that following the introduction of the program, unregulated firms increased energy consumption and pollution emissions by approximately 7.6 percent (0.117×0.652) and 4.3 percent (0.117×0.371), respectively. Panel B examines energy and pollution intensities for unregulated firms. Similar to the regulated sample, the estimated coefficients are close to zero and statistically insignificant, indicating that the increase in emissions was driven primarily by scale expansion rather than deteriorating efficiency. These results suggest that part of the production and pollution activity constrained among regulated firms was reallocated toward unregulated firms within the same local markets.

To assess whether these positive spillovers reflect concurrent policy exposure, we test for mediation through the *National Specially Monitored Firms (NSMF)* initiative.[51] We augment the baseline specification with a triple interaction between Top 1,000 exposure, NSMF treatment, and the post-policy indicator. As shown in Table G.4, the coefficients on the baseline interaction term ($Top\ 1{,}000 \times Post$) remain statistically significant and economically stable, confirming that the observed spillovers are not confounded by the NSMF classification. The coefficients on the triple interaction terms are uniformly small and statistically indistinguishable from zero. This implies that NSMF firms—which are subject to direct supervision by the central government—did not experience less leakage than other unregulated firms. This finding is important: if the spillovers were caused by local governments relaxing environmental standards for unregulated firms, we

[50] We estimate the event study at quarterly frequency to average out temporal fluctuations.

[51] The NSMF initiative was launched in 2007, which placed key industrial polluters under special monitoring at the national level. See Zhang et al. (2018) for detailed analysis of this program.

would expect centrally monitored firms to be less affected. The lack of differential effects suggests that the spillovers are not driven by local regulatory enforcement, but rather reflect a reallocation of production driven by local market linkages.

D Robustness Checks

This section explores the robustness of the results in Section 4.3. We first perform general robustness checks in Section D.1, which shows that our results are robust to controlling for various heterogeneous trends, using alternative weights, using alternative exposure measures, or using alternative inference approach. Next we show that our results are robust to different levels of (dis-)aggregation. Section D.2 shows that our results are robust to province level aggregation, and Section D.3 shows that results are robust to using individual panel on health or mortality. These two exercises address concerns on bias due to migration or spatial spillovers.

D.1 Heterogeneous Trends, Weights, Exposure Measures, and Inference

We first explores the robustness of our results to heterogeneous trends by extending the set of prefecture characteristics used in Figure 4. Results are summarized in Figures G.19 to G.22. To ease comparison across specifications, we multiply the difference-in-differences coefficients by the mean exposure in Figure G.19 so that coefficients represent estimated effects for an averagely exposed prefecture.

Our "Full controls" specification of Figure 4 already used the following statistics:

- *Urban population share.*—Share of population residing in urban areas (cities or townships) as reported in the 2000 Population Census (NBS 2000). This variable accounts for various ways in which more urbanized prefectures might differ from rural prefectures.

- *Shares of young and old people.*—Share of young people aged 0-15 in 2000 and share of old people aged 65 or above in 2000, both of which are obtained from the 2000 Population Census (NBS 2000). These variables account for age structure differences.

- *Infant mortality.*—Infant mortality rate as reported in the 2000 Population Census (NBS 2000), which accounts for differences in initial health conditions.

- *Top 1,000 prefecture indicator.*—A dummy that equals one if the prefecture hosts at least one Top 1,000 firm in 2004 and zero otherwise, measured using the 2004 Economic Census (NBS 2004). This control implies that we are only exploring variation *within* exposed prefectures.

- *Two control zones dummy.*—A dummy that equals one if the prefecture belongs to the *Two Control Zones* (TCZ). The list of TCZ cities are obtained from the official website of Chinese government (`https://www.gov.cn/zhengce/zhengceku/2010-11/22/content_5181.htm`, accessed June 14, 2024). Although the TCZ policy began in 1998, the enforcement became much more stringent since 2006 during the 11-th Five Year Plan of China (Chen et al. 2018) and led to further reduction in mortality rates (Fan et al. 2023).

- *National Specially Monitored Firms (NSMF) share.*—Share of industrial employment working in NSMF in 2004. The list of NSMF is obtained from the official website of Chinese

government, as described in Section A.1. We create this variable in the same way as our exposure measure to Top 1,000 program, by merging the NSMF list with the 2004 Economic Census (NBS 2004). The NSMF program was launched in 2007 to strengthen central supervision of major polluters (Zhang et al. 2018), and thus could confound with the Top 1,000 program.

Results conditional on these heterogeneous trends are reported in columns (1) to (5) of Figure G.19.

Next we explore robustness to additional controls. Results are presented in columns (6) to (14) of Figure G.19 and Figures G.20 to G.22, and all coefficients remain reasonably stable. Below we describe the concerns and the controls in more details.

Additional Controls for Confounding Policies. To achieve the goal of reducing energy use per GDP by 20% during the 11th FYP, local governments might implemented parallel energy saving policies that might confound with the Top 1,000 program. To address this concern, we hand-collected prefecture-level energy-saving targets from local government work reports and policy documents released in 2006, the first year of the Eleventh Five-Year Plan. Among the 292 prefectures for which we obtained official reports, only 141 explicitly articulated quantified energy-saving targets. Panel A of Figure G.20 displays the distribution of these local targets. Most prefectures adopted the 20% reduction goal mandated by the central government, with very limited cross-sectional variation. This limited dispersion implies that prefecture-level heterogeneity in policy ambition was modest and unlikely to drive our main results.

Panel B of Figure G.20 presents an event-study specification analogous to equation (2), but augmented with year fixed effects interacted with each prefecture's energy-saving target. To ensure a consistent comparison, we also re-estimate our baseline specification on this same subsample of 141 prefectures. All resulting coefficients remain close to our baseline.

Additional Controls for Industrial Structure Differences. Our control of Top 1,000 prefecture by year fixed effects already account for any heterogeneous trends specific to exposed prefectures, but one might still concern that our exposure measure might be correlated with industry-specific shocks. To address this concern more systematically, Figure G.21 further controls for year fixed effects interacted with baseline employment share of a 2-digit industry (measured using the 2000 Population Census; NBS 2000) once a time. The figure confirms that our results are not driven by any single two-digit industry, with only three out of 92 regressions (the ones with controls for "fitting and decoration", "instruments, meters, cultural and office machinery", and "printing and record medium reproduction") yield coefficients outside the ninety-five percent confidence interval of our baseline specification.

Province-Year Fixed Effects. Our benchmark specification includes region-by-year fixed effects to absorb broad regional shocks. In columns (6) to (14) of Figure G.19, we further add province-by-year fixed effects, which control for province-level shocks common to all prefectures. Moreover, because our yearbook data are adjusted by province-year-specific multipliers to correct for fluctuations (see Section A.2), controlling for province-by-year fixed effects effectively relies on variation in the unadjusted raw entries.

Age Structure. A limitation of the yearbook data is that mortality rates are not age-adjusted. While prefecture-by-age mortality is unavailable annually, we mitigate this concern by

interacting year fixed effects with changes in the population age distribution between 2000 and 2010 (column (7)).[52]

Insurance Coverage. The 2000s saw rapid expansions of social insurance, notably the *New Rural Pension Scheme* (NRPS; Huang and Zhang 2021) and the *New Cooperative Medical Scheme* (NCMS; Gruber et al. 2023), both of which could confound health outcomes. To account for potential confounding from the concurrent expansion of social safety nets, column (8) interacts year fixed effects with baseline coverage rates in medical and pension insurance, computed using microdata from the 2005 mini-census (NBS 2005a).[53]

2008 Financial Crisis. Because Top 1,000 firms are also major exporters,[54] prefectures with greater exposure to the program may have been disproportionately affected by the 2008 global financial crisis through negative export demand shocks. To address this concern, column (9) interacts year fixed effects with each prefecture's baseline employment share in exporting firms, measured using the 2004 Economic Census (NBS 2004).

Related Firms. As highlighted by Chen et al. (2025), Top 1,000 firms often belong to larger conglomerates and may shift production to related affiliates. Omitting these within-group spillovers could bias our estimates. Column (10) adds year fixed effects interacted with the baseline employment share of related firms.[55]

Cross-Prefecture Spillovers. Prefectures are linked through trade, so a local shock could have spillover effects on nearby prefectures. Therefore, column (11) adds year fixed effects interacted with indirect exposure to Top 1,000 activity in nearby prefectures. Following Adão et al. (2019), we measure indirect exposure as

$$\text{Top 1,000 share}_d^{\text{indirect}} = \sum_{o \neq d} \frac{D_{od}^{-\delta}}{\sum_{o' \neq d} D_{o'd}^{-\delta}} \text{Top 1,000 share}_o, \tag{D.1}$$

where D_{od} denotes the travel time between locations o and d, and $\delta = 5$ governs the rate of distance decay.[56] The estimated direct effects remain virtually unchanged, suggesting that cross-prefecture spillovers are largely orthogonal to the program's direct impact.

We further show in Figure G.22 that the results are not sensitive to our choice of δ or using the 2010 road networks to measure travel times (Panels B-D and F-H). In addition to the fact that our estimates of the program's direct effects are barely affected, we find large and statistically significant indirect effects: mortality rate increased by 2.7-7.4 percent in the average indirectly exposed prefecture, even larger—though not statistically different—from the direct effect. This pattern echoes Adão et al. (2019), who document sizable but orthogonal spillover effects of the "China

[52] Specifically, we control for changes in the shares of population aged 0-15 and 65+.

[53] We use baseline coverage because by 2015 nearly all residents were insured (NBS 2015), so initial coverage is a more informative predictor of differential roll-out.

[54] According to the 2004 Economic Census, Top 1,000 firms account on average for about 15% of total industrial exports in prefectures that host at least one Top 1,000 firm.

[55] Related firms are defined as in Chen et al. (2025). Data sources, cleaning procedures, and summary statistics are provided in Section A.

[56] Travel times are computed from road and railway networks circa 2000; see Section A.7 for details.

shock'' on U.S. labor markets.[57] Hence, our baseline estimates likely represent a conservative lower bound of the program's total impact.

An alternative approach to address potential spillovers is to aggregate the data to a higher geographic level (i.e. province level aggregation). We discuss this approach below in Section D.2.

Regression Weights. We use baseline industrial employment as regression weights to reduce the influence of small, noisy prefectures. Columns (12) and (13) report results without weights and with population weights, respectively. Dropping weights slightly attenuates coefficients, consistent with greater noise in small prefectures. Weighting by population yields estimates close to the benchmark, suggesting that the program's effects were stronger in more industrialized prefectures.

Alternative Exposure. Finally, column (14) replaces the exposure denominator with total (all-industry) employment at baseline, and interacts year fixed effects with baseline industrial employment shares to capture differential industrial trends.

Inference. Figure G.19 reports 95% confidence intervals based on two complementary inference procedures. Throughout, we report confidence intervals constructed from standard errors clustered at the prefecture level. In addition, we report 95% confidence intervals obtained using the wild cluster bootstrap procedure of Cameron et al. (2008), with clustering at the province level. This alternative inference allows for arbitrary correlation in unobserved shocks within provinces over time and is well suited to settings with a limited number of higher-level clusters.

D.2 Province Level Analysis

We next assess the robustness of our findings using province-level data. Aggregation to the province level naturally absorbs cross-prefecture spillovers within provinces and mitigates concerns related to migration or spatial reallocation across prefectures. In addition, richer province-level data allow us to examine heterogeneity along dimensions that are unavailable in the prefecture panel.

Overall mortality. Figure G.23 reports estimates from province-level panels constructed using the *Population & Employment Statistics Yearbook* (NBS 2023). We estimate the following specification:

$$Y_{pt} = \sum_{\tau \neq 2005} \beta_\tau \big(\text{Top 1,000 share}_p \times \text{Year}_t\big) + \boldsymbol{\gamma}' \boldsymbol{x}_{pt} + \varepsilon_{pt}, \tag{D.2}$$

which mirrors specification (2), with prefecture-level variables replaced by their province-level counterparts. The control vector $\boldsymbol{x}_{pt}$ includes province fixed effects, region-by-year fixed effects, and year fixed effects interacted with the Top 10,000 employment share.

Figure G.23 shows that provinces exhibit parallel trends prior to 2005, followed by a clear and sustained increase in mortality after the program's introduction in 2006. The estimated effects are highly persistent, declining only modestly after the program's conclusion in 2011. This persistence is consistent with prior evidence that temporary income shocks can have long-lasting effects on mortality (e.g., Sullivan and von Wachter 2009). Quantitatively, we estimate a 5.7 percent increase in all-cause mortality in the averagely exposed province (mean Top 1,000 share of 0.097).

[57] They further show that under realistic spatial models, the indirect effects typically share the same sign as the direct effects, consistent with our findings.

This effect is roughly twice as large as our prefecture-level estimate for 2006–2010, though not statistically different, suggesting that aggregation may attenuate biases arising from within-province spillovers or migration.

Alternative exposure. Our baseline exposure measure is the employment share of Top 1,000 firms. As an alternative, we construct an exposure measure based on policy intensity: the ratio of the total energy-saving targets assigned to Top 1,000 firms to baseline total energy use. Because location-specific energy use data are available only at the provincial level, we implement this robustness check using the province-level panel in Figure G.23, replacing the benchmark exposure variable with this target-based measure.

Panel A of Figure G.24 plots the relationship between the two exposure measures. They are strongly correlated: the estimated slope is 0.128 (s.e. 0.036) with an R^2 of 0.30, indicating that provinces with greater Top 1,000 presence tended to face more ambitious energy-saving mandates. Panel B reports the corresponding event-study estimates using the target-based exposure. Both the dynamic pattern and magnitude closely resemble the baseline results. Given a mean exposure of 0.037, the estimated coefficient of 1.796 implies a $6.65\% = 0.037 \times 1.796$ increase in mortality in the averagely exposed province, comparable to the 5.7 percent increase obtained using the employment-based measure.

Heterogeneity. We further examine heterogeneity using province-gender-year mortality data disaggregated by cause of death and demographic group. As described in Section 3, cause-of-death information is drawn from Zhou et al. (2016) and is available for the years 1990 and 2013. Mortality rates by demographic group are constructed from tabulations of the 2000 and 2010 Population Censuses (NBS 2000, 2010). Both datasets report outcomes separately for males and females; we pool them to maximize statistical power. Following standard practice, we report standard errors clustered at the province level and complement them with wild cluster bootstrap inference following Cameron et al. (2008). In practice, the two inference procedures yield very similar results.

It is important to emphasize that causes of death differ substantially in baseline prevalence. As a result, heterogeneity in percentage responses across causes does not directly translate into their contribution to aggregate mortality. We therefore interpret the estimates below as describing differential responsiveness across causes and groups, while their aggregate importance is assessed through the decomposition analysis in Figure 5.

Panel A of Figure G.25 reports estimated effects for all-cause mortality, the nine most prevalent causes of death in 1990, and a residual category aggregating all remaining causes. We estimate a 7.2 percent increase in all-cause mortality in the averagely exposed province, consistent with the province-level event-study results in Figure G.23. Across causes, we find statistically significant increases for several categories, including metabolic disorders, chronic respiratory diseases, and neoplasms. While some less prevalent causes exhibit relatively large percentage responses, their mechanical contribution to excess deaths is limited by low baseline incidence. In contrast, more prevalent causes—particularly respiratory diseases and cancers—account for a much larger share of the overall mortality increase, as shown in the decomposition results.

Panels B through D examine heterogeneity by demographic group. Mortality increases are concentrated among urban residents, males, and individuals of working age (15-64). These patterns closely mirror the decomposition results in Figure 5, which show that excess deaths are driven primarily by demographic groups with greater exposure to income losses induced by the program.

D.3 Individual Level Analysis

A limitation of mortality analyses based on aggregate statistics is that migration may bias estimates. We therefore turn to individual-level panel data on mortality and health, which are not affected by migration.

We begin with elderly mortality using the *Chinese Longitudinal Healthy Longevity Survey* (CLHLS), which tracks individuals aged 65 or above across 22 provinces.[58] Following Jensen and Richter (2004), we estimate:

$$Y_{ipt} = \sum_{t \neq 2005} \beta_t \left(\text{Top 1,000 share}_p \times \text{Year}_t \right) + \boldsymbol{\gamma}' \boldsymbol{x}_{ipt} + \varepsilon_{ipt},$$

where Y_{ipt} equals one if individual i at province p dies in year t and zero otherwise. Because the CLHLS only provides province identifiers, we use province-level exposure measures Top 1,000 share$_p$ as defined in Section D.2.

Figure G.26 reports the results. Panel A controls for demographic characteristics (age, gender, and ethnicity), province fixed effects, region-by-year fixed effects, and year effects interacted with baseline employment shares of Top 10,000 firms. We find a sharp post-2005 rise in elderly mortality, with an average post-pre difference of 0.223. Panel B further adds individual fixed effects, and the results change only mildly.

We next use the *China Health and Nutrition Survey* (CHNS), which covers all age groups across 49 prefectures in nine provinces from 2004-2011. Compared with the CLHLS, the CHNS (i) is not limited to the elderly, (ii) measures health conditions during the four weeks prior to each interview, and (iii) includes prefecture identifiers, allowing us to exploit cross-prefecture variation in exposure.[59]

Panel A of Figure G.27 shows the event-study results for heart disease or chest pain, controlling for individual and age fixed effects along with our baseline controls. We find a significant increase in incidence beginning in 2006, rising sharply through 2009 and stabilizing thereafter. The post-pre difference of 0.077 implies that in the average prefecture (mean exposure 0.117), the probability of reporting heart disease or chest pain increased by $0.009 = 0.077 \times 0.117$, a 53% rise relative to the pre-policy mean (0.017). Panel B of Figure G.27 summarizes difference-in-differences estimates across all diseases, showing significant increases only for heart disease. This finding is consistent with the province-level evidence that cardiorespiratory mortality rose sharply following the program.

We also use the CLHLS and CHNS micro data to examine heterogeneity by region (urban versus rural). Figure G.28 presents the results. We find consistently larger effects among urban residents, both for elderly mortality in the CLHLS (Panel A) and for the probability of having heart disease or chest pain in the CHNS (Panel B).The estimated urban-rural difference is highly significant at the 5% level for health outcomes in the CHNS (Panel B). For elderly mortality in the CLHLS (Panel A), the difference is marginally significant at the 10% level ($p \approx 0.08$). The stronger impacts in urban areas align with the program's focus on industrial and energy-intensive enterprises, which are predominantly located in urban non-agricultural sectors.

[58] See Section A.2 for details of the data.

[59] Province-level variation alone is insufficient for identification given the small number of provinces.

E Discussion of Alternative Mechanisms

So far, we have emphasized the misallocation channel, but the Top 1,000 Program may also affect mortality through alternative mechanisms. In this section, we show that these alternative explanations are not consistent with the empirical evidence. We focus on three main channels. First, although prefecture-wide average pollution does not change, factor reallocation within prefectures could increase *exposure* to pollution, as highlighted by Hernandez-Cortes and Meng (2023). Second, the program might induce residents to relocate across townships within prefectures, mechanically increasing mortality by shifting population toward locations with higher baseline mortality rates.[60] Third, because Top 1,000 firms are major taxpayers, reduced production could tighten local fiscal budgets and thereby worsen healthcare supply. Finally, in the last subsection, we present additional evidence supporting reduced income as the primary driver of the mortality response.

E.1 Pollution Exposure

We begin by examining whether the program increased pollution exposure. To this end, we study the program's impact on *population-weighted* pollution exposure. We collect township-level population data from the 2000 and 2010 censuses (NBS 2000, 2010) and compute weighted-average AOD exposure by combining population shares with township-level (log) average AOD concentrations:[61]

$$\text{Exposed pollution}_{dt} = \sum_{k \in d} \ell_{kdt} \text{Pollution}_{kdt}, \tag{E.1}$$

where ℓ_{kdt} denotes the share of the population residing in township k in prefecture d in year t, and Pollution_{kdt} denotes township-level pollution concentration. Changes in exposed pollution can be decomposed using the following accounting identity:

$$\Delta\text{Exposed pollution}_{d} = \underbrace{\sum_{k \in d} \Delta\ell_{kd} \text{Pollution}_{kdt_0}}_{\text{Population reallocation}} + \underbrace{\sum_{k \in d} \ell_{kdt_1} \Delta\text{Pollution}_{kd}}_{\text{Pollution reallocation}}, \tag{E.2}$$

where t_0 denotes the start period, t_1 the end period, and Δ the change between t_0 and t_1. In the analysis below, we set $t_0 = 2000$ and $t_1 = 2010$, given data availability.[62]

Table G.6 reports the estimation results, based on a long-difference analogue of specification (2). Column (1) reports the program's impact on unweighted average pollution across townships. Consistent with Panel E of Figure 2, we find a small and statistically insignificant effect of the

[60] As highlighted by Allcott et al. (2019), Deryugina and Molitor (2020), and Finkelstein et al. (2021), location is an important determinant of residents' health. See Deryugina and Molitor (2021) for a discussion of the broader literature.

[61] Townships are the smallest geographic units for which population data are disclosed. As the lowest-level formal administrative units, townships are comparable in size to small U.S. cities: the average township contains approximately 20 villages, has about 30,000 residents, and spans nearly 80 square kilometers. Township shapefiles and population data are obtained from Dingel et al. (2021). To harmonize boundary changes over time, we apportion 2000 population to 2010 administrative boundaries based on overlapping areas.

[62] Because AOD data are available only starting in 2001, we use 2001 values to proxy for 2000.

program on prefecture-wide average pollution.[63]

Column (2) reports changes in population-weighted pollution exposure. The coefficient declines from −0.8 percent in column (1) to −2.3 percent, although the estimate is imprecisely measured. This larger decline reflects the fact that *exposed* pollution decreased. Columns (3) and (4) decompose this change into the two components in equation (E.2). The results indicate that within-location pollution reductions (column (4)) account for the bulk of the decline in pollution exposure, while population reallocation contributes very little. This pattern is consistent with the fact that AOD concentrations declined in locations near regulated firms (Panel C of Figure 2) and in downwind areas (Table G.3).

In sum, using highly granular population and air-pollution data, we find no evidence that the program increased pollution exposure. If anything, pollution exposure declined slightly, though the effect is not statistically significant.

E.2 Household Relocation

We next examine whether the program induced a systematic relocation of households across townships within prefectures, which is often termed as endogenous household sorting. If the program caused residents to move from relatively healthy areas to locations with higher baseline mortality or inferior public infrastructure, the aggregate mortality rate at the prefecture level would rise mechanically, even in the absence of any change in individual biological health risk (Allcott et al. 2019; Deryugina and Molitor 2020).

Following the decomposition in equation (E.2), we isolate the impact of population reallocation by estimating the program's effect on the population-weighted average of baseline township characteristics. Specifically, for each prefecture d, we construct the dependent variable as:

$$\Delta\text{Sorting Component}_d = \sum_{k \in d} \Delta \ell_{kd} \ln Y_{kdt_0},$$

where $\Delta \ell_{kd}$ is the change in the population share of township k between 2000 and 2010, and Y_{kdt_0} denotes the baseline characteristic of township k measured in the 2000 census. By holding the township characteristics constant at their baseline levels, this measure captures changes in prefecture-level outcomes driven solely by the shifting spatial distribution of the population across townships.

Table G.7 reports the results. We examine a wide range of baseline township characteristics, including mortality rates, infant mortality, and various dimensions of housing quality and infrastructure. Column (1) shows that the program had a small and statistically insignificant effect on the population-weighted average of baseline mortality ($\beta = 0.010, p > 0.10$). Similarly, we find no significant impact on the sorting toward townships with higher baseline infant mortality (column (2)). Beyond health outcomes, we examine whether residents relocated to townships with poorer public services or housing conditions. Columns (3) through (8) report estimates for housing-related indicators. While a few coefficients reach statistical significance, their economic magnitudes are relatively modest and their directions are inconsistent. For instance, although we observe a negative correlation between program exposure and sorting toward townships with tap

[63] The coefficient differs from that in Panel E of Figure 2 for two reasons. First, column (1) of Table G.6 uses a long-difference specification, whereas Panel E of Figure 2 uses an event-study specification with the Delta method. Second, we use the mean of log pollution concentrations as the outcome here, while Panel E of Figure 2 uses the log of mean pollution concentrations (Jensen's inequality).

water (column (4), $\beta = -0.094$), we simultaneously find a positive shift toward townships with independent lavatories (column (6), $\beta = 0.048$). The lack of a consistent downward trend across these multi-dimensional infrastructure proxies suggests that systematic household relocation to lower-quality areas is not the primary driver of our results.

Our main estimates in Figure 4 suggest that the Top 1,000 Program increased all-cause mortality by approximately 3.6 percent (0.311×0.117) in the average exposed prefecture. In comparison, the point estimate for the sorting component in Column (1) of Table G.7 indicates that household relocation led to a negligible mortality increase of only 0.12 percent (0.010×0.117) for the average prefecture. This sorting effect explains only about 3% of the baseline total mortality effect. The fact that this sorting component is both statistically insignificant and economically negligible suggests that our main findings are not driven by the mechanical reshuffling of the population across locations. Instead, the observed rise in mortality predominantly stems from an actual increase in mortality rates within locations.

E.3 Healthcare Supply

Next, we examine whether the program affected local healthcare supply. Columns (1)-(3) of Table G.8 report the program's impacts on the number of hospitals, hospital beds, and doctors, all measured on a per capita basis. We find no statistically significant association between the program and the supply of hospitals (column (1)) or hospital beds (column (2)), but a significant decline in the number of doctors (column (3)). Quantitatively, the average exposed prefecture experienced a 2.7 percent reduction in doctors per capita (-0.235×0.117). Thus, local healthcare supply indeed deteriorated along this dimension.

Do these changes in healthcare supply help explain the observed mortality responses? Column (4) re-estimates the program's impact on mortality while additionally controlling for these healthcare supply measures. The estimated mortality effect is essentially unchanged relative to Panel A of Figure 4, suggesting that reductions in healthcare supply do not meaningfully account for the increase in mortality.

One concern is that directly controlling for healthcare supply may introduce a "bad control" problem, since these variables are potentially endogenous and we lack credible instruments. To address this, columns (5)-(8) explore heterogeneity by the fraction of public hospitals.[64] If the program raised mortality through a deterioration in healthcare supply, one would expect larger mortality increases in prefectures that rely more heavily on the public healthcare system. Consistent with this mechanism, columns (5)-(7) show that prefectures with higher public-hospital shares experienced larger declines in the number of hospitals (column (5)), hospital beds (column (6)), and doctors (column (7)). However, column (8) yields a negative and statistically insignificant interaction effect on mortality, which is not consistent with a healthcare-supply channel driving the mortality increase.

E.4 More Direct Evidence on Income-Driven Mortality Increase

So far, our main argument that reduced income is the primary source relies on the fact that the program increased vulnerability to extreme heat shocks, and the mortality effects are most

[64] We use measure this the fraction of staff in public hospitals among all hospital-sector staff (3-digit CIC code 831) in 2008, using the 2008 Economic Census (NBS 2008). Across 345 prefectures, the average (median) fraction of public hospital is 87% (88%) with standard deviation 9.7%.

pronounced for the demographic groups whose income rely more heavily on regulated firms (Section 4.3). This section presents more direct evidence that the documented mortality increase is primary due to reduced income.

Place of death. We first utilize detailed longitudinal records from the CLHLS to examine the impact of the program on the specific place of death. Specifically, we categorize the place of death into three mutually exclusive groups: at home, in a hospital, and in other places (e.g., work place or public spaces), which serves as a high-frequency proxy for medical resource utilization and the intensity of formal healthcare intervention at the end of life. Following the empirical framework established in Section D.3, we exploit the variation in provincial exposure to the Top 1,000 Program to estimate changes in the probability of dying in different settings. Figure G.30 documents a significant 2.7 percentage points (0.281×0.097) increase in the probability of dying at home in the averagely exposed province, whereas deaths in hospitals show no statistically significant change. As aggregate mortality within the CLHLS sample for the averagely exposed province increased by 2.9 percentage points (0.303×0.097), the vast majority of the mortality surge is attributable to deaths occurring at home. This pattern suggests a deterioration in effective medical access among the elderly. The observed compositional shift in place of death suggests that the program-induced income loss pushed households toward an interior solution where expensive hospital-based care became unaffordable, forcing a substitution toward lower-cost home settings.

Heterogeneity by insurance enrollment. We further investigate the moderating role of financial protection by examining the heterogeneity of health responses according to baseline medical insurance status. We utilize individual-level panel data from CLHLS and CHNS to perform sub-sample difference-in-differences based on pre-program insurance status. The classification of insurance status is tailored to the specific variables available in each dataset. In the CHNS, we define "insured" using a broad measure of public medical insurance, encompassing the Urban Employee Basic Medical Insurance and the New Rural Cooperative Medical Scheme (NCMS). In the CLHLS, we focus on severe disease medical insurance, which historically included supplementary unit-based reimbursement and catastrophic illness schemes. This specific form of coverage is designed to mitigate the prohibitive costs of treating life-threatening conditions, making it a particularly relevant proxy for financial protection against deadly health shocks. Following the identification strategy described in Section D.3, we use death as the dependent variable in the CLHLS and the prevalence of heart disease and chest pain in the CHNS.[65] Exposure is measured at the provincial level for the CLHLS and at the prefecture level for the CHNS.

Table G.9 reports the results from these sub-sample estimations. We find that the adverse health impacts are most robustly identified among individuals without insurance coverage. In the CLHLS sample, uninsured individuals in an averagely exposed province experienced a significant 3.0 percent (0.306×0.097) increase in mortality. Similarly, in the CHNS, the uninsured experienced a 0.9 percentage point (0.077×0.117) increase in the probability of reporting heart disease or chest pain. In contrast, the point estimates for individuals covered by medical insurance are smaller in magnitude and lack statistical precision. While these null results for the insured group are consistent with a protective role of insurance, we acknowledge that the large standard errors likely reflect limited statistical power in these smaller subsamples, and a formal test cannot reject the

[65] The Top 1,000 Program generated significant increases only for heart disease and chest pain in the CHNS baseline (Figure G.27)

equality of coefficients between the two groups. Nonetheless, these findings are highly suggestive that the program's health consequences are mediated by an income mechanism, as the most severe impacts are concentrated among populations lacking adequate financial safety nets (Cheng et al. 2015). Overall, these heterogeneous results provide compelling evidence that the program's adverse health consequences are fundamentally driven by an income mechanism, where the impact is concentrated among populations lacking adequate financial and institutional safety nets.

F A Model of Energy Regulation

We build on Hsieh and Klenow (2009) to derive a model-based sufficient statistic consistent with our empirical exposure measure. The framework nests, under standard parameter restrictions, both the baseline Hsieh and Klenow (2009) environment and the conglomerate production variant in Chen et al. (2025). Two extensions are central for our application: (i) heterogeneous energy intensity across affiliates and (ii) roundabout production that captures propagation of upstream regulation through input-output links.[66]

Demand and market structure. A competitive final producer aggregates varieties $\omega \in \Omega$ by CES:

$$Y = \Big(\int_{\omega} q(\omega)^{\frac{\sigma-1}{\sigma}} \, d\omega \Big)^{\frac{\sigma}{\sigma-1}}, \qquad \sigma > 1.$$

Monopolistic competitors charge a constant markup $\mu \equiv \sigma/(\sigma-1)$. Standard demand implies

$$q(\omega) = \big(P/p(\omega)\big)^{\sigma} R, \qquad p(\omega) = \mu \cdot MC(\omega).$$

Technology and the Top 1,000 shadow tax. Within conglomerate ω, affiliate $i = 1, \ldots, n(\omega)$ produces

$$q(\omega, i) = \varphi(\omega, i) \left[\min\{ l(\omega, i), \nu(\omega, i)^{-1} e(\omega, i) \} \right]^{\alpha} m(\omega, i)^{\beta},$$

with $\alpha, \beta > 0$ and $\alpha + \beta < 1$. Materials m are purchased at price P out of the final good; energy e is purchased at price p_e. The Top 1,000 quota is isomorphic to an affiliate-specific shadow tax $\tau(\omega, i)$ on energy, so the *composite variable-input price* is

$$\tilde{w}(\omega, i) \equiv w + \nu(\omega, i) \, (1 + \tau(\omega, i)) \, p_e.$$

Because of Leontief between l and e, optimal within-plant mix is $e = \nu \, l$, and cost shares imply $Pm = (\beta/\alpha) \, \tilde{w} \, l$. Therefore each affiliate has an equivalent value-added representation in l only:

$$q(\omega, i) = \varphi(\omega, i) \left(\tfrac{\beta}{\alpha} \tfrac{\tilde{w}(\omega, i)}{P} \right)^{\beta} l(\omega, i)^{\alpha+\beta}.$$

[66] To keep the exposition compact, we focus on key steps and omit algebraic derivations that follow standard manipulations; these are available from the authors upon request.

Conglomerate cost minimization. Let $l(\omega) \equiv \sum_i l(\omega, i)$. Minimizing the wage bill $\frac{\alpha+\beta}{\alpha} \sum_i \tilde{w}(\omega, i) l(\omega, i)$ subject to aggregate output $q(\omega) = \sum_i q(\omega, i)$ yields the *labor allocation weights*:

$$l(\omega, i) \;\propto\; \varphi(\omega, i)^{\frac{1}{1-\alpha-\beta}} \; \tilde{w}(\omega, i)^{-\frac{1-\beta}{1-\alpha-\beta}}.$$

Define two conglomerate shifters (both central later):

$$\tilde{\varphi}(\omega) \;\equiv\; \sum_i \varphi(\omega, i)^{\frac{1}{1-\alpha-\beta}} \; \tilde{w}(\omega, i)^{-\frac{\alpha}{1-\alpha-\beta}}, \quad \tilde{\mu}(\omega)^{-1} \;\equiv\; \frac{\omega \sum_i \varphi(\omega, i)^{\frac{1}{1-\alpha-\beta}} \; \tilde{w}(\omega, i)^{-\frac{1-\beta}{1-\alpha-\beta}}}{\sum_i \varphi(\omega, i)^{\frac{1}{1-\alpha-\beta}} \; \tilde{w}(\omega, i)^{-\frac{\alpha}{1-\alpha-\beta}}}.$$

Intuitively, $\tilde{\varphi}(\omega)$ is an "effective productivity" that embeds affiliate wedges, while $\tilde{\mu}(\omega)^{-1}$ is a within-conglomerate cost-share index.

Lemma 1 (Conglomerate revenue index)**.** *There exists $\zeta \in (0, 1)$ such that conglomerate revenue satisfies*

$$r(\omega) \;\propto\; \tilde{\varphi}(\omega)^{\zeta}, \qquad \zeta \equiv \frac{\sigma - 1}{\sigma} \cdot \frac{\frac{1-\alpha-\beta}{\alpha+\beta}}{\frac{1-\alpha-\beta}{\alpha+\beta} + \frac{1}{\sigma}}.$$

Lemma 2 (Labor share and employment)**.** *The conglomerate labor share equals α/μ times a composition term, and employment satisfies*[67]

$$\frac{w\, l(\omega)}{r(\omega)} \;=\; \frac{\alpha}{\mu}\, \tilde{\mu}(\omega)^{-1}, \qquad l(\omega) \;\propto\; \tilde{\mu}(\omega)^{-1} \; \tilde{\varphi}(\omega)^{\zeta}.$$

Aggregation. Labor market clearing $\int_\omega l(\omega)\, d\omega = L$ determines the equilibrium wage w given $\{\tilde{\varphi}, \tilde{\mu}\}$. A standard CES aggregation then delivers:

Proposition F.1 (Output and price index)**.** *Let*

$$\eta_1 \equiv \frac{\sigma - (\sigma - 1)\beta}{(\sigma - 1)(1 - \beta)} > 1.$$

Aggregate output and the price index satisfy

$$Y \;\propto\; L^{\frac{\alpha}{1-\beta}} \; \frac{\left(\int \tilde{\varphi}(\omega)^{\zeta}\, d\omega \right)^{\eta_1}}{\left(\int \tilde{\mu}(\omega)^{-1} \tilde{\varphi}(\omega)^{\zeta}\, d\omega \right)^{\frac{\alpha}{1-\beta}}}, \qquad P \;\propto\; L^{\frac{1-\alpha-\beta}{1-\beta}} \; \frac{\left(\int \tilde{\varphi}(\omega)^{\zeta}\, d\omega \right)^{-\frac{1}{1-\beta}}}{\left(\int \tilde{\mu}(\omega)^{-1} \tilde{\varphi}(\omega)^{\zeta}\, d\omega \right)^{-\frac{1-\alpha-\beta}{1-\beta}}}.$$

Totally differentiating the (log) output expression yields a transparent sufficient statistic.

[67] In a standard framework with constant returns ($\alpha+\beta = 1$) and no markup, the labor share of cost is $\alpha/(\alpha+\beta)$. However, with decreasing returns and markups, the optimal labor-to-revenue ratio is determined by $wl/r = \alpha/\mu$. Consequently, β cancels out in the revenue-based labor share, and the conglomerate labor share simplifies to $(\alpha/\mu)\, \tilde{\mu}(\omega)^{-1}$.

Proposition F.2 (A sufficient statistic for wedges)**.** *Let*

$$s_r(\omega) \equiv \frac{\tilde{\varphi}(\omega)^{\zeta}}{\int \tilde{\varphi}^{\zeta}}, \qquad s_l(\omega) \equiv \frac{\tilde{\mu}(\omega)^{-1}\tilde{\varphi}(\omega)^{\zeta}}{\int \tilde{\mu}^{-1}\tilde{\varphi}^{\zeta}},$$

and for each ω define affiliate weights

$$\tilde{s}_q(\omega,i) \equiv \frac{\varphi(\omega,i)^{\frac{1}{1-\alpha-\beta}}\tilde{w}(\omega,i)^{-\frac{\alpha}{1-\alpha-\beta}}}{\sum_j \varphi(\omega,j)^{\frac{1}{1-\alpha-\beta}}\tilde{w}(\omega,j)^{-\frac{\alpha}{1-\alpha-\beta}}}, \quad \tilde{s}_l(\omega,i) \equiv \frac{\varphi(\omega,i)^{\frac{1}{1-\alpha-\beta}}\tilde{w}(\omega,i)^{-\frac{1-\beta}{1-\alpha-\beta}}}{\sum_j \varphi(\omega,j)^{\frac{1}{1-\alpha-\beta}}\tilde{w}(\omega,j)^{-\frac{1-\beta}{1-\alpha-\beta}}}.$$

Then small changes in affiliate wedges $d\ln\tilde{w}(\omega,i)$ imply

$$\begin{aligned} d\ln Y \;=\; & \frac{\alpha}{1-\beta}\, d\ln L \;-\; \kappa_1 \int \sum_i s_r(\omega)\,\tilde{s}_q(\omega,i)\, d\ln\tilde{w}(\omega,i)\, d\omega \\ & +\; \kappa_2 \int \sum_i s_l(\omega)\,\tilde{s}_l(\omega,i)\, d\ln\tilde{w}(\omega,i)\, d\omega \\ & -\; \kappa_3 \int \sum_i s_l(\omega)\,\tilde{s}_q(\omega,i)\, d\ln\tilde{w}(\omega,i)\, d\omega, \end{aligned}$$

where $\kappa_1 \equiv \dfrac{\alpha}{1-\alpha-\beta}\cdot\dfrac{\sigma-(\sigma-1)\beta}{(\sigma-1)(1-\beta)}\cdot\zeta$, $\kappa_2 \equiv \dfrac{\alpha}{1-\alpha-\beta}$, *and* $\kappa_3 \equiv \dfrac{\alpha^2}{(1-\beta)(1-\alpha-\beta)}(1-\zeta)$.

Connection to our exposure measure. To map to our empirical exposure, impose two empirically plausible normalizations: (i) within a conglomerate, affiliates share a common energy intensity $\nu(\omega,i) \equiv \nu(\omega)$, so $\tilde{s}_q(\omega,i) = \tilde{s}_l(\omega,i)$; (ii) regulated affiliates face a common shadow change $d\ln\tilde{w}(\omega,i) \equiv \bar{\tau}$ (consistent with Chen et al. (2025) who find little cross-firm dispersion).[68] Under (i)-(ii), Proposition F.2 collapses to

$$\begin{aligned} d\ln Y \;=\; & \frac{\alpha}{1-\beta}\, d\ln L \;-\; \frac{\alpha}{1-\alpha-\beta}\Bigg[\underbrace{\frac{s_r}{s_l}\cdot\frac{\sigma-(\sigma-1)\beta}{(\sigma-1)(1-\beta)}\cdot\zeta}_{\text{demand/markup channel}} \\ & +\; \underbrace{\frac{\alpha}{1-\beta}(1-\zeta)}_{\text{intra-conglomerate composition}} \;-\; 1\Bigg]\, s_l\,\bar{\tau} \end{aligned}$$

where $s_r \equiv \int s_r(\omega)\,d\omega$ and $s_l \equiv \int s_l(\omega)\,d\omega$ are the aggregate revenue- and labor-weighted exposures to the Top 1,000 shadow cost. This is exactly the empirical *exposure measure* we implement: a single sufficient statistic that combines (a) how wedges load on effective productivity $\tilde{\varphi}$ (revenue weights) and (b) how they load on the wage bill (labor weights).

Interpretation. The bracketed term is positive for standard parameter values ($\sigma > 1$, $\alpha,\beta \in (0,1)$, $\alpha+\beta<1$). Hence a higher shadow cost $\bar{\tau}$ lowers Y proportionally to the exposure s_l, with an elasticity that (i) rises with substitution possibilities (larger σ); (ii) rises with labor's curvature α; and (iii) is amplified when materials intensity β is high (since $\eta_1 > 1$).

[68] Heterogeneous ν or τ only reweights the sums by $\tilde{s}_q$ and $\tilde{s}_l$; the sufficient statistic remains linear in $d\ln\tilde{w}$.

G Additional Figures and Tables

Panel A. Geographic distribution of Top 1,000 firms



Panel B. Prefecture exposure



Figure G.1: Geographic Distribution of Top 1,000 Firms

Notes: Panel A plots the geographic distribution of Top 1,000 firms (blue dots) as well as the railway network in 1962 (orange lines). Panel B plots the prefecture-level exposure to the program. Shaded areas indicate the share of baseline prefecture employment accounted for by Top 1,000 firms, with darker colors corresponding to higher exposure.
Sources: NBS (2004); Baum-Snow et al. (2017).

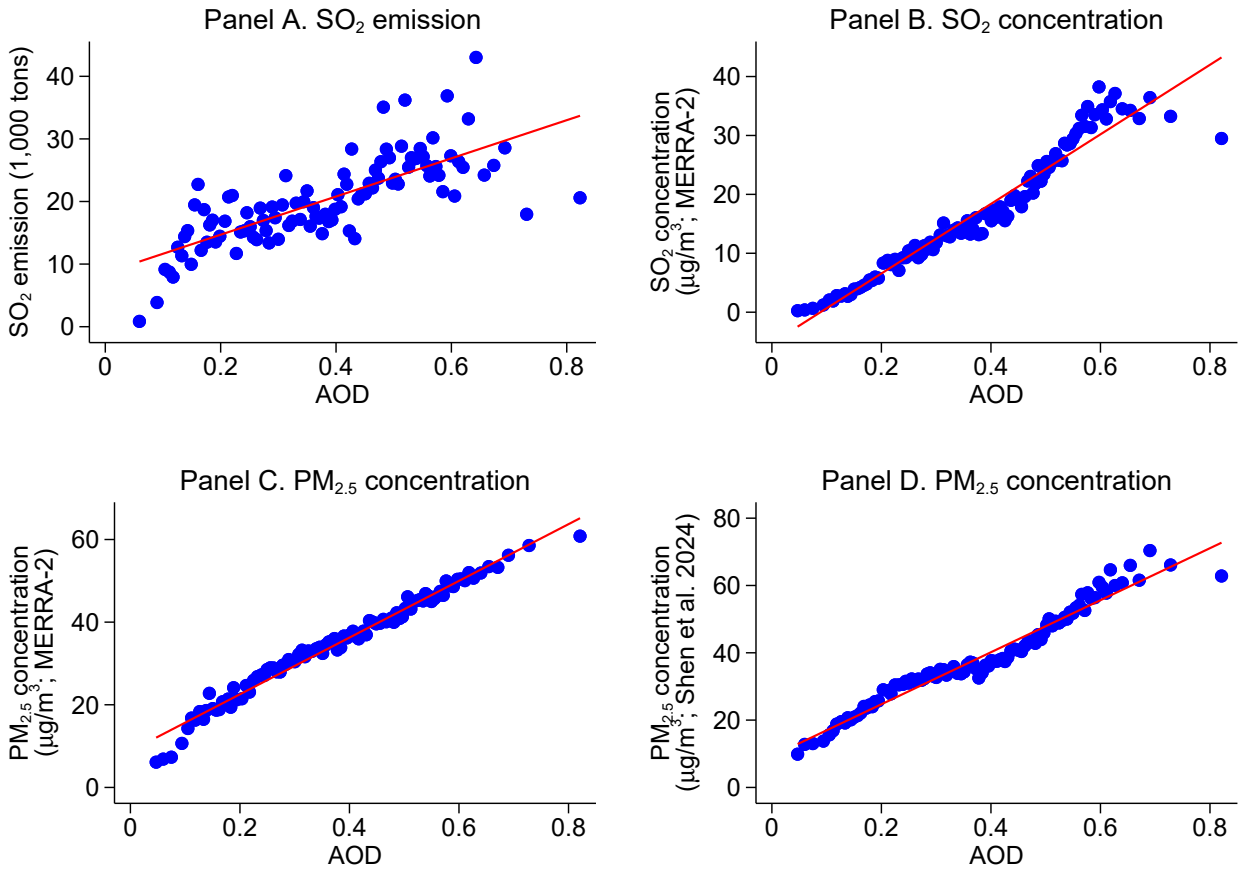


Figure G.2: Correlations between AOD and SO_2 and $PM_{2.5}$

Notes: This graph shows prefecture-year level aggregate SO_2 emission (Panel A), SO_2 concentration (Panel B), $PM_{2.5}$ concentration (Panels C and D) by 100 equal bins of AOD, for years 2001 to 2011. Aggregate SO_2 emission is aggregated using micro data from MEP (2002-2011). SO_2 and $PM_{2.5}$ concentration in Panels B and C are obtained from Modeling and Assimilation Office (GMAO). $PM_{2.5}$ concentration in Panel C is calculated using the formula of Buchard et al. (2016). $PM_{2.5}$ concentration in Panel D is obtained from Shen et al. (2024).
Sources: Lyapustin et al. (2015); Modeling and Assimilation Office (GMAO); Shen et al. (2024); MEP (2002-2011).

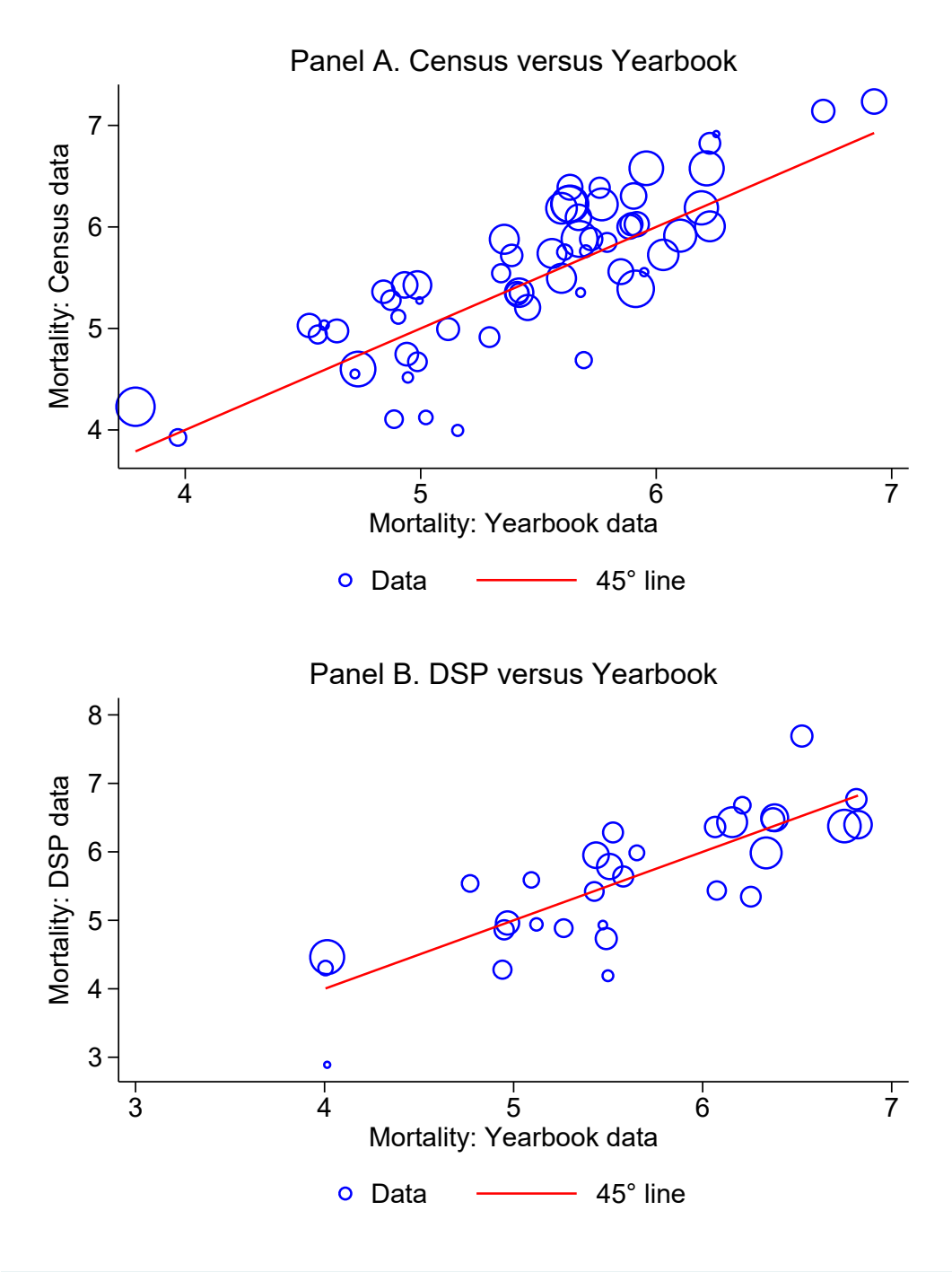


Figure G.3: Quality Check of Mortality Data from Population & Employment Statistics Yearbook

Notes: Panel A compares province-level mortality rates from China Population & Employment Statistics Yearbook against census data in 2000 and 2010. Panel B compares compares province-level mortality rates from China Population & Employment Statistics Yearbook against data from the China's Disease Surveillance Points (DSP) system in 2019. Yearbook data are rescaled by a factor of 0.9 to show that different sources align closely with each other (up to a scalar). This simple multiplicative normalization has no bearing on cross-sectional or temporal variation used in our analysis because we apply a logarithm transformation of mortality rates. Sizes of dots correspond to population.
Sources: NBS (2023, 2000, 2010); Qi et al. (2022).

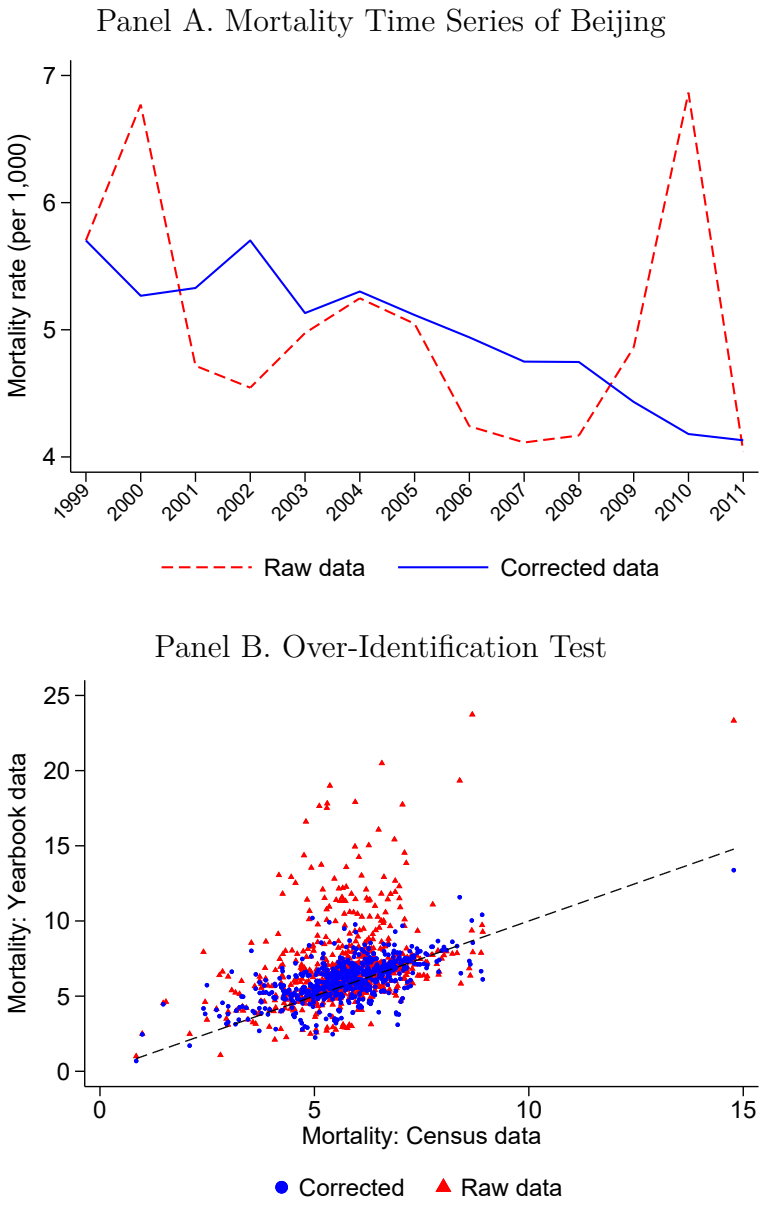


Figure G.4: Correction of the Yearbook Data and Over-Identification Test

Notes: Panel A plots the raw and corrected mortality series for Beijing. The raw yearbook data exhibit implausible fluctuations, while the correction procedure smooths the series and aligns more closely with independent data sources. Panel B compares prefecture-level mortality rates from yearbooks against census data in 2000 and 2010, where we omit one dot with exceptionally high raw mortality rate (62.417 ‰) for readability. The corrected series shows markedly better alignment with the census benchmark, reducing measurement error relative to the raw yearbook values.
Sources: NBS (2000, 2010, 2000-2012).

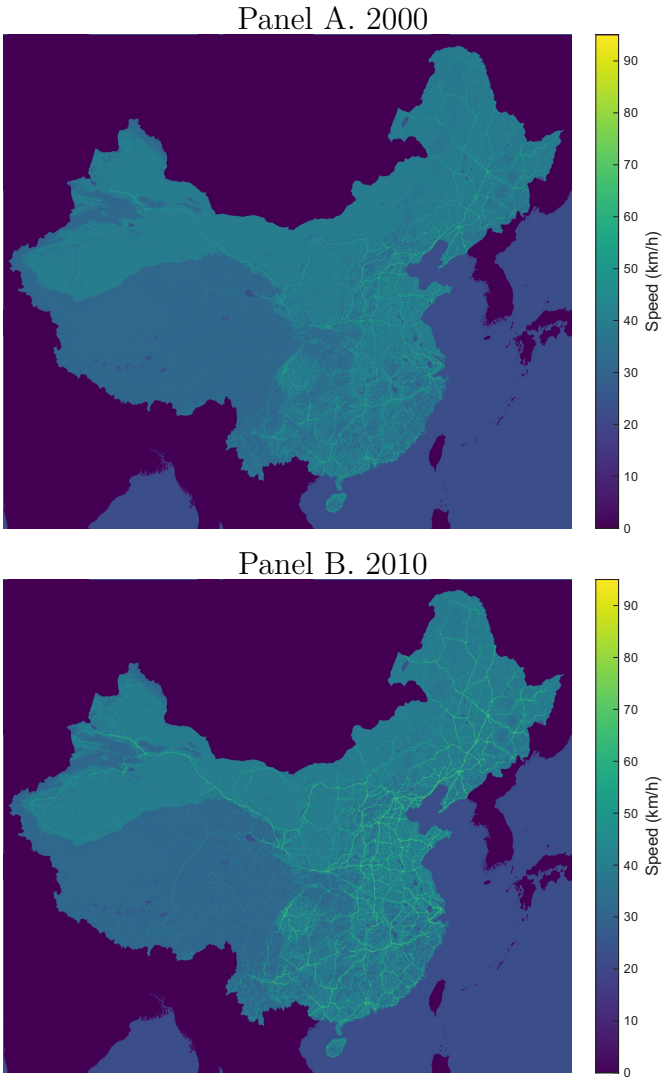


Figure G.5: Travel Speed Map for China in 2000 and 2010

Notes: The figure plots estimated travel speed in each 1 kilometer × 1 kilometer grid point for China in 2000 (Panel A) and 2010 (Panel B).
Sources: Authors' calculations. See Section A.7 for details.

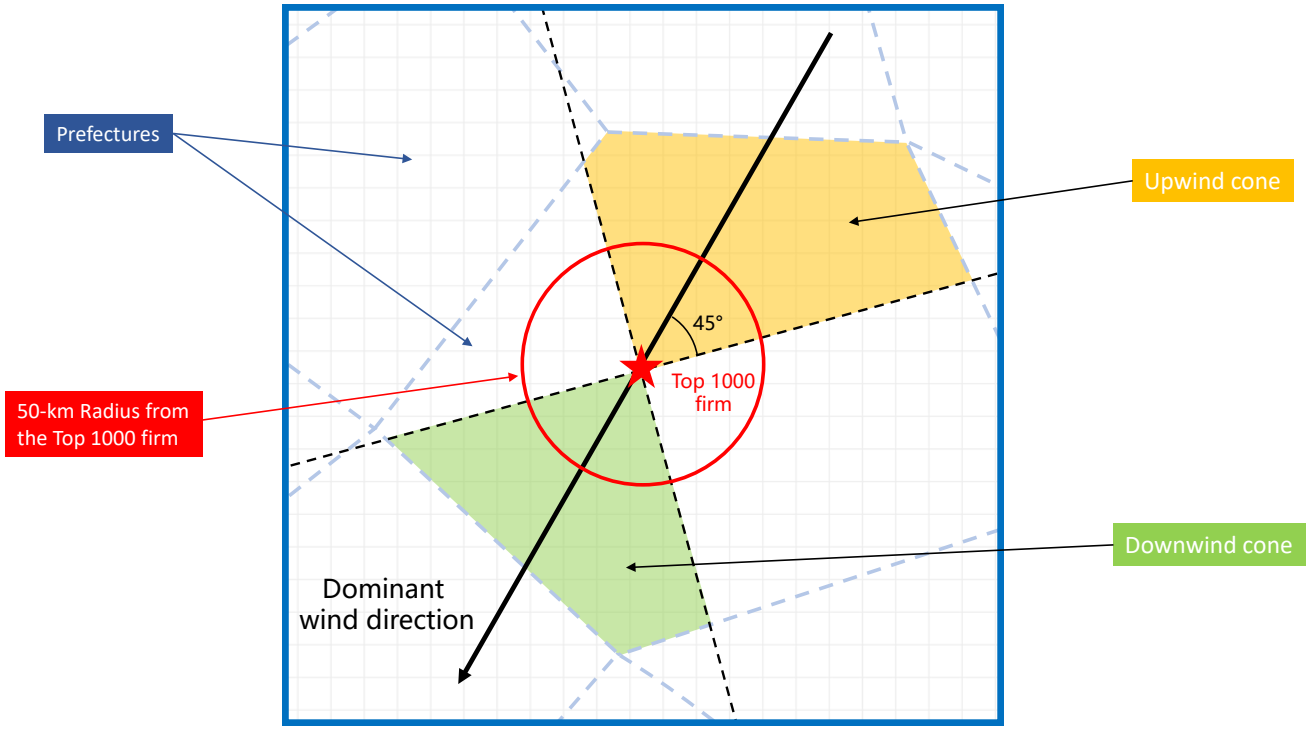


Figure G.6: Illustration of Upwind and Downwind Regions

Notes: This figure illustrates the research design in Table G.3. The black line presents the dominant wind direction. Within each prefecture, we define the downwind region as a $\pm 45°$ cone in the direction of the dominant wind and the upwind region as a $\pm 45°$ cone in the opposite direction. The dashed line represents the prefecture borders.

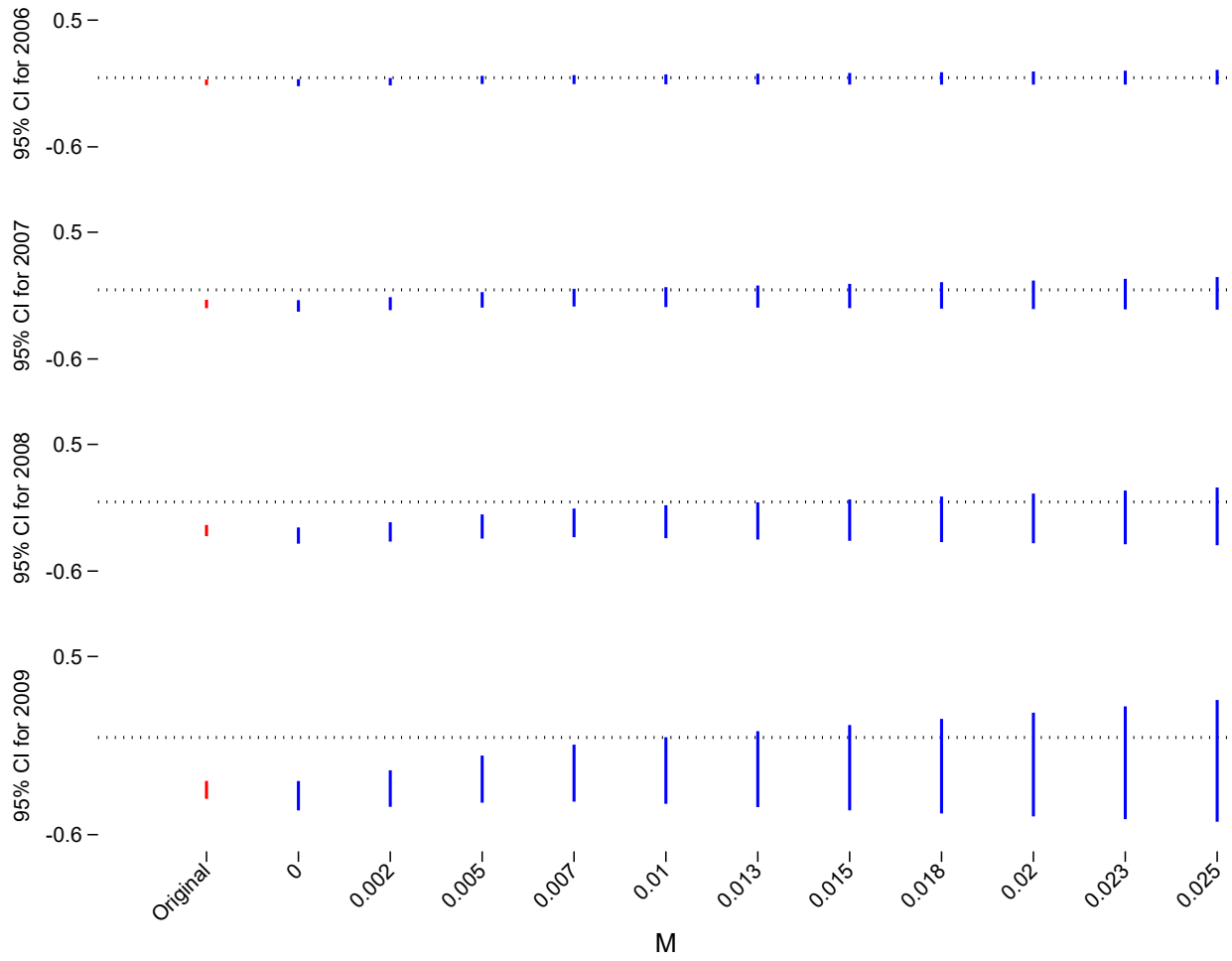


Figure G.7: Sensitivity Analysis of Grid Cell Level Event Study on Labor Following Rambachan and Roth (2023)

Notes: This figure plots sensitivity analysis of β_τ's ($\tau = 2006, ..., 2009$) estimated in the event study plotted in Panel D of Figure 2, following Rambachan and Roth (2023) and posing smoothness restrictions of the form Δ^{SD}. Red lines indicate original estimates, and blue lines indicate fixed length confidence intervals (FLCIs) when $\Delta = \Delta^{\text{SD}}(M)$ for different values of M.
Sources: NBS (2001-2009a).

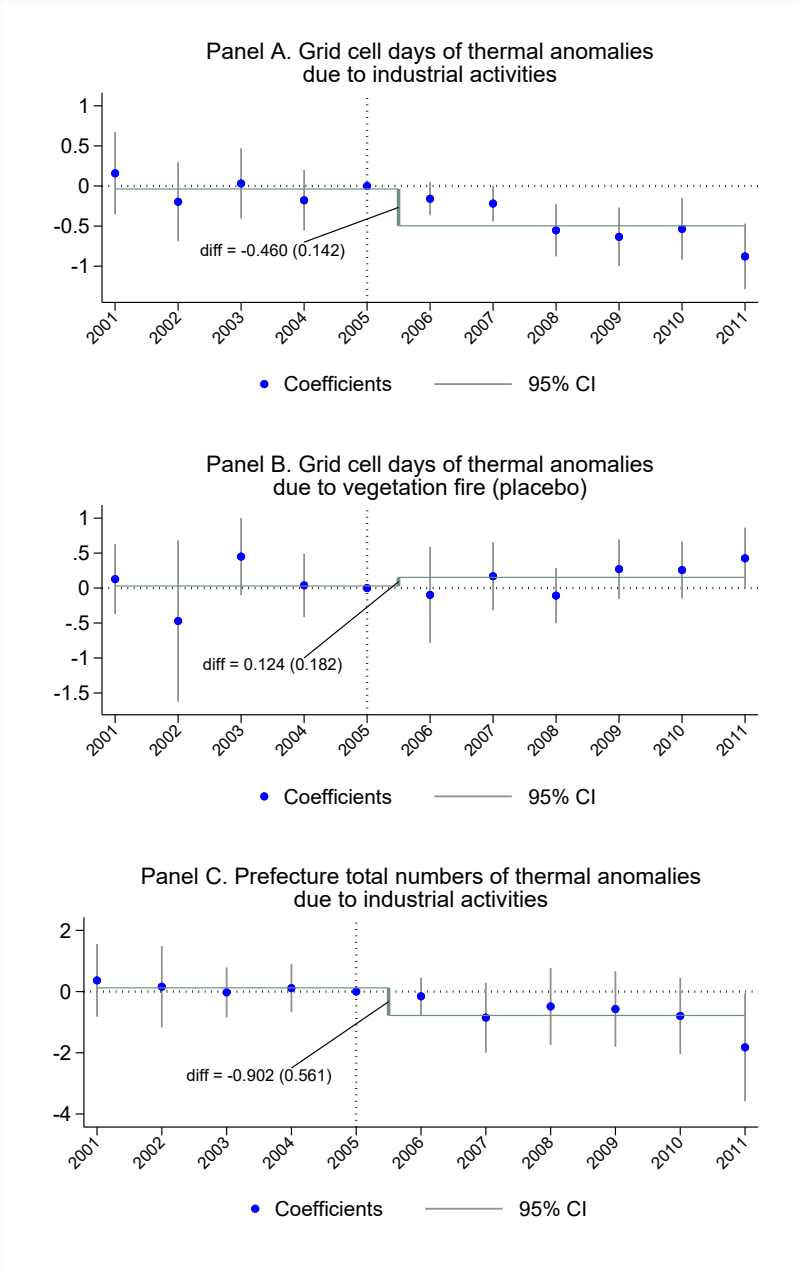


Figure G.8: The Effects of Top 1,000 Program on Reallocation of Thermal Anomalies Activities

Notes: Panels A and B plots Poisson pseudo-maximum-likelihood (PPML) estimators of the following specification, which is similar to specification (1):

$$Y_{it} = \exp\left(\sum_{\tau \neq 2005} \beta_\tau (\text{Top } 1{,}000_i \times \text{Year}_t) + \boldsymbol{\gamma}' \boldsymbol{x}_{it} + \varepsilon_{it}\right),$$

where the dependent variable Y_{it} is the number of thermal anomalies due to industrial activities ("other static land source"; Panel A) and due to vegetation fire (Panel B). The control vector $\boldsymbol{x}_{it}$ contains grid cell fixed effects and prefecture-by-year fixed effects. The sample includes 82,420 (Panel A) and 22,901 (Panel B) grid cell-year observations.

Panel C plots the PPML estimators of the following specification, which is similar to specification (2):

$$Y_{dt} = \exp\left(\sum_{\tau \neq 2005} \beta_\tau (\text{Top } 1{,}000 \text{ share}_d \times \text{Year}_t) + \boldsymbol{\gamma}' \boldsymbol{x}_{dt} + \varepsilon_{dt}\right),$$

where dependent variable Y_{dt} is the total number of thermal anomalies due to industrial activities in prefecture d in year t. Control vector $\boldsymbol{x}_{dt}$ includes prefecture fixed effects and province-by-year fixed effects. The sample includes 3,642 prefecture-year observations. All 95 percent confidence intervals are constructed using standard errors clustered at prefecture level.
Sources: NASA (2025).

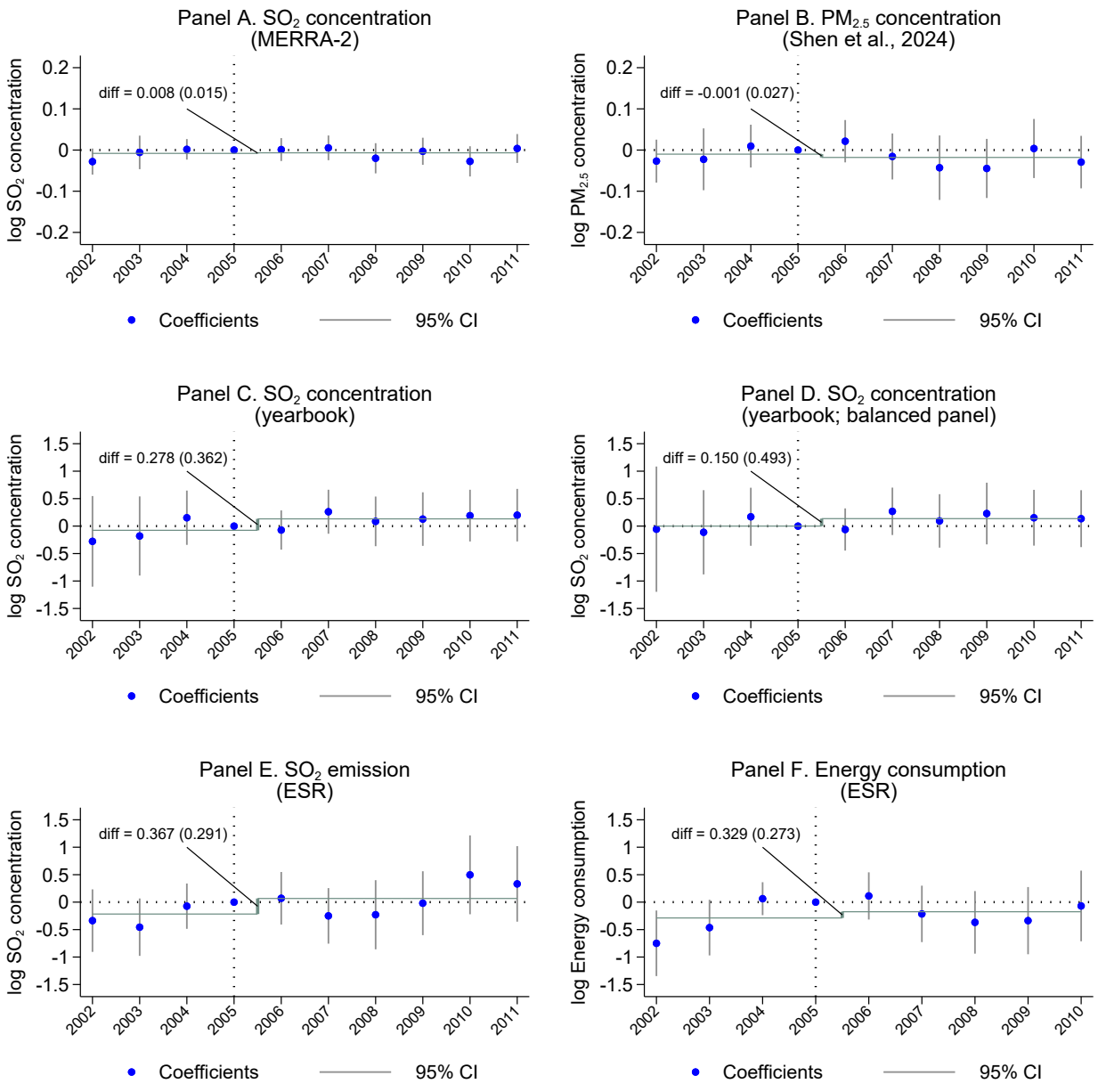


Figure G.9: Effects of the Top 1,000 Program on Prefecture Environment: Alternative Measures

Notes: Event-study estimates of the Top 1,000 program's effects on aggregate prefecture-level pollution using specification (2). Dependent variables are the logarithm of prefecture-year level pollution concentration and emission: SO_2 concentration from the MERRA-2 data (Modeling and Assimilation Office GMAO) (Panel A), $PM_{2.5}$ concentration from Shen et al. (2024) (Panel B), SO_2 concentration from MEP (2002-2009, 2007-2012) (Panels C and D), total SO_2 emission from the ESR data (MEP 2002-2011) (Panel E), and total energy consumption from the ESR data (MEP 2002-2011) (Panel F). The sample includes 3,450 (Panels A and B), 1,673 (Panel C), 1,002 (Panel D), 3,303 (Panel E) and 2,967 (Panel F) prefecture-year observations. The balanced panel in Panel D refers to 112 prefectures with non-missing SO_2 concentration readings from 2003 to 2011. All regressions include prefecture and province-by-year fixed effects, weighted by base industrial employment. 95% confidence intervals are constructed using standard errors clustered at the prefecture level.
Sources: Modeling and Assimilation Office (GMAO); Shen et al. (2024); MEP (2002-2011,-, 2007-2012).

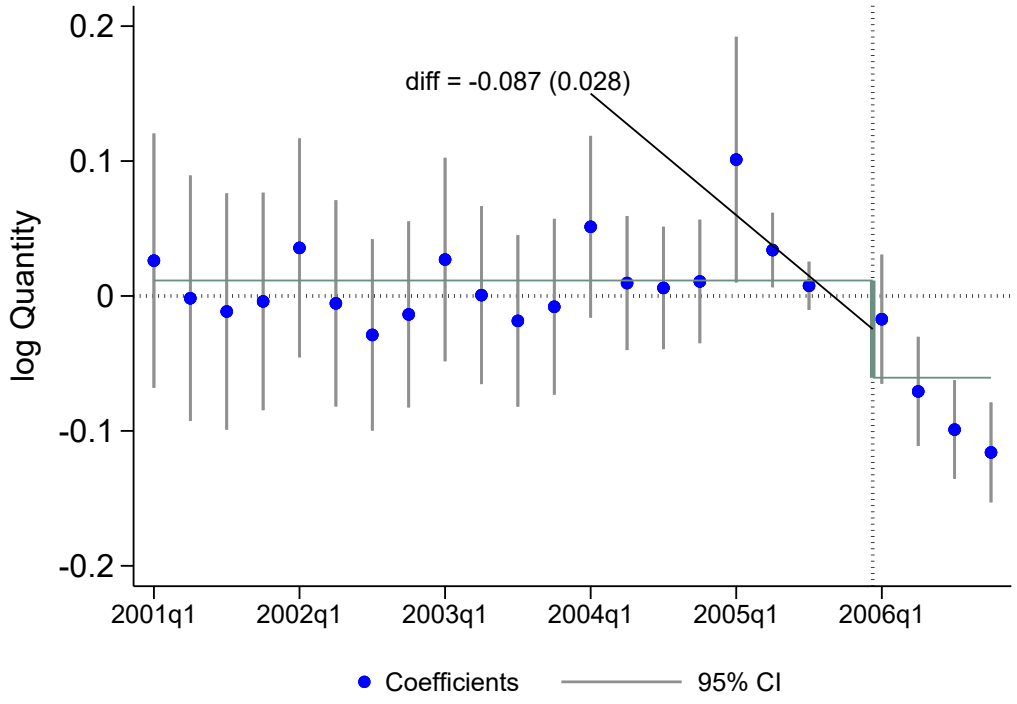


Figure G.10: Effects of the Top 1,000 Program on Product Quantity of Regulated Firms

Notes: The figure plots event-study estimates of the Top-1000 program's effects on regulated firms using the following quarterly specification:

$$Y_{fpq} = \sum_{q \neq 2005Q4} \beta_\tau \left(\text{Top } 1,000_f \times Quarter_q \right) + \boldsymbol{\gamma}' \boldsymbol{x}_{fpq} + \varepsilon_{fpq}$$

where Y_{fpq} denotes the logarithm of product quantity for firm f, product p, and quarter q. The summation indexes quarters τ from 2000Q1 to 2006Q4, with 2005Q4 omitted as the reference period. All regressions include firm-product fixed effects, product-year-quarter fixed effects, and province-year-quarter fixed effects. Firms that change prefecture during the sample period are excluded from the regression. The value labeled "diff" denotes the difference between post- and pre-policy means, computed from the event-study coefficients using the Delta method. These estimates may differ slightly from those obtained from a standard difference-in-differences specification. Numbers of observations are 524,457. 95% confidence intervals are constructed using standard errors clustered two-way at the firm and product level.
Sources: NBS (2000-2006).

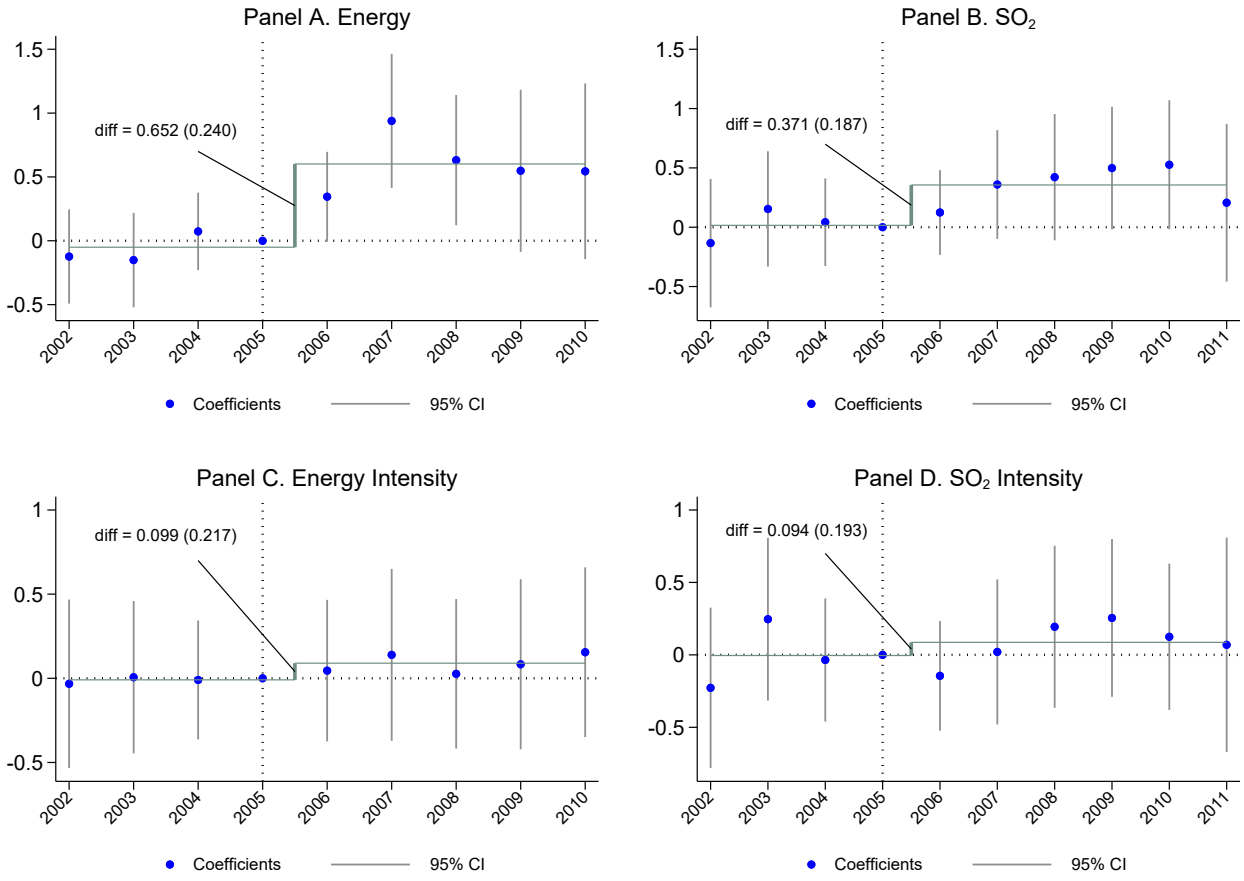


Figure G.11: Effects of the Top 1,000 Program on Energy Use and SO_2 Emission of Unregulated Firms

Notes: The figure plots event-study estimates of the Top-1000 program's effects on unregulated firms using the following specification:

$$Y_{fdt} = \sum_{\tau \neq 2005} \beta_\tau (\text{Top 1,000 share}_d \times \text{Year}_t) + \boldsymbol{\gamma}' \boldsymbol{x}_{fdt} + \varepsilon_{fdt},$$

where Y_{fdt} denotes outcomes for firm f, prefecture d, and year t. The dependent variable is logarithm of energy consumption in Panel A, logarithm of SO_2 in Panel B, logarithm of energy intensity (energy consumption per unit of output) in Panel C and SO_2 intensity (SO_2 emissions per unit of output) in Panel D. All regressions include firm fixed effects, industry-by-year fixed effect and province-by-year fixed effects. The value labeled "diff" denotes the difference between post- and pre-policy means, computed from the event–study coefficients using the Delta method. These estimates may differ slightly from those obtained from a standard difference-in-differences specification. Numbers of observations are: 70,049 (Panel A), 267,408 (Panels B), 59,192 (Panels C) and 207,628 (Panels D). 95% confidence intervals are constructed using standard errors clustered at the prefecture level.
Sources: MEP (2002-2011).

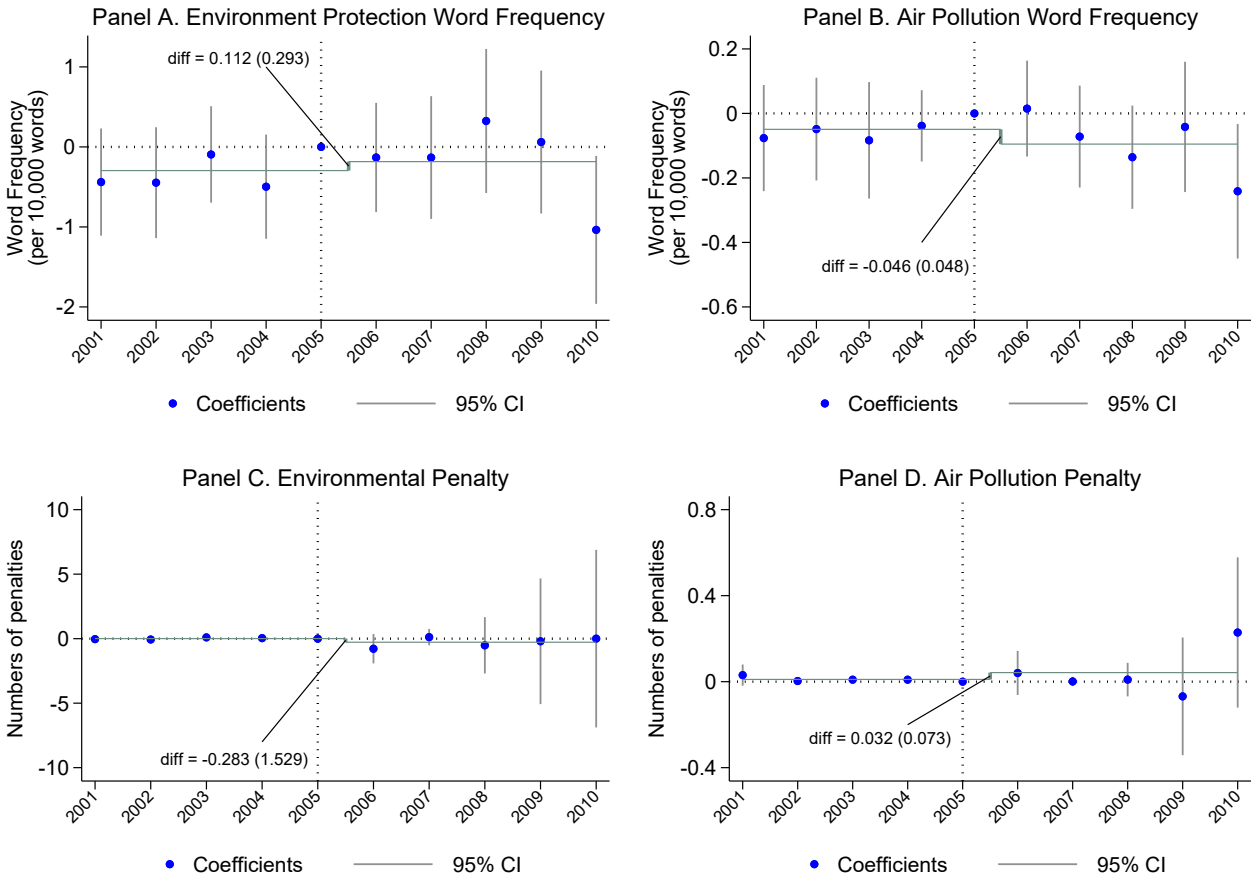


Figure G.12: Environmental Policy Effect after the Top 1,000 Program

Notes: Event-study estimates of environmental policy effect after the Top 1,000 Program using specification (2). We use two datasets to measure environmental policy: word frequency from government report (panel A and B) and environmental penalty (panel C and D). Numbers of observations are 2,698 in panel A and B and 3,150 in panel C and D. Regressions include prefecture and province by year fixed effects, weighted by base industrial employment. 95% confidence intervals are constructed using standard errors clustered at the prefecture level.
Sources: Various. See Section A.6 for details.

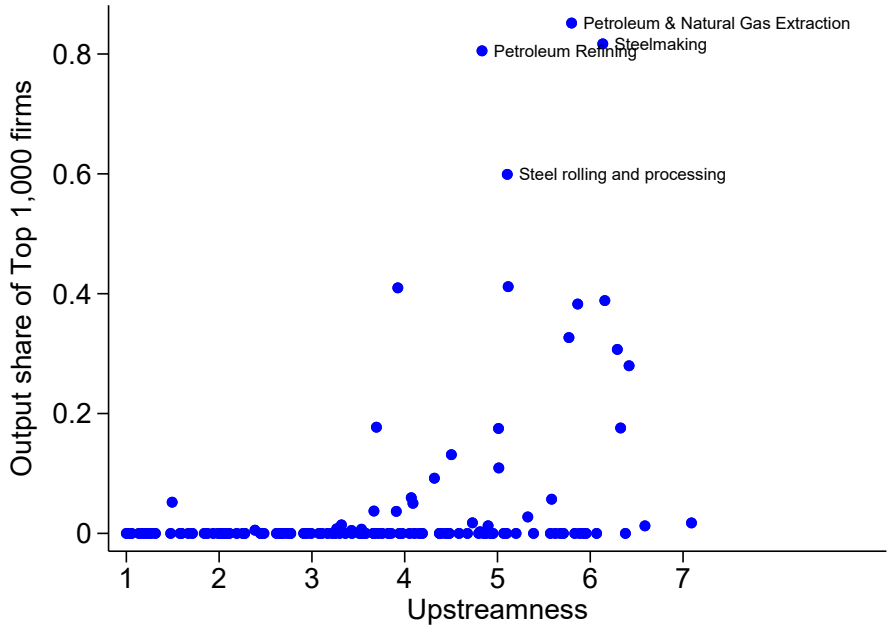


Figure G.13: Upstreamness of Regulated Firms

Notes: A dot is an IO industry in the 2007 Input-Output Table of China. Upstreamness is calculated using the method proposed by Antràs et al. (2012).
Sources: NBS (2007).

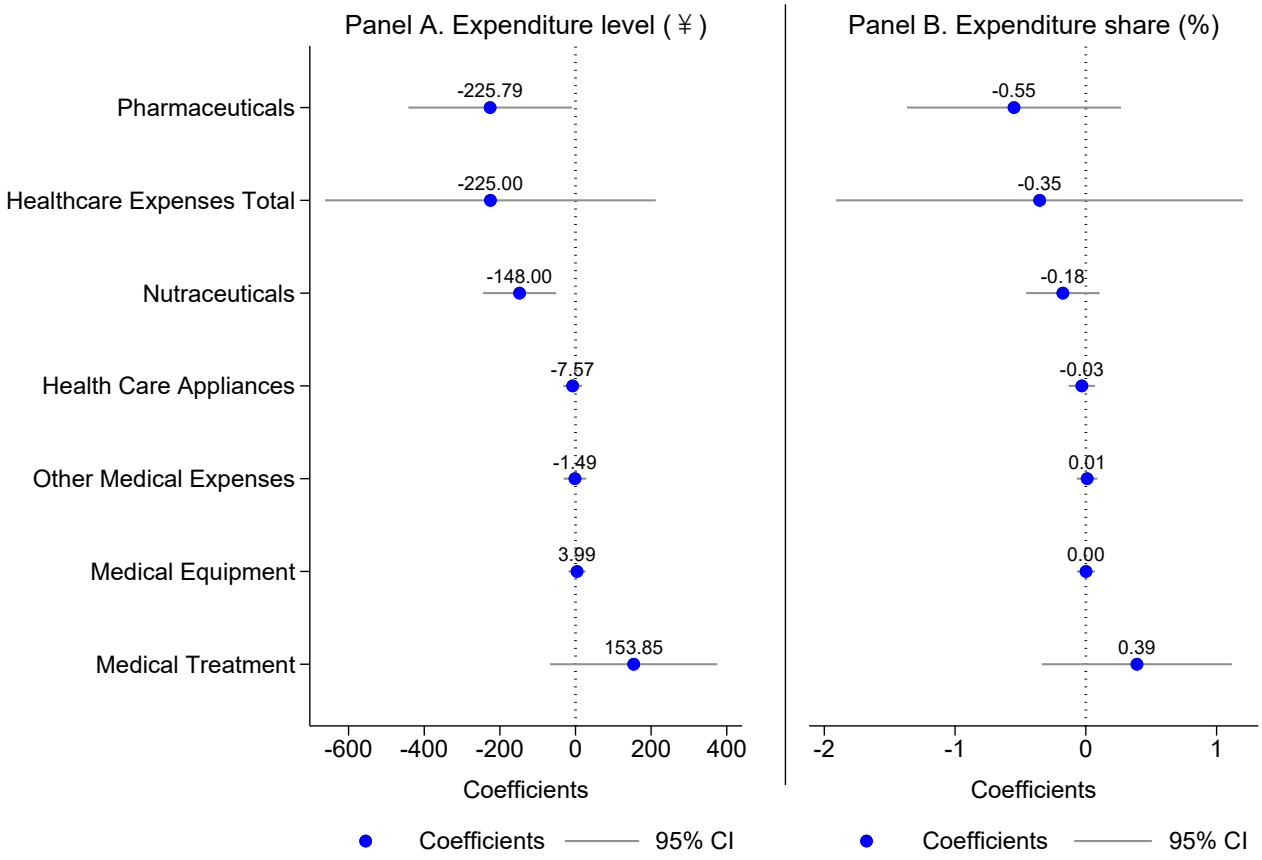


Figure G.14: Detailed Health Spending Changes

Notes: This figure plots the difference-in-differences estimates of individual and household responses to the Top 1,000 Program based on the following specification:

$$Y_{hdt} = \beta_t \left(\text{Top 1,000 share}_d \times \text{Post}_t\right) + \boldsymbol{\gamma}' \boldsymbol{x}_{hdt} + \varepsilon_{hdt},$$

where Y_{hdt} denotes household expenditure in household h, prefecture d, and year t. The dependent variables is household expenditure on total healthcare expense and different type of healthcare service. Panels A use the absolute amount and Panels B use its share in total household expenditure as dependent variables. All income and expenditure variables are deflated using the CPI compiled by the National Bureau of Statistics, with 2002 as the base year. All regressions include individual demographic controls (household head's age, education, and gender, as well as household size), prefecture fixed effects and province-by-year fixed effects. Numbers of observations are 256,077 in Panel A and B. All regressions are weighted by base industrial employment. 95% confidence intervals are constructed using standard errors clustered at the prefecture level.
Source: NBS (2002-2009b).

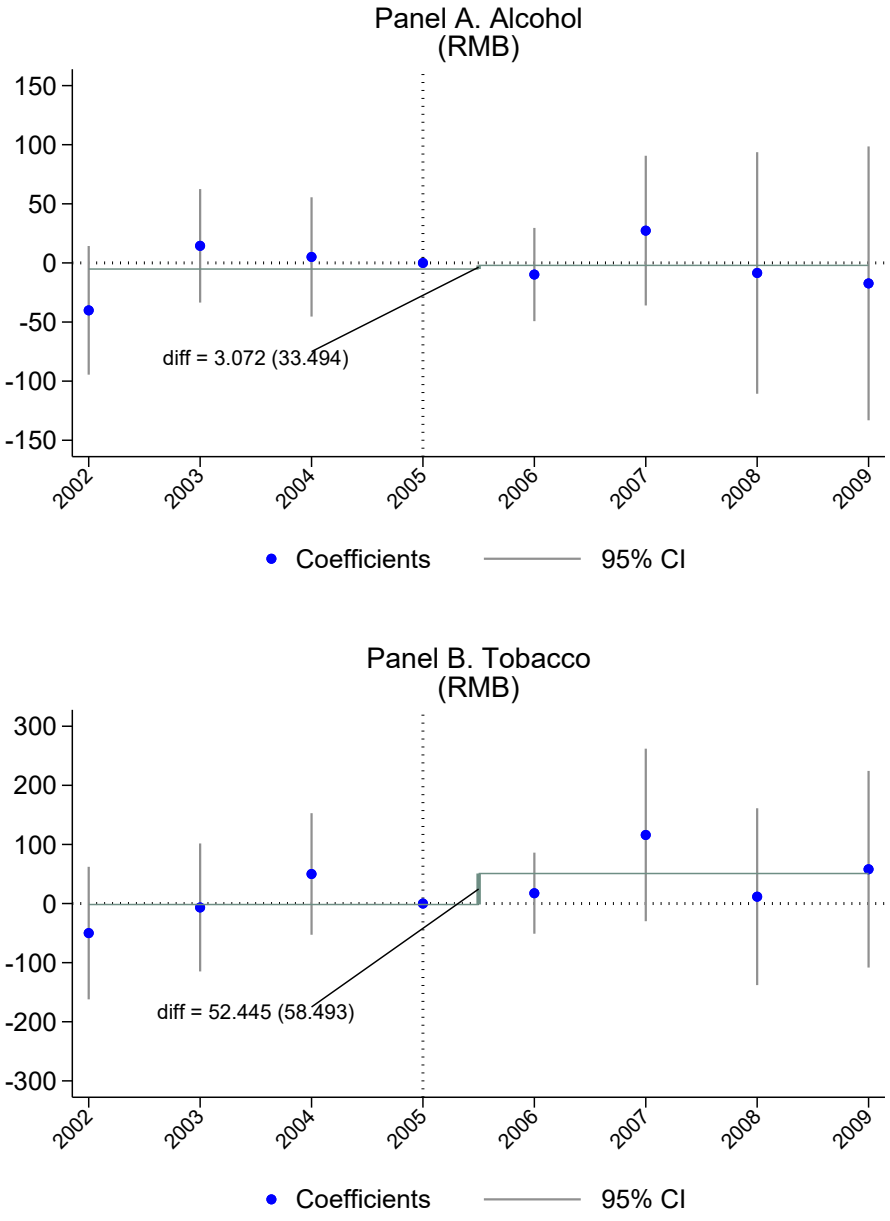


Figure G.15: Spending on Alcohol and Tobacco

Notes: This figure plots the event-study estimates of individual consumption on alcohol and tobacco responses to the Top 1,000 Program based on the following specification:

$$Y_{\iota dt} = \sum_{t \neq 2005} \beta_t \left(\text{Top 1,000 share}_d \times \text{Year}_t\right) + \boldsymbol{\gamma}' \boldsymbol{x}_{\iota dt} + \varepsilon_{\iota dt},$$

where $Y_{\iota dt}$ denotes outcomes for household ι, prefecture d, and year t. The dependent variable the spending on alcohol in Panel A and the spending on tobacco in Panel B. All regressions include prefecture fixed effects and province-by-year fixed effects, as well as household-head demographics including age, gender, ethnicity, and years of education. The value labeled "diff" denotes the difference between post- and pre-policy means, computed from the event-study coefficients using the Delta method. These estimates may differ slightly from those obtained from a standard difference-in-differences specification. Numbers of observations are 256,077 in Panels A and Panel B. 95% confidence intervals are constructed using standard errors clustered at the prefecture level.
Source: NBS (2002-2009b).

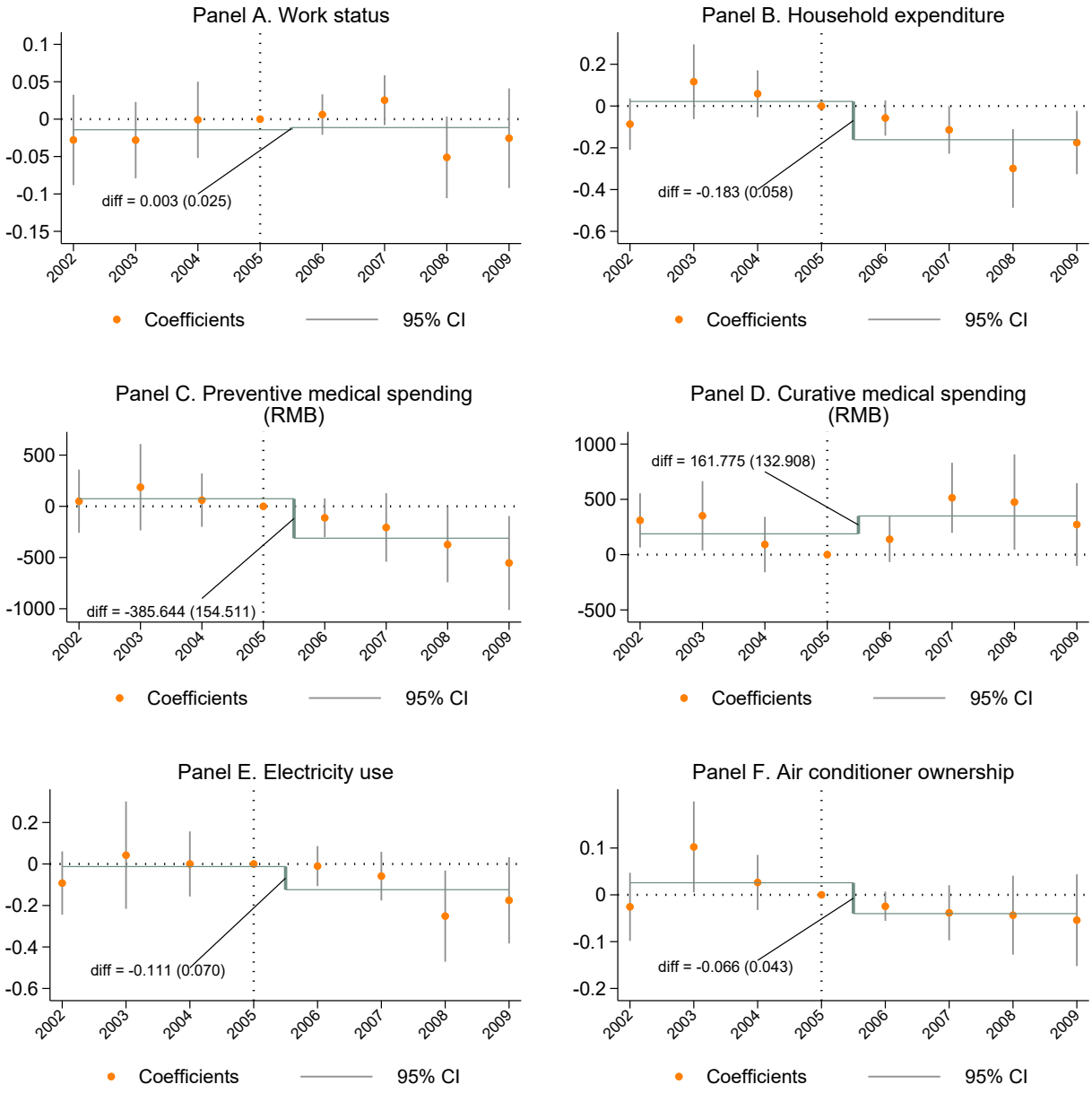


Figure G.16: Household Responses to the Top 1,000 Program: Robustness to Additional Controls

Notes: This figure re-estimates the specifications in Figure 3, but further control for year fixed effects interacted with baseline prefecture characteristics on demographics (urban population share, share of the population with a high school degree or above, share of the population aged 0-15, and share of the population aged 65 or above), health (infant mortality rate), industrial structure (indicator for Top 1,000 prefectures), and concurrent environmental regulations (indicator for inclusion in the *Two Control Zones* and employment shares of *National Specially Monitored Firms*).. Numbers of observations are: 587,652 (Panel A), 256,077 (Panels B-D), 247,028 (Panel E) and 256,652 (Panel F). 95% confidence intervals are constructed using standard errors clustered at the prefecture level.
Source: NBS (2002-2009b).

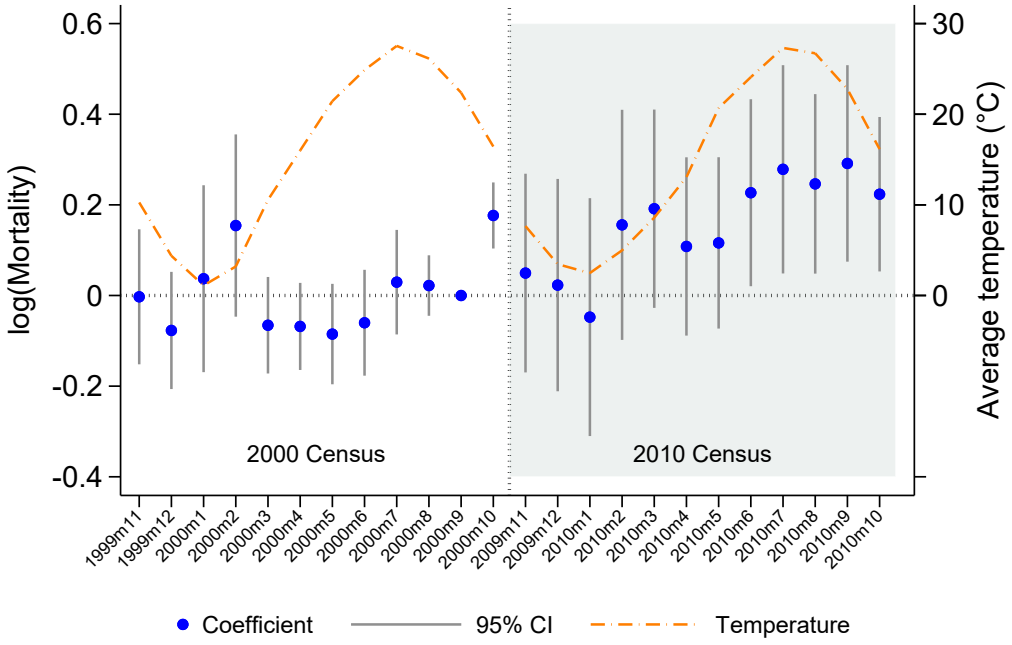


Figure G.17: Monthly Mortality Event Study Based on Population Census

Notes: This figure plots the monthly event study of log mortality rate using specification (2). The regression includes prefecture and gender fixed effects and region-by-month-of-sample fixed effects and is weighted by baseline industrial employment. The sample includes 16,200 prefecture-gender-month observations. Orange dashed line plots the weighted average temperature in Top 1,000 prefectures. 95 percent confidence intervals are constructed using standard errors clustered at prefecture level.
Sources: NBS (2000, 2010); NOAA (2024).

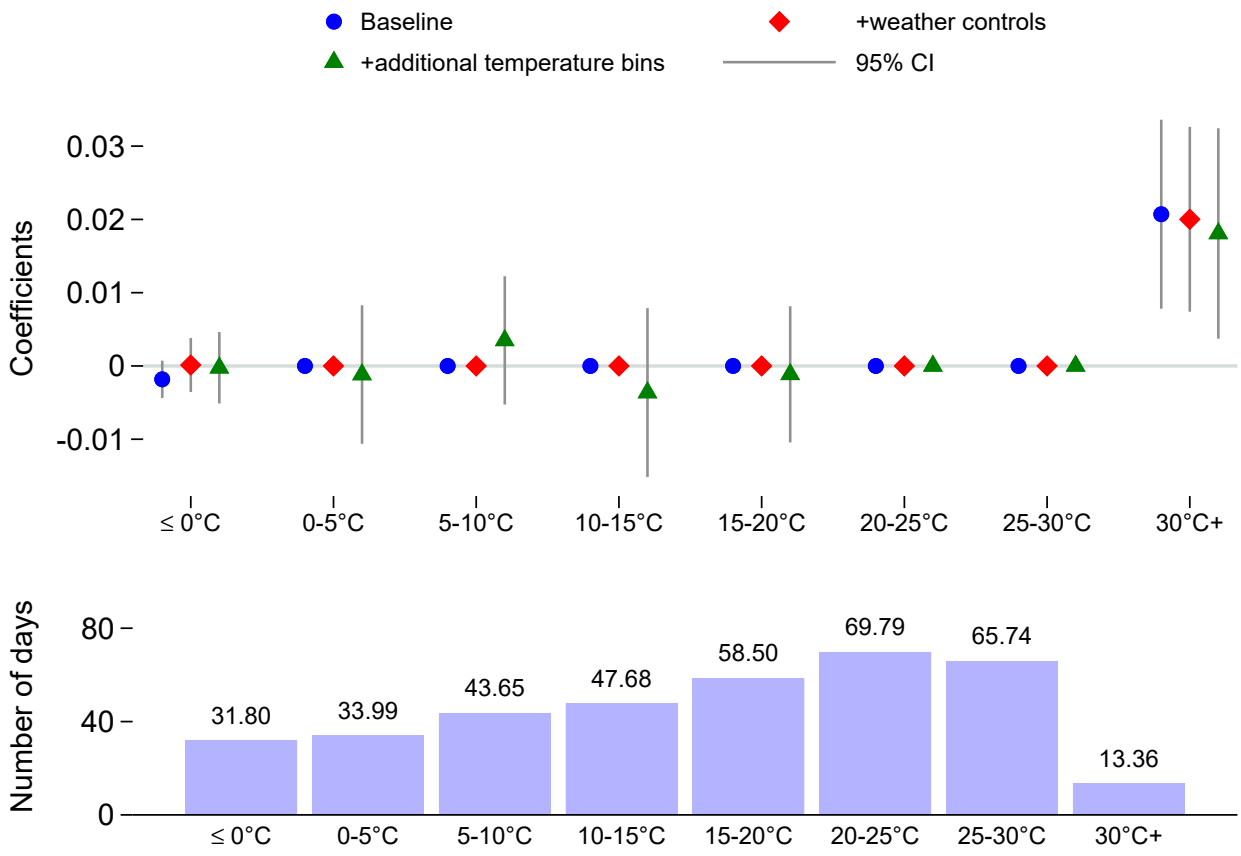


Figure G.18: The Effects of Top 1,000 Program on Vulnerability to Extreme Temperature Shocks: Additional Controls

Notes: The top panel plots the estimated $\hat{\beta}^k$ of the following specification, which is similar to specification (3):

$$\begin{aligned} Y_{dt} =& \beta(\text{Top 1,000 share}_d \times \text{Post}_t) \\ &+ \sum_k \beta^k \left(\text{TBin}_{dt}^k \times \text{Top 1,000 share}_d \times \text{Post}_t\right) + \boldsymbol{\gamma}' \boldsymbol{x}_{dt} + \varepsilon_{dt}. \end{aligned}$$

In the baseline specification, the control vector $\boldsymbol{x}_{dt}$ includes prefecture fixed effects, region-by-year fixed effects, and year fixed effects interacted with baseline shares of Top 10,000 firms, as well as all lower-order terms including the temperature bins $\{\text{TBin}_{dt}^k\}$, their interaction terms with year fixed effects, and their interaction terms with Top 1,000 shares; in "+weather controls", we further controls for pollution (log $\text{PM}_{2.5}$), wind speed, precipitation, and bins of humidity; and in "+additional temperature bins", we interact Top 1,000 $\text{share}_d \times \text{Post}_t$ with additional temperature bins, as plotted in the figure. 95 percent confidence intervals are constructed using standard errors clustered at prefecture level. All regressions include 3,990 prefecture-year observations and are weighted by baseline industrial employment.

The bottom panel plots the weighted average number of days in each temperature bin in Top 1,000 prefectures during the sample period.

Sources: NBS (2000-2012); NOAA (2024).

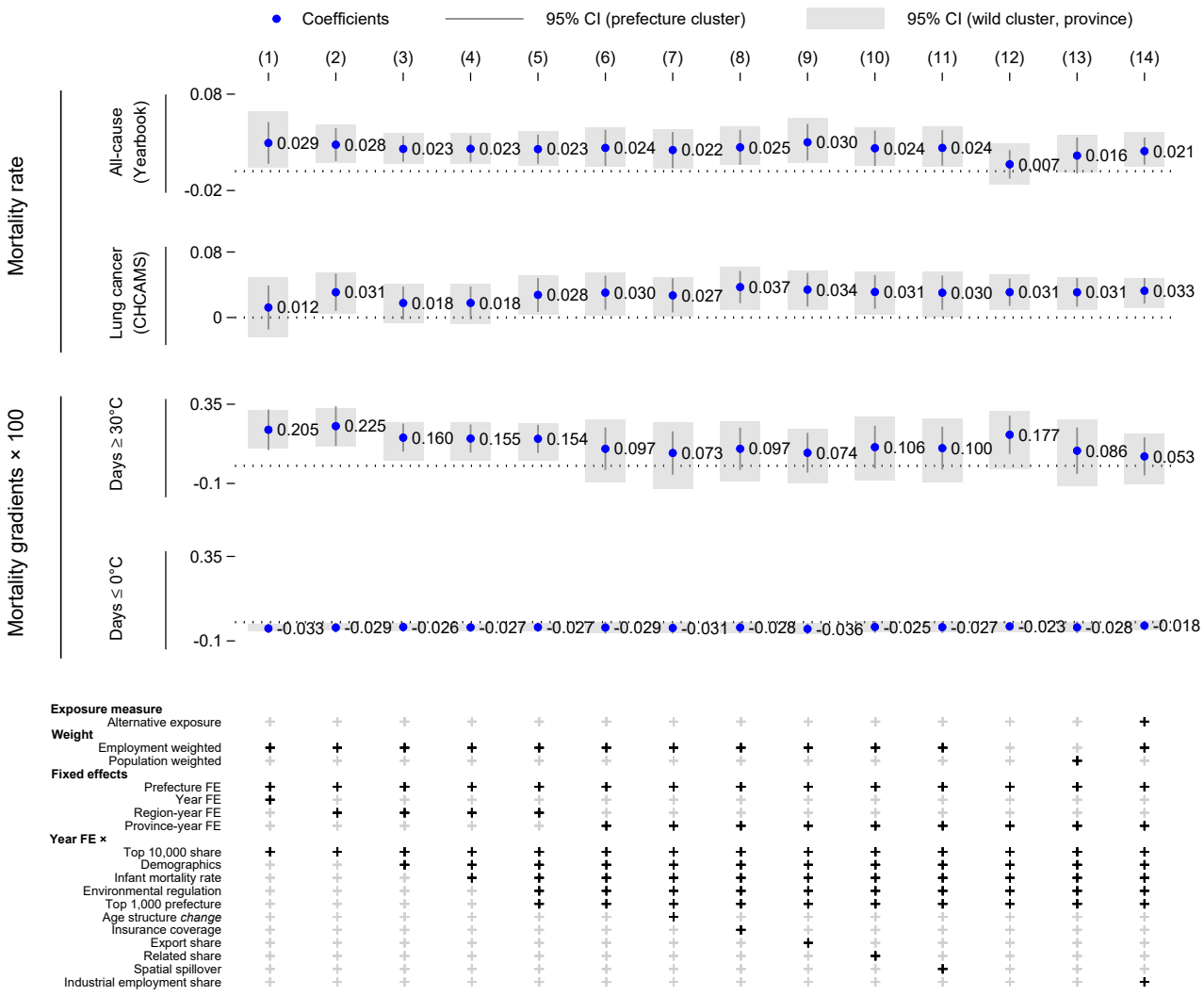


Figure G.19: Effects of the Top 1,000 Program on Mortality: Robustness to Heterogeneous Trends, Weights, and Exposure Measures

Notes: This figure reports the difference-in-differences estimates of the Top 1,000 Program and its interaction with temperature on mortality. The first two rows labeled "Mortality rate'' plots difference-in-differences estimates of the Top 1,000 program on mortality rates:

$$Y_{dt} = \beta \left(\widetilde{\text{Exposure}}_d \times \text{Post}_t\right) + \boldsymbol{\gamma}' \boldsymbol{x}_{dt} + \varepsilon_{dt},$$

The second two rows labeled "Mortality gradients × 100'' plots the estimates of the interaction of Top 1,000 program shock with temperature shocks:

$$Y_{dt} = \beta \left(\widetilde{\text{Exposure}}_d \times \text{Post}_t\right) + \left(\sum_k \beta_k \text{TBin}^k_{dt} \times \widetilde{\text{Exposure}}_d \times \text{Post}_t\right) + \boldsymbol{\gamma}' \boldsymbol{x}_{dt} + \varepsilon_{dt}.$$

These specifications above parallels specification (2) and (3) respectively, except that the post-treatment effect is summarized by the interaction between prefecture exposure Exposure_d and a post-2005 dummy Post_t. To ease comparison across specifications, we normalize exposure measure x so that variable $\tilde{x}$ defined as the raw exposure divided by its sample mean among exposed ($x > 0$) prefectures. Thus, the coefficients represent the effect for an averagely exposed prefecture. Sample in the first rows includes 4,271 prefecture-year observations for years 1999 to 2011. Sample in the second two rows includes 2,070 prefecture-gender-year observations for years 1990-1992, 2004-2005, and 2014. For comparability across specifications, exposure is normalized to have mean one among exposed prefectures. Dependent variables: "Yearbook" and "Mortality gradients × 100"–all-cause mortality rate (logarithm) from NBS (2000-2012) and "Lung cancer (CHCAMS)"–lung-cancer mortality rate (logarithm) from CHCAMS (2017). In the bottom panel, black plus signs indicate the inclusion of corresponding exposure measures, weighting schemes, and control sets for each specification

vertically aligned above. *Exposure measures*: the baseline exposure equals the share of industrial employment in Top 1,000 firms; "Alternative exposure" divides Top 1,000 employment by total employment. *Weights*: "Employment weight" uses baseline industrial employment; "Population weight" uses baseline urban population. *Baseline characteristics*: "Top 10,000 share"– the share of industrial employment in Top 1,000 firms; "Demographics"–share of urban population, share of share of the population with a high school degree or above, share of the population aged 0-15, and share of the population aged 65 or above); "Infant mortality rate"–infant mortality rate; "Environmental regulation"–indicator for inclusion in the *Two Control Zones* and employment shares of *National Specially Monitored Firms* (NSMF); "Top 1,000 prefecture"–indicator for Top 1,000 prefectures; "Age structure *change*"–changes in share of the population aged 0-15, and changes in share of the population aged 65 or above, both from 2000 to 2010; "Insurance coverage"–fraction of population aged 15 or above covered by medical insurance, and fraction of population aged 15 or above covered by pension insurance; "Export share" share of industrial employment in exporting firms; "Related share"–share of industrial employment in firms related to Top 1,000 firms as defined in Chen et al. (2025); "Spatial spillover"—indirect exposure to neighboring prefectures, computed using equation (D.1) following Adão et al. (2019); "Industrial employment share"–share of employment working in the industrial sector. Top 10,000 firms, NSMF firms, and related firms are defined *excluding* any firm that also belongs to the Top 1,000 group. Spike lines represent 95% confidence intervals based on standard errors clustered at the prefecture level. Shading errors represent 95% confidence intervals based on wild cluster bootstrap procedures developed by Cameron et al. (2008).
Sources: NBS (2000, 2005a, 2010, 2000-2012); CHCAMS (2017).

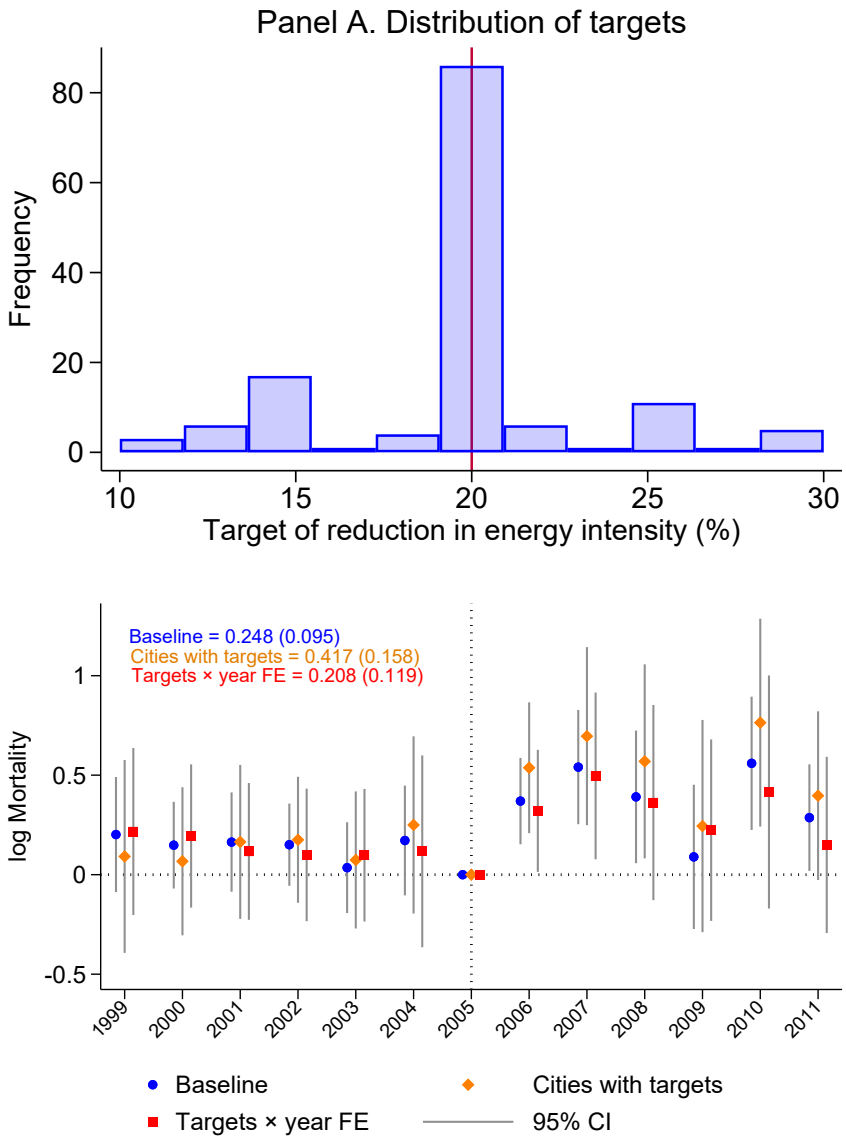


Figure G.20: Effects of the Top 1,000 Program on Mortality:
Robustness to Controlling for Local Governments' Energy Saving Targets during the 11th FYP

Notes: Panel A plots the distribution of prefecture-level targets for the reduction in energy intensity (energy consumption per unit of GDP) set during the Eleventh Five-Year Plan (2006-2010), for 141 prefectures with available data. Targets are hand-collected from local government reports issued in 2006. Panel B replicates the baseline event-study specification (2) (blue circles), restricts sample to the prefectures with energy saving targets (orange diamonds), and additionally controls for year fixed effects interacted with these prefecture-specific targets (red squares). 95% confidence intervals are based on standard errors clustered at the prefecture level.
Sources: Authors' compilation from local government reports. See Section D.1 for details.

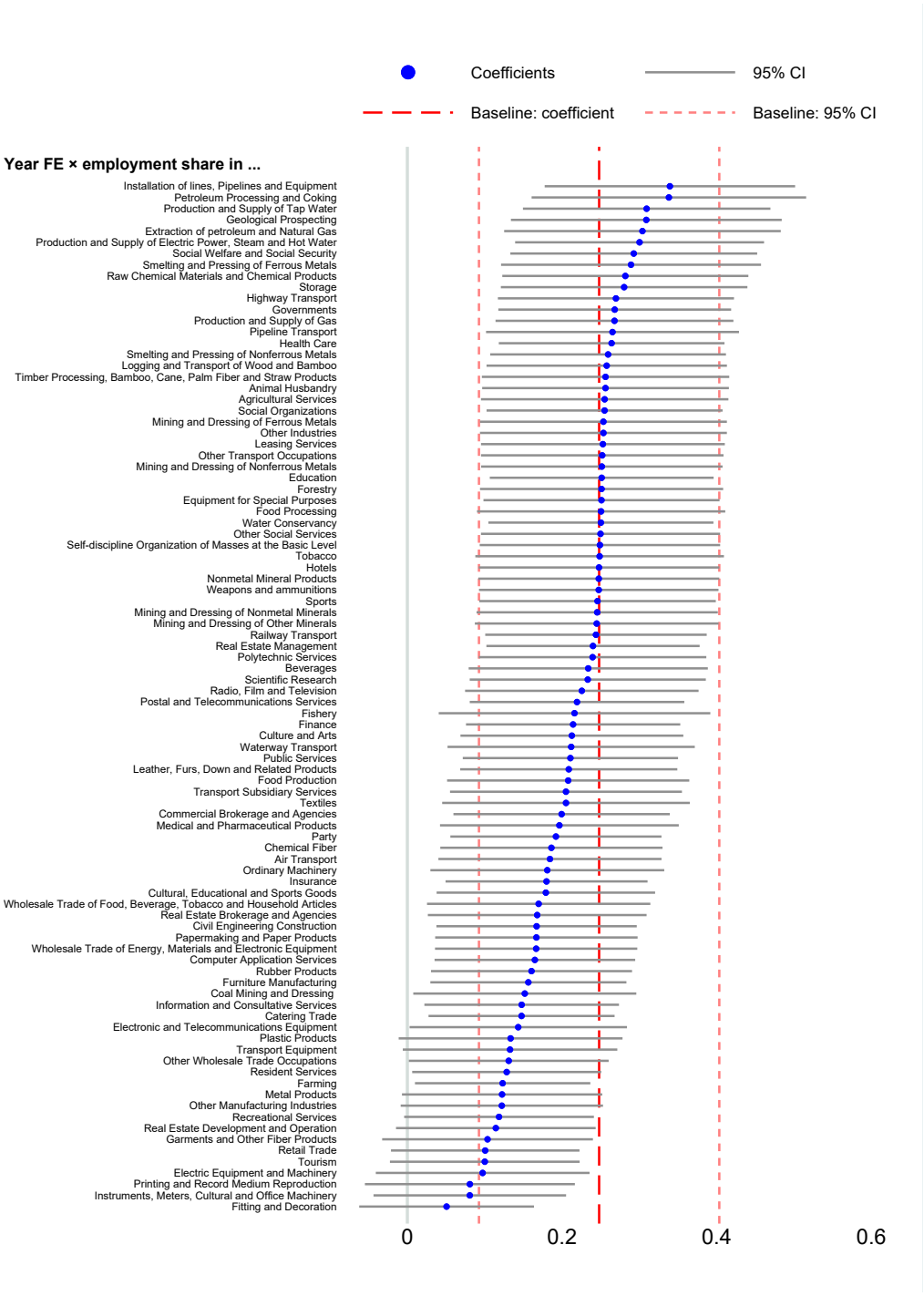


Figure G.21: Effects of the Top 1,000 Program on Mortality: Robustness to Industry-Specific Time-Varying Shocks

Notes: This figure demonstrates the robustness to controlling for industry-specific time varying shocks. Each coefficient corresponds to one separate regression result of:

$$Y_{dt} = \beta \left(\text{Exposure}_d \times \text{Post}_t\right) + \boldsymbol{\gamma}' \boldsymbol{x}_{dt} + \gamma_{st} \text{Employment share}_s + \varepsilon_{dt},$$

where Y_{dt} is the logarithm of all-cause mortality; $\boldsymbol{x}_{dt}$ the control vector including prefecture fixed effects, region-year fixed effects, and year fixed effects interacted with Top 10,000 share; Employment share$_s$ the baseline employment share in sector s, measured using the 2000 Population Census (NBS 2000). Samples include 4,332 prefecture-year observations for 1999-2011. 95% confidence intervals are based on standard errors clustered at prefecture level.
Sources: NBS (2000), NBS (2000-2012).

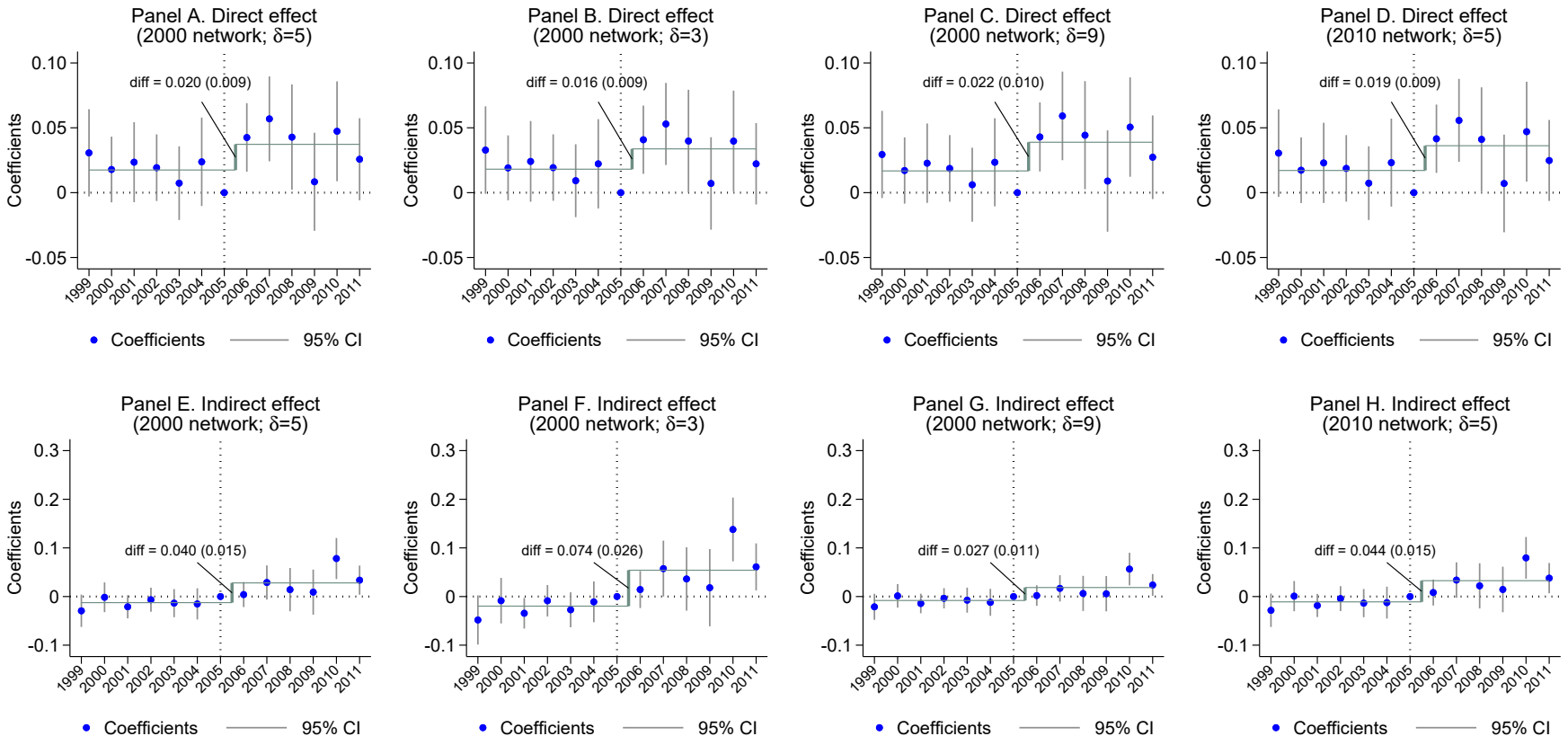


Figure G.22: Spatial Spillovers of the Top 1,000 Program

Notes: This figure plots the event studies of the Top 1,000 program on mortality rates based on the following specification:

$$Y_{dt} = \sum_{t \neq 2005} \beta_t \left(\text{Top } \widetilde{1{,}000 \text{ share}}_d \times \text{Year}_t \right) + \sum_{t \neq 2005} \beta_t^{\text{indirect}} \left(\text{Top } \widetilde{1{,}000 \text{ share}}_d^{\text{indirect}} \times \text{Year}_t \right) + \boldsymbol{\gamma}' \boldsymbol{x}_{dt} + \varepsilon_{dt},$$

which augments baseline specification (2) by adding controls for indirect spillover Top 1,000 $\text{share}_d^{\text{indirect}}$, which is constructed using equation (D.1). To ease comparison across specifications, we normalize exposure measure x so that variable $\tilde{x}$ defined as the raw exposure divided by its sample mean among exposed ($x > 0$) prefectures. Thus, the coefficients represent the effect for an averagely exposed prefecture. Each column corresponds to one specification. Panels A to D plot the estimated direct effects (β_t's) and panels E to H plot the estimated indirect effects ($\beta_t^{\text{indirect}}$'s). Panels A to C and E to G use the road networks in 2000, while Panels D and H use the road networks in 2010. Panels A, D, E, and H set the spatial decay parameter $\delta = 5$, Panels B and F set $\delta = 3$, and Panels C and G set $\delta = 9$. All regressions include prefecture fixed effects, region-by-year fixed effects, and year fixed effects interacted with (i) a dummy for Top 1,000 prefectures and (ii) the employment share of Top 10,000 firms. The labeled "diff" denotes the difference between post- and pre-policy means, computed from the event-study coefficients using the Delta method. These estimates may differ slightly from those obtained from a standard difference-in-differences specification. The number of observations is 3,307. 95% confidence intervals are constructed using standard errors clustered at prefecture level.
Sources: NBS (2000-2012).

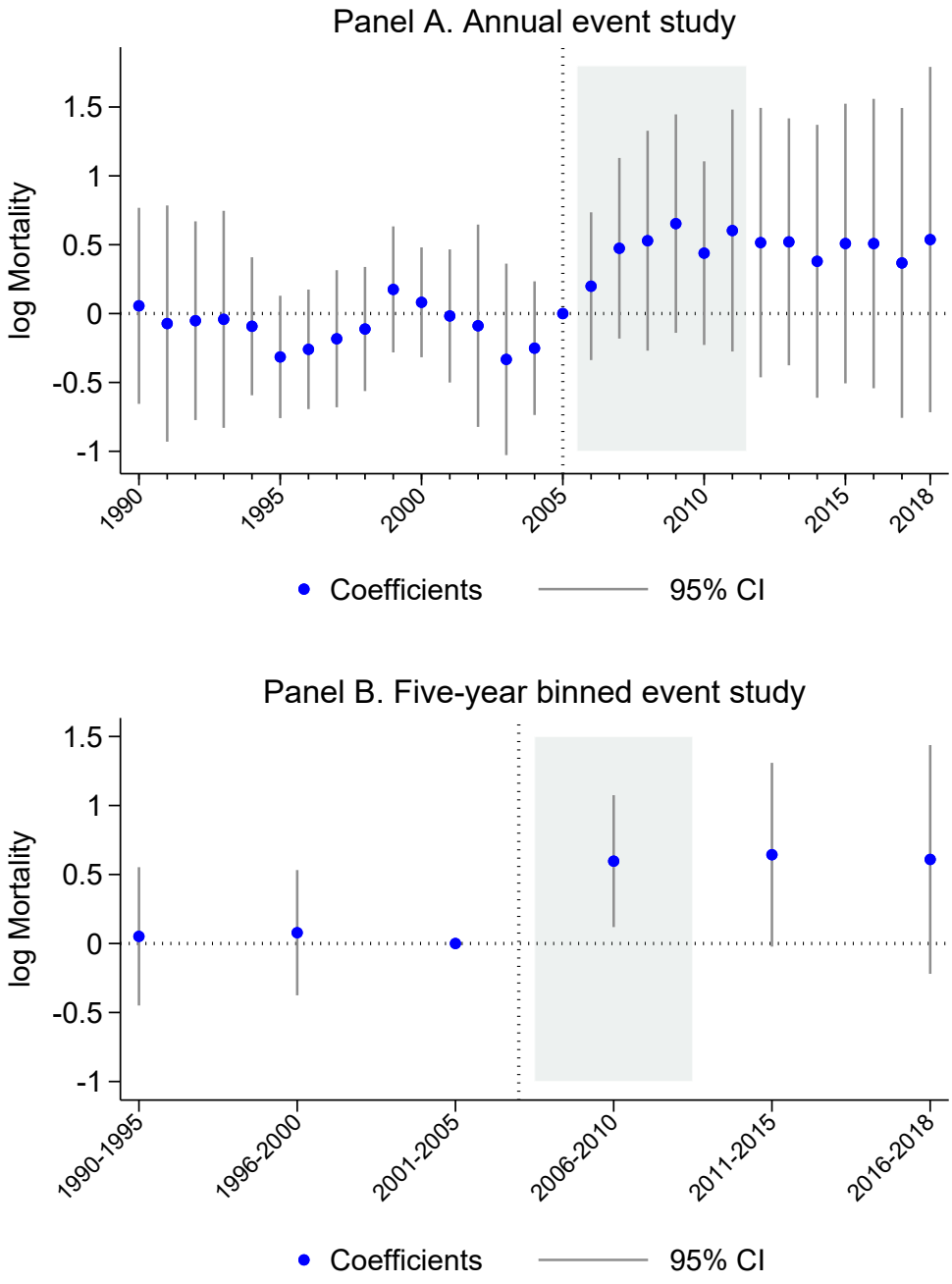


Figure G.23: Province Level Mortality Event Studies: Extended Time Window

Notes: The figure plots event-study estimates of the Top 1,000 program's effects on provincial all-cause mortality. Panel A estimates the dynamic effects annually, while Panel B estimates the dynamic effects using five-year bins. An observation is a province-year. The number of observations is 892. All regressions control for province fixed effects, region-by-year fixed effects, and year fixed effects interacted with baseline employment shares of Top 10,000 firms. 95% confidence intervals are constructed from standard errors clustered at the province level.
Sources: NBS (2023).

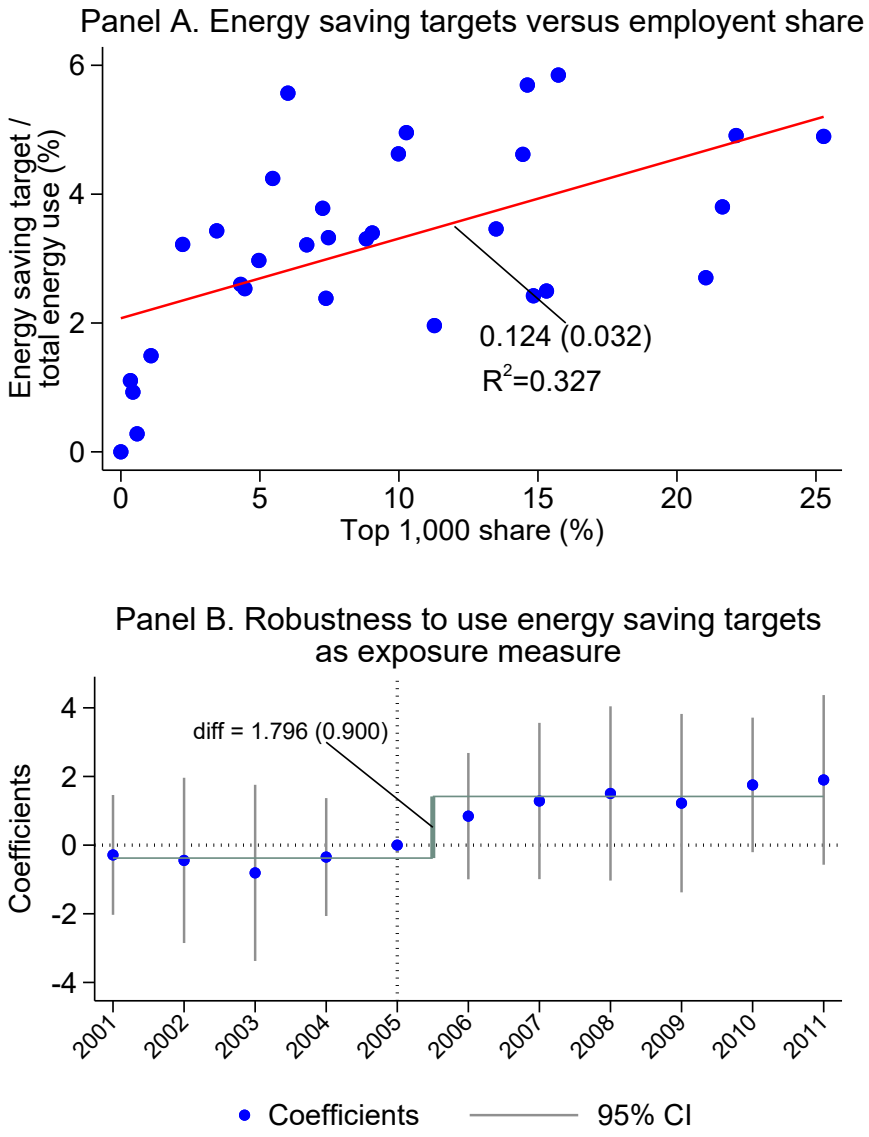


Figure G.24: Effects of the Top 1,000 Program on Mortality: Robustness to Using Top 1,000 Firms' Energy Saving Targets as Exposure Measure

Notes: Panel A compares the alternative exposure measure proposed by Chen et al. (2025), total energy saving target of Top 1,000 firms divided by total energy use, versus our baseline Top 1,000 share measure. Panel B plots event-study estimates of the Top 1,000 program's effects on provincial mortality based on the alternative exposure measure. An observation is a province-year. The number of observations is 372. All regressions control for province fixed effects and region-by-year fixed effects. 95% confidence intervals are constructed from standard errors clustered at the province level.
Sources: NBS (2023, 2005b).

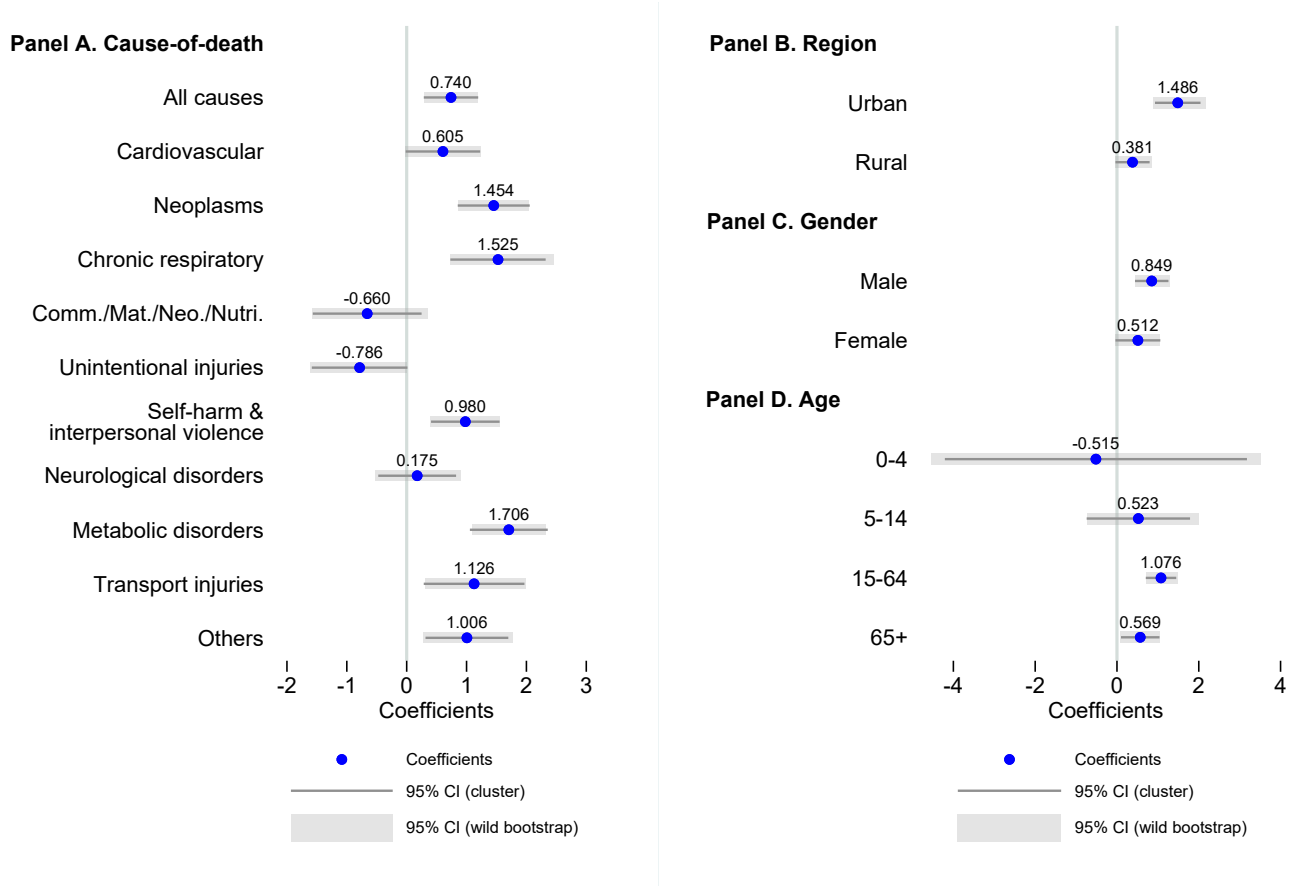


Figure G.25: Effects of the Top 1,000 Program on Mortality: Heterogeneity

Notes: The figure plots the difference in difference estimates of the following specification:

$$Y_{gpt} = \beta(\text{Top 1,000 share}_p \times \text{Post}_t) + \boldsymbol{\gamma}' \boldsymbol{x}_{gpt} + \varepsilon_{gpt},$$

where the dependent variable Y_{gpt} is the logarithm of mortality rate of gender g in province p in year t. The control vector $\boldsymbol{x}_{gpt}$ includes province and gender fixed effects, region-by-year fixed effects, and year fixed effects interacted with baseline employment shares of Top 10,000 firms. These specifications apply to all results except for Panel C (gender heterogeneity), which does not incorporate the full set of gender dimensions. Panel A uses data for 1990 and 2013 from Zhou et al. (2016), and Panels B to D use data for 2000 and 2010 from the population censuses (NBS 2000, 2010). The cause-of-death classification follows the Global Burden of Disease (GBD) 2013. Abbreviations: "Metabolic disorders" is death due to diabetes, urogenital, blood, and endocrine; "Comm./Mat./Neo./Nutri." is death due to communicable, maternal, neonatal, and nutritional. Samples include 124 observations (31 provinces × 2 genders × 2 years) in Panels A, B (Rural) and D 120 observations (30 provinces × 2 genders × 2 years) in Panel B (Urban), and 62 observations (31 provinces × 2 years) in Panel C. We exclude Tibet when estimating mortality rate responses for urban residents in Panel B because there are few urban residents in Tibet. The short lines are 95 percent confidence intervals constructed using standard errors clustered at province level, and the shaded areas are 95 percent confidence intervals constructed using wild bootstrap procedure developed by Cameron et al. (2008) with clustering at the provincial level, based on 1,000 repetitions.
Sources: NBS (2000, 2010); Zhou et al. (2016).

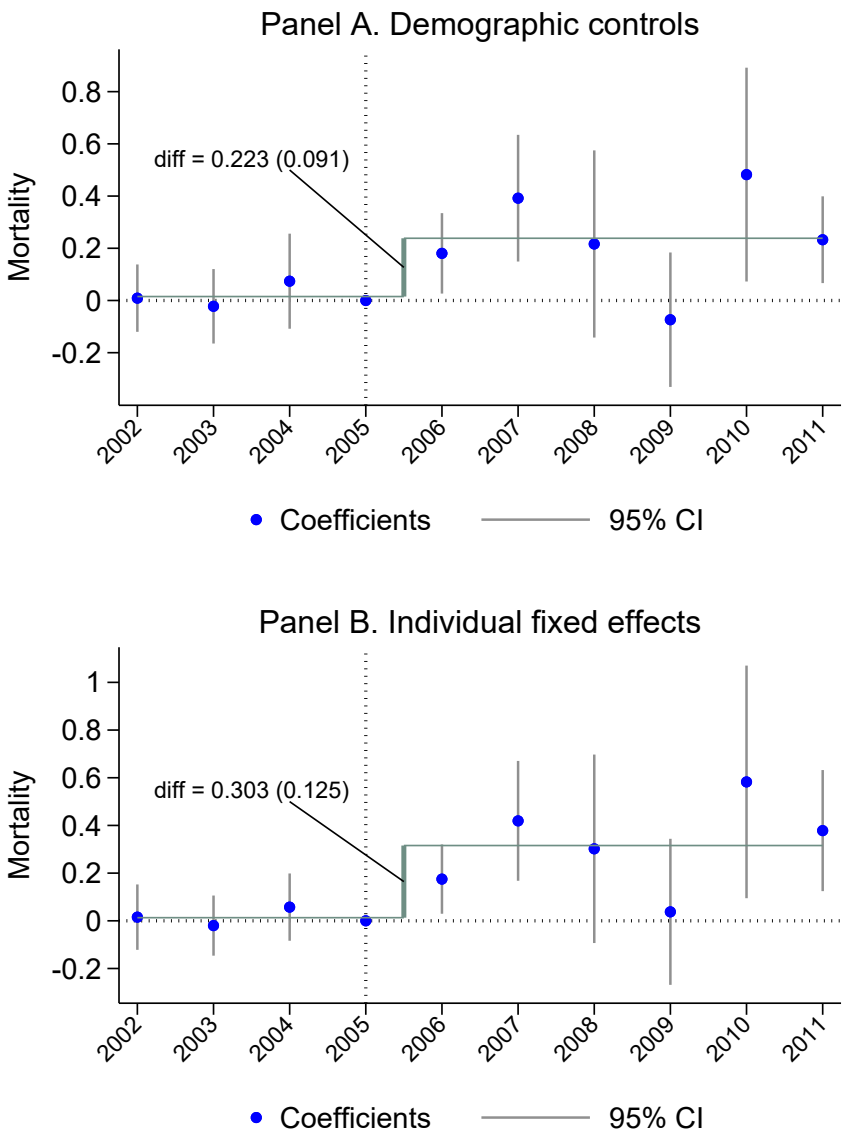


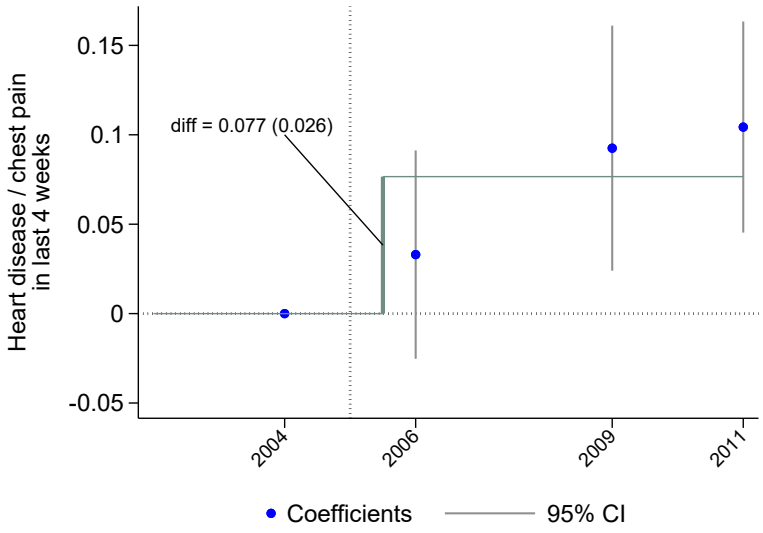
Figure G.26: Effects of the Top 1,000 Program on Mortality: Estimates Based on CLHLS Individual Panel

Notes: The figure reports event study of the Top 1,000 program on one-year mortality rates based on a panel of elderly aged 65 or above in 2002 from 22 provinces in CLHLS (2002-2011):

$$Y_{it} = \sum_{t \neq 2005} \beta_t \left(\text{Top 1,000 share}_p \times \text{Year}_t \right) + \boldsymbol{\gamma}' \boldsymbol{x}_{it} + \varepsilon_{it},$$

where dependent variable Y_{it} is a dummy that takes the value of one if individual i deceased in year t and zero otherwise. The exposure measure Top 1,000 share$_p$ is the baseline employment share of Top 1,000 firms in province p. $\boldsymbol{x}_{it}$ is a vector of controls. We use province level exposure because there is no prefecture identifiers in the CLHLS (2002-2011) dataset. Panel A controls for province, age, ethnicity, sex, and region-by-year fixed effects, as well as year fixed effects interacted with baseline employment share of Top 10,000 firms; Panel B further controls for individual fixed effects. The labeled "diff" denotes the difference between post- and pre-policy means, computed from the event-study coefficients using the Delta method. The numbers of observations are 70,958 and 71,752 in Panel A and B respectively. Sampling weights provided by the data providers are applied. 95% confidence intervals are based on standard errors clustered at province level.
Sources: CLHLS (2002-2011).

Panel A. Event study on having heart disease/chest pain



Panel B. Difference-in-differences estimates on all diseases

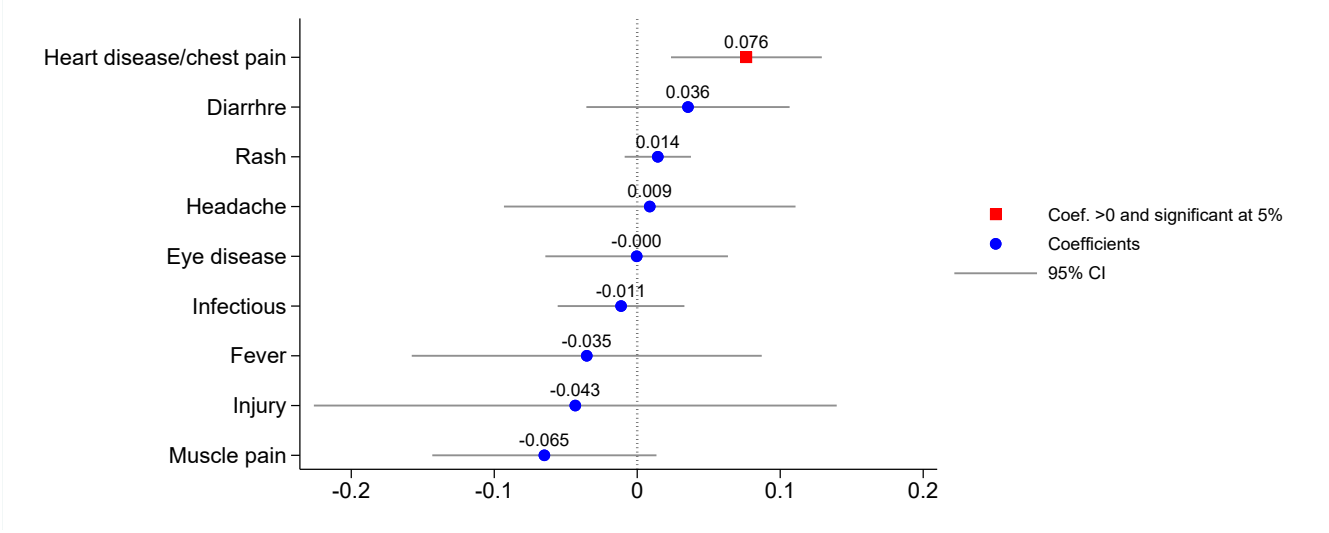


Figure G.27: Effects of the Top 1,000 Program on Health: Estimates Based on CHNS Data

Notes: Panel A reports the event study using the following specification:

$$Y_{it} = \sum_{t \neq 2005} \beta_t \left(\text{Top 1,000 share}_d \times \text{Year}_t\right) + \boldsymbol{\gamma}' \boldsymbol{x}_{it} + \varepsilon_{it},$$

where the outcome Y_{it} is an indicator equal to one if individual i reported heart disease or chest pain in the four weeks prior to the survey in year t, and zero otherwise.

Panel B reports the difference-in-differences estimates:

$$Y_{it} = \beta \left(\text{Top 1,000 share}_d \times \text{Post}_t\right) + \boldsymbol{\gamma}' \boldsymbol{x}_{it} + \varepsilon_{it},$$

where Post_t is a dummy for years after 2005.

All regressions control for individual fixed effects, age fixed effects, and region-by-year fixed effects. The label "diff" in Panel A denotes the post-pre mean difference computed from the event-study coefficients using the Delta method, which may slightly differ from the corresponding difference-in-differences estimate. The sample includes 22,422 individual-year observations. 95% confidence intervals are constructed using standard errors clustered at prefecture level.

Sources: Zhang et al. (2014).

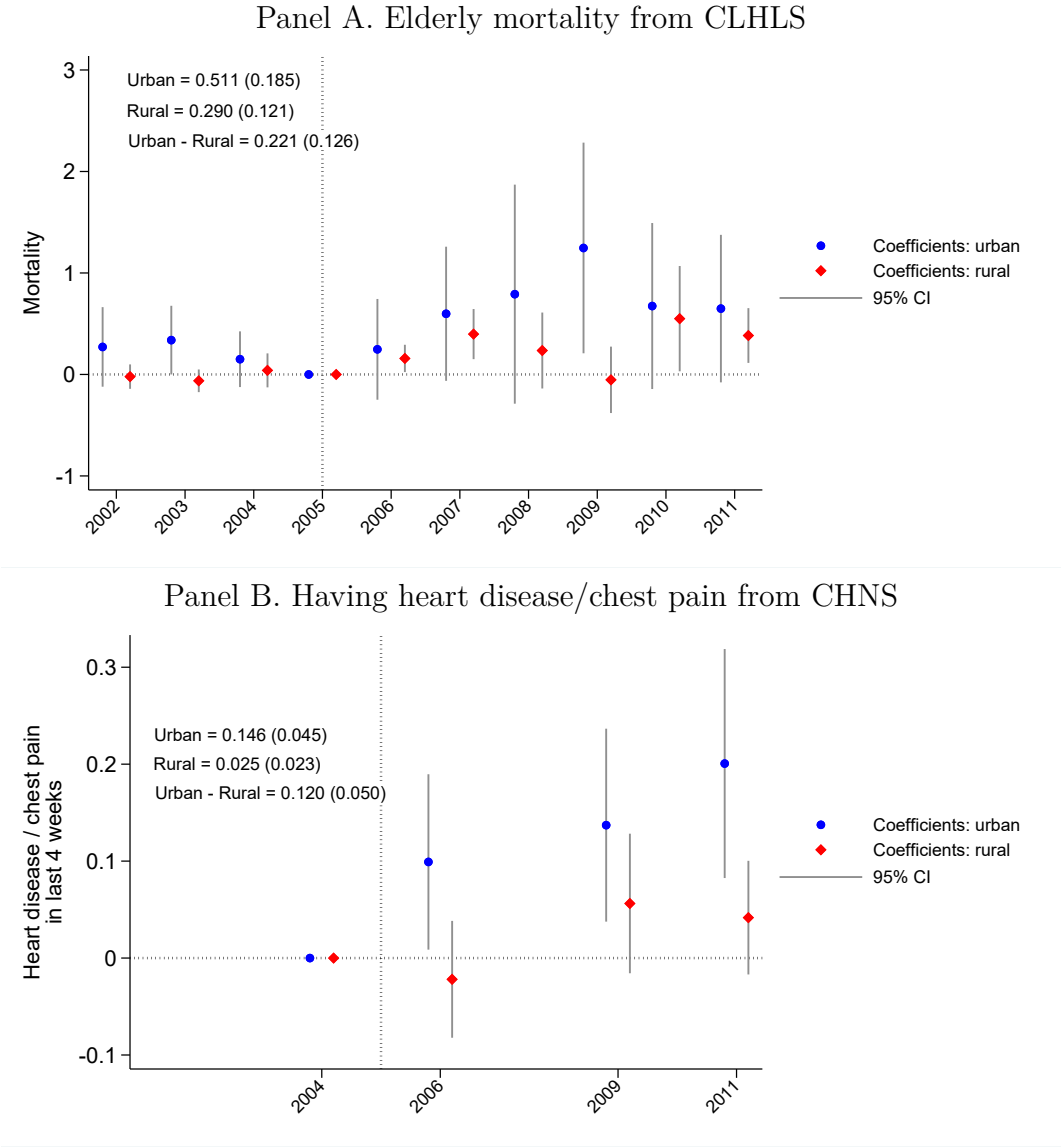


Figure G.28: Effects of the Top 1,000 Program on Health and Mortality by Region (Urban/Rural)

Notes: The figure plots the heterogeneous effects of the Top 1,000 program by region (urban versus rural), using micro data from CLHLS (2002-2011; Panel A) and CHNS (2004-2011; Panel B). The exposure is measured at province level in Panel A, and at prefecture level in Panel B. All regressions control for individual fixed effects, age fixed effects, and region-by-year fixed effects. Regression in Panel B further controls for year fixed effects interacted with a dummy for Top 1,000 prefectures. The numbers of observations are 9,828 (urban) and 61,130 (rural) in Panel A; 6,828 (urban) and 15,590 (rural) in Panel B. 95% confidence intervals are constructed using standard errors clustered at province level in Panel A, and standard errors clustered at prefecture level in Panel B, respectively.
Sources: CLHLS (2002-2011); Zhang et al. (2014).

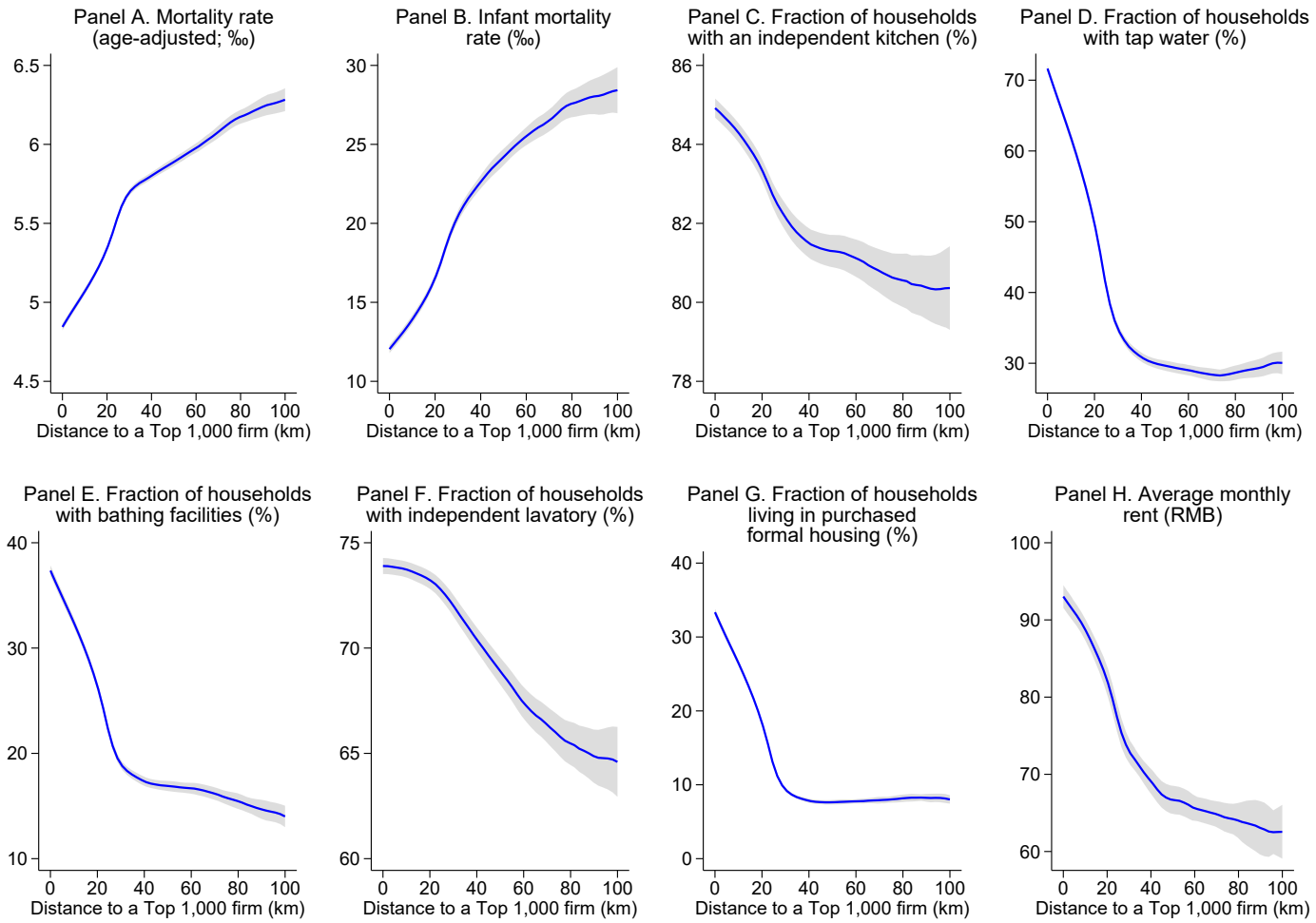


Figure G.29: Baseline Township Characteristics

Notes: This figure plots polynomial smooths of baseline township characteristics in 2000 against the distance to the nearest Top 1,000 firm within the same prefecture. The y-axis variables are defined as follows. Panel A reports the age-adjusted mortality rate using the age structure of China in 2000. Panel B reports the infant mortality rate. Panel C reports the fraction of households with an independent kitchen. Panel D reports the fraction of households with tap water. Panel E reports the fraction of households with bathing facilities. Panel F reports the fraction of households with an independent lavatory. Panel G reports the fraction of family households living in purchased formal housing, including purchased commercial housing, purchased affordable housing, and purchased privatized public housing. Panel H reports the average monthly rent among households living in rented formal housing. Because households are surveyed about monthly rents in bins (below 20 RMB, 20–50 RMB, 50–100 RMB, 100–200 RMB, 200–500 RMB, 500–1,000 RMB, 1,000–1,500 RMB, 1,500–2,000 RMB, and above 2,000 RMB), we use bin midpoints to impute monthly rents. For the bottom-coded category (below 20 RMB), we assume a monthly rent of 20 RMB, and for the top-coded category (above 2,000 RMB), we assume a monthly rent of 2,000 RMB. In the 2000 population census, "households" include both family households and collective households. All series are estimated using an Epanechnikov kernel with a bandwidth of 10 km. The underlying sample excludes townships in Zhejiang province, for which township-level data are not available.
Sources: NBS (2000).

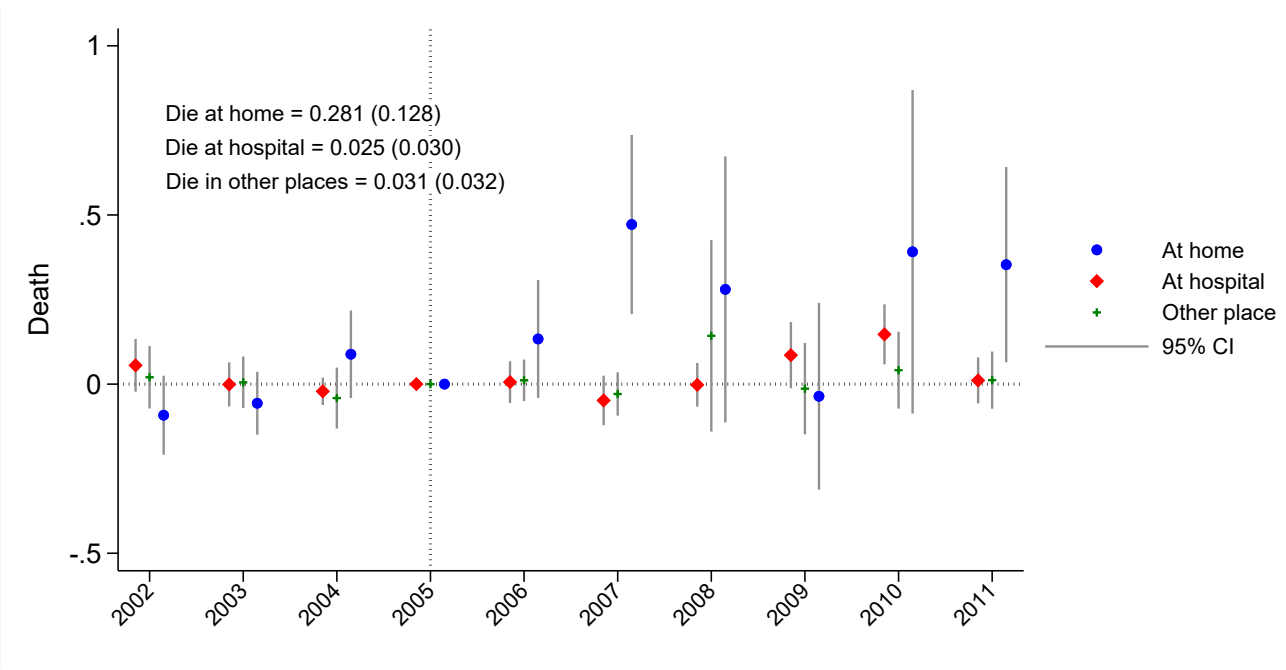


Figure G.30: Effects of the Top 1,000 Program: Place of Death

Notes: This figure presents event-study estimates of the Top 1,000 Program on the probability of dying in specific locations using the CLHLS sample. The dependent variables are dummy variables equal to one if an individual's death occurred at home, in a hospital, or in another location, respectively. The exposure is measured at province level. All regressions control for individual fixed effects, age fixed effects, and region-by-year fixed effects. The number of observations is 70,958. 95% confidence intervals are constructed using standard errors clustered at province level.
Sources: CLHLS (2002-2011).

Table G.1: Summary Statistics of Main Data

	Source	Obs.	Mean	S.D.	Median	p25	p75
Panel A. Grid cell level variables							
Top 1,000 grid cell	NBS (2001-2009a)	510,721	0.02	0.14	0.00	0.00	0.00
Wage (skill-adjusted)	NBS (2004)	510,721	3.51	3.27	3.10	2.35	4.11
Aerosol optical depth (pollution index)	Lyapustin et al. (2015)	509,315	0.50	0.16	0.52	0.40	0.60
Labor (thousand people)	NBS (2001-2009a)	449,052	1.55	4.58	0.36	0.12	1.22
Panel B. Prefecture level variables							
Top 1,000 prefecture	NBS (2004)	345	0.72	0.45	1.00	0.00	1.00
Top 1,000 employment share (if > 0)	NBS (2004)	247	0.12	0.15	0.06	0.02	0.15
Top 10,000 employment share (if > 0)	NBS (2004)	333	0.10	0.07	0.08	0.05	0.13
Related firms' employment share (if > 0)	NBS (2004)	263	0.02	0.03	0.01	0.00	0.03
Aerosol optical depth (pollution index)	Lyapustin et al. (2015)	3,795	0.38	0.17	0.38	0.24	0.52
Labor (million people)	NBS (2001-2009a)	3,448	0.21	0.34	0.11	0.05	0.21
Days above 30°C	NOAA (2024)	3,674	10.40	13.44	4.00	0.00	18.00
Days below 0°C	NOAA (2024)	3,674	47.27	53.88	21.00	0.00	93.00
Mortality rate (corrected; ‰)	NBS (2000-2012)	3,417	5.95	1.37	5.96	5.11	6.77
Lung cancer mortality (per 100,000)	CHCAMS (2017)	2,070	23.46	13.52	19.60	12.63	34.21
Panel C. Indivdual level variable							
Work Status (among working age)	NBS (2002-2009b)	587,652	0.66	0.47	1.00	0.00	1.00
Age	NBS (2002-2009b)	757,572	39.46	18.64	41.00	26.00	53.00
Ethnic Han	NBS (2002-2009b)	757,572	0.97	0.17	1.00	1.00	1.00
Years of education	NBS (2002-2009b)	757,572	10.43	3.83	12.00	9.00	12.00
Female	NBS (2002-2009b)	757,572	0.50	0.50	1.00	0.00	1.00
Panel D. Household level variable							
Total expenditure (RMB)	NBS (2002-2009b)	256,077	23075.81	20059.48	18189.27	12205.03	27476.22
Preventive medical spending (RMB)	NBS (2002-2009b)	256,077	1246.28	2522.50	504.00	154.90	1335.96
Curative medical spending (RMB)	NBS (2002-2009b)	256,077	650.63	2327.41	82.00	0.00	470.00
Electricity use (kWh)	NBS (2002-2009b)	256,077	1301.55	1006.54	1090.00	656.00	1704.00
Air conditioner ownership	NBS (2002-2009b)	256,652	0.54	0.50	1.00	0.00	1.00

Notes: The table reports the summary statistics of the main datasets. Panel A reports the grid cell level variables aggregated from firm level data (NBS 2001-2009a) and 1 km × 1 km MODIS AOD data from NASA's TERRA and AQUA satellites (Lyapustin et al. 2015). Panel B reports the prefecture level variables, including exposure measures calculated from 2004 Economic Census (NBS 2004), AOD data calculated from the NASA's TERRA and AQUA satellites (Lyapustin et al. 2015), labor data aggregated from the ASIF data for 2001-2009 (NBS 2001-2009a), temperature data from NOAA (2024), all-cause mortality data from *China Statistical Yearbook For Regional Economy* (NBS 2000-2012) and prefecture-gender-year level lung cancer mortality from CHCAMS (2017). For all-cause mortality rate, "corrected" means adjustment by province-year specific factors to match province-year mortality rates published on the *China Population & Employment Statistics Yearbook* (NBS 2023). Panels C and D report the individual and household variables from the UHS (NBS 2002-2009b), respectively.
Sources: NBS (2004, 2002-2013, 2001-2009a, 2002-2009b); Lyapustin et al. (2015); NOAA (2024); CHCAMS (2017).

Table G.2: Summary Statistics of Auxiliary Data on Mortality and Health

Variable	Unit	Years available	Coverage	Source	Mean	SD
All-causes mortality rate (per 1,000)	Province-year	1990-2018	31 provinces	NBS (2023)	6.228	0.771
Mortality rate (CLHLS)	Individual-year	2002-2011	22 provinces	CLHLS (2002-2011)	0.050	0.218
Mortality rate (CLHLS; urban)	Individual-year	2002-2011	22 provinces	CLHLS (2002-2011)	0.047	0.211
Mortality rate (CLHLS; rural)	Individual-year	2002-2011	22 provinces	CLHLS (2002-2011)	0.050	0.218
Been sick or injured in last 4 weeks? (CHNS)	Individual-year	2004, 2006, 2009, 2011	49 prefectures in 9 provinces	Zhang et al. (2014)	0.152	0.359
Last 4 weeks: fever, sore throat, cough (CHNS)	Individual-year	2004, 2006, 2009, 2011	49 prefectures in 9 provinces	Zhang et al. (2014)	0.079	0.269
Last 4 weeks: diarrhre, stomachache (CHNS)	Individual-year	2004, 2006, 2009, 2011	49 prefectures in 9 provinces	Zhang et al. (2014)	0.022	0.147
Last 4 weeks: headache, dizziness (CHNS)	Individual-year	2004, 2006, 2009, 2011	49 prefectures in 9 provinces	Zhang et al. (2014)	0.051	0.221
Last 4 weeks: joint, muscle pain (CHNS)	Individual-year	2004, 2006, 2009, 2011	49 prefectures in 9 provinces	Zhang et al. (2014)	0.052	0.223
Last 4 weeks: rash, dermatitis (CHNS)	Individual-year	2004, 2006, 2009, 2011	49 prefectures in 9 provinces	Zhang et al. (2014)	0.006	0.077
Last 4 weeks: eye/ear disease (CHNS)	Individual-year	2004, 2006, 2009, 2011	49 prefectures in 9 provinces	Zhang et al. (2014)	0.010	0.098
Last 4 weeks: heart disease/chest pain (CHNS)	Individual-year	2004, 2006, 2009, 2011	49 prefectures in 9 provinces	Zhang et al. (2014)	0.018	0.131
Last 4 weeks: other infectious disease (CHNS)	Individual-year	2004, 2006, 2009, 2011	49 prefectures in 9 provinces	Zhang et al. (2014)	0.012	0.108

Notes: This table reports the unit, temporal and geographic coverage, and summary statistics of auxiliary data on mortality and health. Except for the CHNS data, all other data sets are national or nationally representative in scope. The 22 provinces covered by the CLHLS are Beijing, Tianjin, Hebei, Shanxi, Liaoning, Jilin, Heilongjiang, Shanghai, Jiangsu, Zhejiang, Anhui, Fujian, Jiangxi, Shandong, Henan, Hubei, Henan, Guangdong, Guangxi, Chongqing, Sichuan, and Shaanxi. The 9 provinces covered by the CHNS data are Liaoning, Heilongjiang, Jiangsu, Shandong, Henan, Hubei, Hunan, Guangxi, and Guizhou.
Sources: NBS (2023); CLHLS (2002-2011); Zhang et al. (2014).

Table G.3: Reallocation of AOD and Labor within Prefectures: Heterogeneity by Wind Patterns

	(1)	(2)	(3)	(4)
Panel A. AOD				
Top 1,000 cell × Post	-0.006	-0.008	-0.006	-0.009
	(0.002)	(0.002)	(0.002)	(0.002)
Downwind cell × Post		-0.004		-0.005
		(0.002)		(0.002)
Upwind cell × Post			0.001	-0.001
			(0.002)	(0.002)
Observations	509,296	509,296	509,296	509,296
Clusters	343	343	343	343
Panel B. Labor				
Top 1,000 cell × Post	-0.189	-0.189	-0.192	-0.195
	(0.026)	(0.027)	(0.027)	(0.028)
Downwind cell × Post		0.001		-0.006
		(0.013)		(0.015)
Upwind cell × Post			-0.013	-0.015
			(0.013)	(0.015)
Observations	405,337	405,337	405,337	405,337
Clusters	344	344	344	344
Grid cell FE	✓	✓	✓	✓
Prefecture × year FE	✓	✓	✓	✓

Notes: An observation is a $0.03° \times 0.03°$ grid cell from 2001 to 2011 in Panel A and from 2001 to 2009 in Panel B. The dependent variable is the logarithm of annual aerosol optical depth (AOD) concentration in Panel A and the logarithm of total industrial employment in Panel B. Panel B serves as a placebo test: unlike AOD, industrial labor reallocation should be orthogonal to wind patterns, conditional on distance. The key explanatory variables are defined as follows. "Top 1,000 cell" is a dummy equal to one if a grid cell hosts at least one Top 1,000 firm and zero otherwise. "Downwind cell" is a dummy equal to one if a grid cell hosts no Top 1,000 firm but lies within 50 kilometers and downwind of a Top 1,000 firm, and zero otherwise. "Upwind cell" is a dummy equal to one if a grid cell is neither a "Top 1,000 cell" nor a "Downwind cell" but lies within 50 kilometers and upwind of a Top 1,000 firm, and zero otherwise. "Post" is a dummy equal to one for years after 2005, and zero otherwise. We identify upwind and downwind grid cells in three steps. First, we obtain daily wind directions from the fifth-generation European Centre for Medium-Range Weather Forecasts reanalysis dataset (ECMWF ERA-5; Hersbach et al. (2020)) and sample the raster data at county centroids to construct county-by-day wind patterns. Second, we define a county's dominant wind direction as the direction with the largest total wind speed in 2005, and merge this dominant wind direction to Top 1,000 grid cells using geographic coordinates and county shapefiles. Third, within each prefecture, we define the downwind region as a $\pm 45°$ cone in the direction of the dominant wind and the upwind region as a $\pm 45°$ cone in the opposite direction, as illustrated in Figure G.6. Non-Top 1,000 grid cells are assigned to the upwind or downwind regions based on their relative coordinates. All specifications include grid-cell fixed effects and prefecture-by-year fixed effects. Standard errors clustered at the prefecture level are reported in parentheses.
Sources: Lyapustin et al. (2015); NBS (2001-2009a); Hersbach et al. (2020).

Table G.4: Effects of the Top 1,000 Program on Unregulated Firms: Interaction with the NSMF Program

Outcome	Energy	SO_2
	(1)	(2)
Top 1,000 share × Post	0.451	0.364
	(0.190)	(0.183)
Top 1,000 share × Post	-0.009	-0.399
× NSMF (Air)	(0.445)	(0.388)
Top 1,000 share × Post	0.299	0.070
× NSMF (Water)	(0.448)	(0.380)
Observations	59,192	207,628
Clusters	330	333
Firm FE	✓	✓
Industry-year FE	✓	✓
Province-year FE	✓	✓
NSMF (Air)-year FE	✓	✓
NSMF (Water)-year FE	✓	✓

Notes: An observation is a firm-year from 2002 to 2011. Top 1,000 firms are excluded from the sample. The dependent variable is the logarithm of energy use (column (1)) and SO_2 emissions (columns (2)). The number of observations varies across columns because firms report different pollutants. Standard errors clustered at prefecture level are reported in parentheses.
Sources: MEP (2002-2011).

Table G.5: Mortality Income Gradient

Study	Mortality-Income Gradient ($\times -1$)	Sample	Identification Strategy & Shock	Note
Panel A: Correlational Estimates				
Pritchett and Summers (1996)	0.2 $\sim$ 0.4	Cross-country (Infant Mortality) 1960–1990,	**Instrumental Variables.** Uses terms of trade shocks, investment rates, and education as exogenous determinants of income growth.	A 1% increase in per capita income leads to a 0.2%–0.4% relative decrease in Infant Mortality Rate.
Deaton (2003)	0.27	USA (NLMS), 1980 (Baseline)	**Baseline Prediction.** Uses 1980 baseline income to predict future mortality, mitigating reverse causality.	Implied elasticity from $\sim$27% mortality reduction associated with doubling income.
Panel B: Positive Income Shocks (Transfers & Pensions)				
Barham and Rowberry (2013)	0.62	Mexico, 1997-2000	**Progresa (CCT).** Phased rollout benefiting elderly in poor households.	Ratio of elderly mortality decline (13.6%) to income increase (22%).
Walker et al. (2024)	0.64	Kenya, 2011-2021	**RCT / UCT.** Large, one-time unconditional cash transfer ($\sim$\$1,000) via NGO.	Ratio of infant mortality reduction (-48%) to household expenditure increase (+75%).
Richterman et al. (2025)	0.8	37 LMICs, 2000-2019	**Gov. Cash Transfers.** Staggered rollout of national programs in developing countries.	Median transfers ($\sim$10% GDPpc) reduced child mortality by 8%.
Aizer et al. (2016)	0.3 $\sim$ 0.5	USA, 1911-1935	**Mothers' Pensions.** Early welfare program tracking children's long-run longevity.	Reduced-form effect of childhood transfers (+20–30% income) on adult mortality ($\sim$-10%).
Huang and Zhang (2021)	0.38	China, 2009-2012	**Social Pension (NRPS).** County rollout of non-contributory pension (55 RMB/mo).	Based on nominal replacement rate ($\sim$40%) and mortality decline (-14.5%).
Panel C: Negative Economic Shocks				
Sullivan and von Wachter (2009)	0.60	USA, 1980-2006	**Job Displacement.** Mass layoffs causing persistent earnings losses.	Ratio of sustained mortality hazard (+15%) to permanent earnings loss (-25%).
Burgess et al. (2017)	1.29	India, 1957-2000	**Weather/Credit.** Heat shocks reducing yields in unbanked regions.	Comparison of weather-induced mortality rise (+0.9%) and income decline (-0.7%).
Adda and Fawaz (2020)	0.87	USA, 1991-2011	**Import Competition.** Rising Chinese import penetration post-WTO accession.	Import shocks reduced income by 0.83% and raised mortality by 0.74%.
Schwandt and Von Wachter (2019)	1.54	USA, 1979-2016	**Recession at Entry.** Entry during high unemployment causing scarring.	Ratio of mid-life mortality rise (+2%) to permanent income loss (-1.3%).
Xiao et al. (2024)	0.84	China, 1989-2015	**Serial Income Shock.** Severe negative income shocks during economic transition.	Based on HR=1.42 (+42% risk) associated with severe income drop ($\geq$50%).
Bellemare et al. (2025)	1.11	USA (Midwest), 1980-2019	**Commodity Shocks.** Exogenous soybean revenue variation.	Scaled by low pass-through of declining crop revenue to farm income (-0.009) and mortality (0.01) .

Note: "Mortality-Income Gradient" refers to the negative mortality-income elasticity (percentage change in mortality / percentage change in income $\times$ -1), unless otherwise specified."PIR" denotes Poverty Income Ratio.

Table G.6: Impacts of the Top 1,000 Program on Pollution Exposure

Dependent variable	ΔPollution	ΔExposed pollution$_d$	$\sum_{k\in d} \Delta\ell_{kd}$Pollution$_{kdt_0}$	$\sum_{k\in d} \ell_{kdt_1}\Delta$Pollution$_{kd}$
	(1)	(2)=(3)+(4)	(3)	(4)
Top 1,000 share	-0.008	-0.023	-0.001	-0.022
	(0.047)	(0.047)	(0.003)	(0.048)
Observations	345	345	345	345
Province FE	✓	✓	✓	✓

Notes: This table reports long-difference estimates of the effects of the *Top 1,000 Program* on pollution exposure from 2000 to 2010. The estimating equation is:

$$Y_d = \beta(\text{Top 1,000 share}_d) + \delta_p + \varepsilon_d,$$

where Y_d denotes the outcome of interest, Top 1,000 share$_d$ is the baseline employment share of Top 1,000 firms in prefecture d, and δ_p is the province fixed effect. An observation is a prefecture. Column (1) reports changes in unweighted average pollution across townships. Column (2) reports changes in population-weighted pollution exposure. Column (3) reports the change in predicted exposure holding township pollution fixed at 2000 levels while allowing population shares to vary. Column (4) reports the change in predicted exposure holding population shares fixed at 2010 levels while allowing township pollution to vary. See Section E.1 for details. Township pollution is measured as the logarithm of township-average aerosol optical depth (AOD). Because AOD data are available only starting in 2001, we use 2001 AOD concentrations to proxy for 2000 levels. All specifications control for province fixed effects and are weighted using baseline industrial employment. Robust standard errors are reported in parentheses.
Sources: Lyapustin et al. (2015); NBS (2000, 2010).

Table G.7: Impacts of the Top 1,000 Program on Household Sorting

Dependent variable Y	$\sum_{k\in d} \Delta\ell_{kd} \ln Y_{kdt_0}$							
	Mortality	Infant mortality	Independent kitchen	Tap water	Bathing facilities	Independent lavatory	Purchased formal housing	Rent
	(1)	(2)	(3)	(4)	(5)	(6)	(7)	(8)
Top 1,000 share	0.010	0.136	0.000	-0.094	-0.076	0.048	-0.097	0.050
	(0.013)	(0.125)	(0.010)	(0.038)	(0.051)	(0.021)	(0.056)	(0.089)
Observations	334	334	334	334	334	334	334	334
Province FE	✓	✓	✓	✓	✓	✓	✓	✓

Notes: This table reports long-difference estimates of the effects of the *Top 1,000 Program* on household sorting behaviors. The estimating equation is:

$$\sum_{k\in d} \Delta\ell_{kd} \ln Y_{kdt_0} = \beta(\text{Top 1,000 share}_d) + \delta_p + \varepsilon_d,$$

where Y_{kdt_0} denotes the outcome of interest in township k of prefecture d in baseline $t_0 = 2000$, Top 1,000 share$_d$ is the baseline employment share of Top 1,000 firms in prefecture d, and δ_p is the province fixed effect. Y variables are defined as follows. "Mortality" is the age-adjusted mortality rate using the age structure of China in 2000. "Infant mortality" is the infant mortality rate. "Independent kitchen" is the fraction of households with an independent kitchen. "Tap water" is the fraction of households with tap water. "Bathing facilities" is the fraction of households with bathing facilities. "Independent lavatory" is the fraction of households with an independent lavatory. "Purchased formal housing" is the fraction of family households living in purchased formal housing, including purchased commercial housing, purchased affordable housing, and purchased privatized public housing. "Rent" is the average monthly rent among households living in rented formal housing. See Figure G.29 for baseline spatial patterns and more details on data construction. An observation is a prefecture. The underlying sample excludes prefectures in Zhejiang province, for which township-level data are not available. Robust standard errors are reported in parentheses.
Sources: NBS (2000, 2010).

Table G.8: Impacts of the Top 1,000 Program on Healthcare Supply

Dependent variable	Hospital	Hospital beds	Doctors	Mortality	Hospital	Hospital beds	Doctors	Mortality
	(1)	(2)	(3)	(4)	(5)	(6)	(7)	(8)
Top 1,000 share × Post	0.013	-0.128	-0.235	0.283	0.925	0.119	0.054	0.779
	(0.100)	(0.076)	(0.097)	(0.090)	(0.502)	(0.453)	(0.440)	(0.365)
Top 1,000 share × Post					-1.094	-0.296	-0.346	-0.608
× Public hospital share					(0.603)	(0.536)	(0.566)	(0.420)
Hospitals				0.004				
				(0.014)				
Hospital beds				0.081				
				(0.089)				
Doctors				0.004				
				(0.063)				
Observations	3,849	3,849	3,849	3,849	3,849	3,849	3,849	3,849
Clusters	343	343	343	343	343	343	343	343
Prefecture FE	✓	✓	✓	✓	✓	✓	✓	✓
Region × year FE	✓	✓	✓	✓	✓	✓	✓	✓
Top 10,000 share × year FE	✓	✓	✓	✓	✓	✓	✓	✓

Notes: An observation is a prefecture-year from 2000 to 2011. We drop data for 1999 due to lack of data on number of hospitals. The dependent variables are defined as follows. "Hospital" is the logarithm of the number of hospitals per capita. "Hospital beds" is the logarithm of the number of hospital beds per capita. "Doctors" is the logarithm of the number of doctors per capita. "Mortality" is the logarithm of the mortality rate. The key explanatory variables are defined as follows. "Top 1,000 share" is the baseline employment share of Top 1,000 firms. "Top 10,000 share" is the baseline employment share of Top 10,000 firms. "Public hospital share" is the fraction of staff in public hospitals among all hospital-sector staff (3-digit CIC code 831) in 2008, measured using the 2008 Economic Census (NBS 2008). "Hospitals," "Hospital beds," and "Doctors" (when included as controls) are defined analogously to the dependent variables. All specifications include prefecture fixed effects, region-by-year fixed effects, and Top 10,000 share-by-year fixed effects. Standard errors clustered at the prefecture level are reported in parentheses.
Sources: NBS (2000-2012).

Table G.9: Effects of the Top 1,000 Program: Medical Insurance Heterogeneity

Dependent variable	Death: CLHLS		Heart Disease : CHNS	
	Uninsured	Insured	Uninsured	Insured
	(1)	(2)	(3)	(4)
Top 1,000 share × Post	0.306	0.036	0.077	0.048
	(0.120)	(0.194)	(0.025)	(0.093)
Observations	55,577	2,122	15,249	5,326
Clusters	22	21	49	47
Individual FE	✓	✓	✓	✓
Age FE	✓	✓	✓	✓
Region × year FE	✓	✓	✓	✓
Top 10,000 share × year FE	✓	✓	✓	✓

Notes: An observation is an individual-year, using micro data from CLHLS (2002-2011; Column (1)-(2)) and CHNS (2004,2006, 2009 and 2011; Column (3)-(4)). The dependent variable is a dummy variable of individual's death in Column (1)-(2), and a dummy variable equals to one if individual have heart disease/chest pain in last 4 weeks. The "Top 1,000 share" refers to provincial level Top 1,000 employment share in Column (1)-(2) and prefectural level in Column(3)-(4). Insurance definitions vary by data source: in ClHLS (Columns (1)-(2)), "Insured" specifically refers to individuals covered by severe disease insurance,whereas in CHNS (Columns 3-4), it denotes a broader measure of general medical insurance. Standard errors clustered at provincial level in Column (1)-(2) and prefecture level in Column (3)-(4), reported in parentheses.
Sources: CLHLS (2002-2011); Zhang et al. (2014).

References

Adda, Jérôme and Yarine Fawaz, "The health toll of import competition," *Economic Journal*, 2020, *130* (630), 1501–1540.

Adão, Rodrigo, Costas Arkolakis, and Federico Esposito, "General Equilibrium Effects in Space: Theory and Measurement," Working Paper 25544, National Bureau of Economic Research February 2019.

Ai, Hongshan, Yang Hu, and Ke Li, "Impacts of environmental regulation on firm productivity: evidence from China's Top 1000 Energy-Consuming Enterprises Program," *Applied Economics*, 2021, *53* (7), 830–844.

Aizer, Anna, Shari Eli, Joseph Ferrie, and Adriana Lleras-Muney, "The long-run impact of cash transfers to poor families," *American Economic Review*, 2016, *106* (4), 935–971.

Allcott, Hunt, Rebecca Diamond, Jean-Pierre Dubé, Jessie Handbury, Ilya Rahkovsky, and Molly Schnell, "Food Deserts and the Causes of Nutritional Inequality," *Quarterly Journal of Economics*, 2019, *134* (4), 1793–1844.

Allen, Treb and Costas Arkolakis, "Trade and the Topography of the Spatial Economy," *Quarterly Journal of Economics*, 2014, *129* (3), 1085–1140.

Antràs, Pol, Davin Chor, Thibault Fally, and Russell Hillberry, "Measuring the Upstreamness of Production and Trade Flows," *American Economic Review*, 2012, *102* (3), 412–16.

Barham, Tania and Jacob Rowberry, "Living longer: The effect of the Mexican conditional cash transfer program on elderly mortality," *Journal of Development Economics*, 2013, *105*, 226–236.

Baum-Snow, Nathaniel, Loren Brandt, J. Vernon Henderson, Matthew A. Turner, and Qinghua Zhang, "Roads, Railroads, and Decentralization of Chinese Cities," *Review of Economics and Statistics*, 2017, *99* (3), 435–448.

Bellemare, Marc F., Jhih-Yun Liu, and Joleen Hadrich, "Commodity Revenue Shocks and Mortality," *Journal of Human Resources*, December 2025. Published online before print.

Brandt, Loren, Johannes Van Biesebroeck, and Yifan Zhang, "Challenges of working with the Chinese NBS firm-level data," *China Economic Review*, 2014, *30*, 339–352.

Buchard, V., A.M. da Silva, C.A. Randles, P. Colarco, R. Ferrare, J. Hair, C. Hostetler, J. Tackett, and D. Winker, "Evaluation of the surface PM2.5 in Version 1 of the NASA MERRA Aerosol Reanalysis over the United States," *Atmospheric Environment*, 2016, *125*, 100–111.

Burgess, Robin, Olivier Deschenes, Dave Donaldson, and Michael Greenstone, "Weather, Climate Change and Death in India," Working Paper, Energy Policy Institute at the University of Chicago 2017.

Cameron, A. Colin, Jonah B. Gelbach, and Douglas L. Miller, "Bootstrap-Based Improvements for Inference with Clustered Errors," *Review of Economics and Statistics*, 2008, *90* (3), 414–427.

CHCAMS, "Nationwide County-Level Cancer Mortality Rates (1973–1975, 1990–1992, 2004–2005, 2014)," Cancer Hospital, Chinese Academy of Medical Sciences 2017.

Chen, Qiaoyi, Zhao Chen, Zhikuo Liu, Juan Carlos Suárez Serrato, and Daniel Yi Xu, "Regulating Conglomerates: Evidence from an Energy Conservation Program in China," *American Economic Review*, 2025, *115* (2), 408–47.

Chen, Yvonne Jie, Pei Li, and Yi Lu, "Career concerns and multitasking local bureaucrats: Evidence of a target-based performance evaluation system in China," *Journal of Development Economics*, 2018, *133*, 84–101.

Cheng, Lixin, Hong Liu, Yanfeng Zhang, Keping Shen, and Yi Zeng, "The Impact of Health Insurance on Health Outcomes and Spending of the Elderly: Evidence from China's New Cooperative Medical Scheme," *Health Economics*, 2015, *24* (6), 672–691.

CLHLS, "The Chinese Longitudinal Healthy Longevity Survey (CLHLS)-Longitudinal Data (2002-2011)," Center for Healthy Aging and Development Studies 2002-2011.

Deaton, Angus, "Health, Inequality, and Economic Development," *Journal of Economic Literature*, 2003, *41* (1), 113–158.

Deryugina, Tatyana and David Molitor, "Does When You Die Depend on Where You Live? Evidence from Hurricane Katrina," *American Economic Review*, 2020, *110* (11), 3602–33.

_ **and** _ , "The Causal Effects of Place on Health and Longevity," *Journal of Economic Perspectives*, 2021, *35* (4), 147–70.

Dingel, Jonathan I., Antonio Miscio, and Donald R. Davis, "Cities, lights, and skills in developing economies," *Journal of Urban Economics*, 2021, *125*, 103174.

Ebenstein, Avraham, Maoyong Fan, Michael Greenstone, Guojun He, and Maigeng Zhou, "New evidence on the impact of sustained exposure to air pollution on life expectancy from China's Huai River Policy," *Proceedings of the National Academy of Sciences*, 2017, *114* (39), 10384–10389.

Fan, Maoyong, Hanchen Jiang, and Maigeng Zhou, "Beyond particulate matter: New evidence on the causal effects of air pollution on mortality," *Journal of Health Economics*, 2023, *91*, 102799.

Feng, Shuaizhang, Yingyao Hu, and Robert Moffitt, "Long run trends in unemployment and labor force participation in urban China," *Journal of Comparative Economics*, 2017, *45* (2), 304–324.

Finkelstein, Amy, Matthew Gentzkow, and Heidi Williams, "Place-Based Drivers of Mortality: Evidence from Migration," *American Economic Review*, 2021, *111* (8), 2697–2735.

_ **, Matthew J. Notowidigdo, Frank Schilbach, and Jonathan Zhang**, "Lives Versus Livelihoods: The Impact of the Great Recession on Mortality and Welfare," *Quarterly Journal of Economics*, 2025, *140* (3), 2269–2328.

Ge, Suqin and Dennis Tao Yang, "Changes in China's Wage Structure," *Journal of the European Economic Association*, 2014, *12* (2), 300–336.

Ghanem, Dalia and Junjie Zhang, "'Effortless Perfection:' Do Chinese cities manipulate air pollution data?," *Journal of Environmental Economics and Management*, 2014, *68* (2), 203–225.

Greenstone, Michael, Guojun He, Ruixue Jia, and Tong Liu, "Can Technology Solve the Principal-Agent Problem? Evidence from China's War on Air Pollution," *American Economic Review: Insights*, 2022, *4* (1), 54–70.

Gruber, Jonathan, Mengyun Lin, and Junjian Yi, "The largest insurance program in history: Saving one million lives per year in China," *Journal of Public Economics*, 2023, *226*, 104999.

Han, Chao, Zhen Chen, and Zhen Wang, "Mechanisms of Firms' Pollution Reduction under Energy-Saving Target Constraints," *China Industrial Economics (in Chinese)*, 2020, (10), 43–61.

He, Guojun, Shaoda Wang, and Bing Zhang, "Watering Down Environmental Regulation in China," *Quarterly Journal of Economics*, 2020, *135* (4), 2135–2185.

Hernandez-Cortes, Danae and Kyle C. Meng, "Do environmental markets cause environmental injustice? Evidence from California's carbon market," *Journal of Public Economics*, 2023, *217*, 104786.

Hersbach, Hans, Bill Bell, Paul Berrisford, Shoji Hirahara, András Horányi, Joaquín

Muñoz-Sabater, Julien Nicolas, Carole Peubey, Raluca Radu, Dinand Schepers, Adrian Simmons, Cornel Soci, Saleh Abdalla, Xavier Abellan, Gianpaolo Balsamo, Peter Bechtold, Gionata Biavati, Jean Bidlot, Massimo Bonavita, Giovanna De Chiara, Per Dahlgren, Dick Dee, Michail Diamantakis, Rossana Dragani, Johannes Flemming, Richard Forbes, Manuel Fuentes, Alan Geer, Leo Haimberger, Sean Healy, Robin J. Hogan, Elías Hólm, Marta Janisková, Sarah Keeley, Patrick Laloyaux, Philippe Lopez, Cristina Lupu, Gabor Radnoti, Patricia de Rosnay, Iryna Rozum, Freja Vamborg, Sebastien Villaume, and Jean-Noël Thépaut, "The ERA5 global reanalysis," *Quarterly Journal of the Royal Meteorological Society*, 2020, *146* (730), 1999–2049.

Hsieh, Chang-Tai and Peter J. Klenow, "Misallocation and Manufacturing TFP in China and India," *Quarterly Journal of Economics*, 2009, *124* (4), 1403–1448.

Huang, Wei and Chuanchuan Zhang, "The Power of Social Pensions: Evidence from China's New Rural Pension Scheme," *American Economic Journal: Applied Economics*, 2021, *13* (2), 179–205.

Jensen, Robert T and Kaspar Richter, "The health implications of social security failure: evidence from the Russian pension crisis," *Journal of Public Economics*, 2004, *88* (1), 209–236.

Ke, Jing, Lynn Price, Stephanie Ohshita, David Fridley, Nina Zheng Khanna, Nan Zhou, and Mark Levine, "China's industrial energy consumption trends and impacts of the Top-1000 Enterprises Energy-Saving Program and the Ten Key Energy-Saving Projects," *Energy Policy*, 2012, *50*, 562–569.

Kong, Dongmin and Chenhao Liu, "Centralization and Regulatory Enforcement: Evidence from Personnel Authority Reform in China," *Journal of Public Economics*, 2024, *229*, 105030.

Li, Ruoxin and Xiaohui Li, "Energy Saving Sprint Set Production Limit, Energy-Intensive Firms All Suffered," *China Securities Journal*, 2010. News report.

Liu, Nicole Ning, Carlos Wing-Hung Lo, Xueyong Zhan, and Wei Wang, "Campaign-Style Enforcement and Regulatory Compliance," *Public Administration Review*, 2014, *75* (1), 85–95.

Lyapustin, Alexei, Yujie Wang, and NASA MODAPS SIPS, "MCD19A2 MODIS/Terra + Aqua Aerosol Optical Thickness Daily L2G Global 1 km SIN Grid (Collection 6)," 2015.

Ma, Lin and Yang Tang, "The distributional impacts of transportation networks in China," *Journal of International Economics*, 2024, *148*, 103873.

Meng, Xin, "Labor Market Outcomes and Reforms in China," *Journal of Economic Perspectives*, 2012, *26* (4), 75–102.

MEP, "China Environment Yearbook," Ministry of Environmental Protection 2002-2009.

_ , "Environmental Survey and Reporting Database," Ministry of Environmental Protection 2002-2011.

_ , "Zhongguo Huanjing Zhiliang Baogao (Environmental Annual Quality Reports)," Ministry of Environmental Protection 2007-2012.

Modeling, Global and NASA/GSFC Assimilation Office (GMAO), "MERRA-2 tavgM_2d_aer_Nx: 2D Monthly Mean Time-Averaged Single-Level Assimilation Aerosol Diagnostics V5.12.4," 2015. Version 5.12.4.

MOF, "Propping Up a Blue Sky for Environmental Protection: A Review of National Fiscal Support for Energy Conservation and Emission Reduction in Recent Years," China Financial and Economic News may 2012. Ministry of Finance.

NASA, "Fire Information for Resource Management System (FIRMS): Active Fire Data Attributes for MODIS and VIIRS," Technical Report, NASA Earth Science Data and Information

System (ESDIS) Project, Goddard Space Flight Center 2025.
NBS, "Fifth National Population Census," National Bureau of Statistics 2000.
_ , "Industrial Product Output Database," National Bureau of Statistics 2000-2006.
_ , "China Statistical Yearbook For Regional Economy," National Bureau of Statistics 2000-2012.
_ , "Annual Survey of Industrial Firms," National Bureau of Statistics 2001-2009.
_ , "Urban Household Survey (16 provinces)," National Bureau of Statistics 2002-2009.
_ , "China Statistical Yearbook," National Bureau of Statistics 2002-2013.
_ , "First National Economic Census," National Bureau of Statistics 2004.
_ , "2005 1% Population Survey," National Bureau of Statistics 2005.
_ , "China Energy Statistical Yearbook," National Bureau of Statistics 2005.
_ , "Input-Output Tables of China," National Bureau of Statistics 2007.
_ , "Second National Economic Census," National Bureau of Statistics 2008.
_ , "Sixth National Population Census," National Bureau of Statistics 2010.
_ , "2015 1% Population Survey," National Bureau of Statistics 2015.
_ , "China Population & Employment Statistics Yearbook," National Bureau of Statistics 2023.
NDRC, "Implementation Plan for the Top 1,000 Enterprises Energy Conservation Action," Circular [2006] No. 571 apr 2006. National Development and Reform Commission.
_ , "Comprehensive Work Plan for Energy Conservation and Emission Reduction," Official Document No. 15 [2007] of the State Council 2007. Released on May 23, 2007.
_ **and NBS**, "Report on the State of the Energy Use of the Top-1,000 Enterprises (Year 2007)," Official Bulletin September 2007. National Development and Reform Commission and National Bureau of Statistics.
NOAA, "Global Surface Summary of the Day," National Climatic Data Center 2024.
Price, Lynn, Mark D. Levine, Nan Zhou, David Fridley, Nathaniel Aden, Hongyou Lu, Michael McNeil, Nina Zheng, Yining Qin, and Ping Yowargana, "Assessment of China's energy-saving and emission-reduction accomplishments and opportunities during the 11th Five Year Plan," *Energy Policy*, 2011, *39* (4), 2165–2178.
_ **, Xuejun Wang, and Jiang Yun**, "The challenge of reducing energy consumption of the Top-1000 largest industrial enterprises in China," *Energy Policy*, 2010, *38* (11), 6485–6498.
Pritchett, Lant and Lawrence H. Summers, "Wealthier is Healthier," *Journal of Human Resources*, 1996, *31* (4), 841–868.
Qi, Jinlei, Dandan Zhang, Xiang Zhang, Tanakao Takana, Yuhang Pan, Peng Yin, Jiangmei Liu, Shuocen Liu, George F. Gao, Guojun He, and Maigeng Zhou, "Short- and medium-term impacts of strict anti-contagion policies on non-COVID-19 mortality in China," *Nature Human Behaviour*, 2022, *6* (1), 55–63.
Rambachan, Ashesh and Jonathan Roth, "A More Credible Approach to Parallel Trends," *Review of Economic Studies*, 2023, *90* (5), 2555–2591.
Richterman, Aaron, Tra-My Ngoc Bùi, Elizabeth F. Bair, Gregory Jerome, Christophe Millien, Jean Christophe Dimitri Suffrin, Jere R. Behrman, and Harsha Thirumurthy, "The effects of government-led cash transfer programmes on behavioural and health determinants of mortality: a difference-in-differences study," *Lancet*, 2025, *405* (10476), 483–494.
Rubens, Michael, "Market Structure, Oligopsony Power, and Productivity," *American Economic Review*, 2023, *113* (9), 2382–2410.
Schwandt, Hannes and Till Von Wachter, "Socioeconomic Decline and Death: The Life-Cycle Impacts of Recessions for Labor Market Entrants," Working Paper 26638, National Bureau of Economic Research 2019.

Shen, Siyuan, Chi Li, Aaron van Donkelaar, Nathan Jacobs, Chenguang Wang, and Randall V. Martin, "Enhancing Global Estimation of Fine Particulate Matter Concentrations by Including Geophysical a Priori Information in Deep Learning," *ACS EST Air*, 2024, *1* (5), 332–345.

Sullivan, Daniel and Till von Wachter, "Job Displacement and Mortality: An Analysis Using Administrative Data," *Quarterly Journal of Economics*, 2009, *124* (3), 1265–1306.

van Donkelaar, Aaron, Randall V. Martin, Michael Brauer, N. Christina Hsu, Ralph A. Kahn, Robert C. Levy, Alexei Lyapustin, Andrew M. Sayer, and David M. Winker, "Global Estimates of Fine Particulate Matter using a Combined Geophysical-Statistical Method with Information from Satellites, Models, and Monitors," *Environmental Science & Technology*, 2016, *50* (7), 3762–3772.

Walker, Michael W., Nick Shankar, Edward Miguel, Dennis Egger, and Grady Killeen, "Can Cash Transfers Save Lives? Evidence from a Large-Scale Experiment in Kenya," Working Paper 32204, National Bureau of Economic Research 2024.

Wang, Shaoda and David Y. Yang, "Policy Experimentation in China: The Political Economy of Policy Learning," *Journal of Political Economy*, 2025, *133* (7), 2180–2228.

Xia, Haiping, Yunhao Chen, and Jinling Quan, "A simple method based on the thermal anomaly index to detect industrial heat sources," *International Journal of Applied Earth Observation and Geoinformation*, 2018, *73*, 627–637.

Xiao, Na, Zhaohui Ye, Huijuan Li et al., "Associations of serial negative income shock and all-cause mortality: a longitudinal study in China," *BMJ Public Health*, 2024, *2* (1), e000414.

Zhang, B., F. Y. Zhai, S. F. Du, and B. M. Popkin, "The China Health and Nutrition Survey, 1989-2011," *Obes Rev*, 2014, *15 Suppl 1* (0 1), 2–7.

Zhang, Bing, Xiaolan Chen, and Huanxiu Guo, "Does central supervision enhance local environmental enforcement? Quasi-experimental evidence from China," *Journal of Public Economics*, 2018, *164*, 70–90.

Zhang, Yanli, "Private Steel Firms Face a Cold Autumn," *China Economy and Informatization*, September 2010. News report.

Zhao, Xiaofan, Huimin Li, Liang Wu, and Ye Qi, "Implementation of energy-saving policies in China: How local governments assisted industrial enterprises in achieving energy-saving targets," *Energy Policy*, 2014, *66*, 170–184.

Zhou, Maigeng, Haidong Wang, Jun Zhu, Wanqing Chen, Linhong Wang, Shiwei Liu, Yichong Li, Lijun Wang, Yunning Liu, Peng Yin, Jiangmei Liu, Shicheng Yu, Feng Tan, Ryan M. Barber, Matthew M. Coates, Daniel Dicker, Maya Fraser, Diego González-Medina, Hannah Hamavid, Yuantao Hao, Guoqing Hu, Guohong Jiang, Haidong Kan, Alan D. Lopez, Michael R. Phillips, Jun She, Theo Vos, Xia Wan, Gelin Xu, Lijing L. Yan, Chuanhua Yu, Yong Zhao, Yingfeng Zheng, Xiaonong Zou, Mohsen Naghavi, Yu Wang, Christopher J. L. Murray, Gonghuan Yang, and Xiaofeng Liang, "Cause-specific mortality for 240 causes in China during 1990-2013: a systematic subnational analysis for the Global Burden of Disease Study 2013," *Lancet*, 2016, *387* (10015), 251–272.

Misallocation May Kill: Evidence from the World's Largest Energy-Saving Program
Disclosure Statement for Qirui Wang

The author declares that he has no relevant or material financial interests that relate to the research described in this paper.

Misallocation May Kill: Evidence from the World's Largest Energy-Saving Program
Disclosure Statement for Yuan Chen

The author declares that he has no relevant or material financial interests that relate to the research described in this paper.